

Western  Graduate&PostdoctoralStudies

Western University
Scholarship@Western

Electronic Thesis and Dissertation Repository

1-9-2013 12:00 AM

Theory of Model Kohn-Sham Potentials and its Applications

Alex P. Gaiduk
The University of Western Ontario

Supervisor
Prof. Viktor N. Staroverov
The University of Western Ontario

Graduate Program in Chemistry
A thesis submitted in partial fulfillment of the requirements for the degree in Doctor of
Philosophy
© Alex P. Gaiduk 2013

Follow this and additional works at: <https://ir.lib.uwo.ca/etd>

 Part of the [Atomic, Molecular and Optical Physics Commons](#), and the [Physical Chemistry Commons](#)

Recommended Citation

Gaiduk, Alex P., "Theory of Model Kohn-Sham Potentials and its Applications" (2013). *Electronic Thesis and Dissertation Repository*. 1099.
<https://ir.lib.uwo.ca/etd/1099>

This Dissertation/Thesis is brought to you for free and open access by Scholarship@Western. It has been accepted for inclusion in Electronic Thesis and Dissertation Repository by an authorized administrator of Scholarship@Western. For more information, please contact wlsadmin@uwo.ca.

**THEORY OF MODEL KOHN–SHAM POTENTIALS AND
ITS APPLICATIONS**

(Thesis format: Integrated Article)

by

Alex P. Gaiduk

Graduate Program in Chemistry

A thesis submitted in partial fulfillment
of the requirements for the degree of
Doctor of Philosophy

The School of Graduate and Postdoctoral Studies
The University of Western Ontario
London, Ontario, Canada

© Alex P. Gaiduk 2013

THE UNIVERSITY OF WESTERN ONTARIO
School of Graduate and Postdoctoral Studies

CERTIFICATE OF EXAMINATION

Supervisor:

.....
Prof. Viktor N. Staroverov

Supervisory Committee:

.....
Prof. Martin J. Stillman

Examiners:

.....
Prof. Styliani Conostas

.....
Prof. J. Clara Wren

.....
Prof. Lyudmila V. Goncharova

.....
Prof. Paul W. Ayers

The thesis by

Alex P. Gaiduk

entitled:

Theory of model Kohn–Sham potentials and its applications

is accepted in partial fulfillment of the
requirements for the degree of
Doctor of Philosophy

.....
Date

.....
Chair of the Thesis Examination Board

Abstract

The purpose of Kohn–Sham density functional theory is to develop increasingly accurate approximations to the exchange–correlation functional or to the corresponding potential. When one chooses to approximate the potential, the resulting model must be integrable, that is, a functional derivative of some density functional. Non-integrable potentials produce unphysical results such as energies that are not translationally or rotationally invariant. The thesis introduces methods for constructing integrable model potentials, developing properly invariant energy functionals from model potentials, and designing model potentials that yield accurate electronic excitation energies. Integrable potentials can be constructed using powerful analytic integrability conditions derived in this work. Alternatively, integrable potentials can be developed using the knowledge about the analytic structure of functional derivatives. When these two approaches are applied to the model potential of van Leeuwen and Baerends (which is non-integrable), they produce an exchange potential that has a parent functional and yields accurate energies. It is also shown that model potentials can be used to develop new energy functionals by the line-integration technique. When a model potential is not a functional derivative, the line integral depends on the choice of the integration path. By integrating the model potential of van Leeuwen and Baerends along the path of magnitude-scaled density, an accurate and properly invariant exchange functional is developed. Finally, a simple method to improve exchange–correlation potentials obtained from standard density-functional approximations is proposed. This method is based on the observation that an approximate Kohn–Sham potential of a fractionally ionized system is a better representation of the exact potential than the approximate Kohn–Sham potential of the corresponding neutral system. Removing $1/2$ of an electron leads to the greatest improvement of the highest occupied molecular orbital energy, which explains why the Slater transition state method works well for predicting ionization energies. Removing about $1/4$ of an electron improves orbital energy gaps and, when used in time-dependent density functional calculations, reduces errors of Rydberg excitation energies by almost an order of magnitude.

Keywords: quantum chemistry, density functional theory, self-interaction error, model exchange–correlation potentials, functional derivative, calculus of variations

Co-Authorship Statement

Chapter 1 includes two examples of line integration from the paper “Reconstruction of density functionals from Kohn–Sham potentials by integration along density scaling paths” by A. P. Gaiduk, S. K. Chulkov, and V. N. Staroverov [JCTC 5, 699 (2009)]. Alex Gaiduk performed the derivations and contributed to revising the manuscript prepared by Viktor Staroverov. Chapter 2 combines modified papers “Virial exchange energies from model exact-exchange potentials” [JCP 128, 204101 (2008)] and “How to tell when a model Kohn–Sham potential is not a functional derivative” [JCP 131, 044107 (2009)] by A. P. Gaiduk and V. N. Staroverov. Alex Gaiduk performed all the calculations in the Chapter and wrote its text. Chapter 3 is based on the paper “Construction of integrable model Kohn–Sham potentials by analysis of the structure of functional derivatives” by A. P. Gaiduk and V. N. Staroverov [PRA 83, 012509 (2011)]. Alex Gaiduk did all the derivations and calculations in the paper and wrote the draft of the manuscript. Chapter 4 contains the paper “Explicit construction of functional derivatives in potential-driven density-functional theory” by A. P. Gaiduk and V. N. Staroverov [JCP 133, 101104 (2010)]. Alex Gaiduk derived the integrability conditions, proposed their applications, and prepared the draft of the manuscript. Chapter 5 is based on the paper “A generalized gradient approximation for exchange derived from the model potential of van Leeuwen and Baerends” by A. P. Gaiduk and V. N. Staroverov [JCP 136, 064116 (2012)]. Alex Gaiduk performed all the derivations, calculations, and wrote the draft of the manuscript. Chapter 6 includes the paper “Self-interaction correction scheme for approximate Kohn–Sham potentials” by A. P. Gaiduk, D. Mizzi, and V. N. Staroverov [PRA 86, 052518 (2012)]. Dan Mizzi assembled the test set for Table 6.1 and did preliminary calculations with exchange-only potentials for Secs. 6.2–6.4. Alex Gaiduk performed the final calculations with the full exchange-correlation potentials and prepared the draft of the manuscript. Some of the results in Sec. 6.5 are from the paper “Improved electronic excitation energies from shape-corrected semilocal Kohn–Sham potentials” by A. P. Gaiduk, D. S. Firaha, and V. N. Staroverov [PRL 108, 253005 (2012)]. Dzmitry Firaha assembled the test set and determined the optimal depopulations for all functionals. Alex Gaiduk performed the time-dependent density-functional-theory calculations and assigned the symmetry of the excited states.

Acknowledgments

I would like to take this opportunity to thank my advisor, Professor Viktor Staroverov. I am indebted to Viktor for inviting me to visit his group in the summer of 2007 and helping me to make a transition to a completely new field. I am grateful for Viktor’s skillful mentoring and for the freedom in the choice of working habits. I also thank Viktor for showing me the importance of clear writing and presentation of the results. I am now convinced that the success of research critically depends on the way it is presented in a journal article or in a talk. I am sure that Viktor’s clarity in writing will remain the model and the reference to me for a long time even after graduate school. Finally, I am thankful for Viktor’s support and encouragement during all these years. It has been a privilege and pleasure to work with Viktor.

I want to thank Dr. Ilya Ryabinkin for being my colleague and my friend. I am very glad indeed to have been working with Ilya for the 3.5 years he’s been a member of our group. Ilya was always available for discussion when my research “stuck” or went astray. A great deal of my knowledge about theoretical chemistry (and not only chemistry) comes from our conversations. And surely, experience with Ilya convinced me that the morning coffee can be an efficient research tool. The ideas for a couple of papers that we are currently preparing together have been conceived during some of those ‘medium double-double’ morning hours.

I am thankful to the current and former members of the Staroverov group—Pavel Elkind, Brian Nikkel, Alexei Kananenka, Amin Torabi, Dzmitry Firaha, Sviataslau Kohut, Dan Mizzi, and Victoria Karner—for the science we did together and for the friendly and enjoyable atmosphere they all maintained.

I want to acknowledge my references Professors Arne Nylandsted Larsen and Martin H. Müser for their support of my scholarship and postdoctoral applications. I am grateful for the valuable time they spent preparing recommendation letters for me.

I would like to thank Olga and Andrei Smirnov for their warmest hospitality. They truly made me feel at home at their place in Richmond Hill. I also greatly appreciate the support of my friends in London—Siargei Kanaplianik, Eric Tenkorang, Warren Furnival, Ilya Kossovskiy, Sergey Dedyulin, Fanny Mahy, and Niloufar Naderi—for making my life here easier and more enjoyable.

Last but certainly not least, I want to thank my parents, Peter and Alla Gaiduk, and my sister, Olga Gaiduk, for their love and support throughout all these years. It was them who encouraged me to pursue a doctorate in Canada, and I am sure they are very happy to see me finishing my Ph.D. I could not be where I am without you.

Посвящается моим дорогим родителям,
Петру Ивановичу и Алле Васильевне Гайдук

Contents

Certificate of Examination	ii
Abstract	iii
Co-Authorship Statement	iv
Acknowledgments	v
Dedication	vi
List of Figures	x
List of Tables	xi
List of Abbreviations	xii
List of Symbols	xiii
1 Introduction	1
1.1 Density functional theory	1
1.2 Kohn–Sham method	2
1.3 Functionals and functional derivatives	5
1.3.1 Definition of functionals and functional derivatives	5
1.3.2 Calculation of functional derivatives	7
1.4 Potential-driven density functional theory	9
1.4.1 Model potentials	9
1.4.2 Reconstruction of density functionals	15
1.4.3 Potentials that are not functional derivatives	19
1.4.4 Problems of non-integrable model potentials	22
1.5 Objectives of the study	23
Bibliography	25
2 Tests for functional derivatives	31
2.1 Introduction	31
2.2 Methodology	32
2.2.1 Self-consistent-field convergence test	32
2.2.2 Line-integral test	32

2.2.3	Virial-energy test for exact-exchange potentials	33
2.2.4	Zero-force and zero-torque tests	33
2.3	Results and discussion	34
2.3.1	SCF convergence pattern	35
2.3.2	Path dependence of the line integral	37
2.3.3	Virial energies from exact-exchange potentials	39
2.3.4	Exchange-correlation force and torque on the density	42
2.4	Conclusion	43
	Bibliography	45
3	Analytic structure of functional derivatives	48
3.1	Introduction	48
3.2	Methodology	49
3.2.1	Functional derivatives of GGAs	49
3.2.2	Ingredients of functional derivatives of GGAs	51
3.2.3	Analytic structure of functional derivatives of exchange GGAs	53
3.3	Application	56
3.4	Conclusion	59
	Bibliography	60
4	Integrability conditions for model potentials	63
4.1	Introduction	63
4.2	Methodology	64
4.2.1	Integrability from the symmetry of the kernel	65
4.2.2	Integrability from the symmetry of second differential	67
4.3	Analytic integrability conditions	67
4.4	Direct construction of integrable potentials	69
4.5	Conclusion	72
	Bibliography	73
5	Energy functionals based on model Kohn–Sham potentials	74
5.1	Introduction	74
5.2	Methodology	75
5.3	Application	76
5.3.1	Λ -LB94 and Q-LB94 functionals	76
5.3.2	Refinement of the Q-LB94 functional	79
5.3.3	Performance of the Q-revLB94 functional	80
5.3.4	The Q-revLB94 exchange potential	82
5.4	Relation to other methods	84
5.5	Conclusion	85
	Bibliography	86
6	Self-interaction correction scheme for Kohn–Sham potentials	90
6.1	Introduction	90
6.2	Self-interaction error in Kohn–Sham potentials	91
6.3	Self-interaction correction for Kohn–Sham potentials	93

6.4	Vertical ionization energies	97
6.5	Electronic excitation energies	99
6.5.1	Methodology	99
6.5.2	Computational details	100
6.5.3	Results	102
6.6	Conclusion	102
	Bibliography	114
7	Summary and outlook	121
	Bibliography	124
A	Properties of the delta function	127
B	Functional derivative of the Levy–Perdew energy expression	130
C	Copyright permissions	134
	Curriculum Vitæ	141

List of Figures

2.1	Convergence of the total energy in the self-consistent-field procedure with the functional derivatives of the LDA, Gill, Becke exchange functionals, and with the Fermi–Amaldi model potential	36
2.2	Convergence of the total energy in the self-consistent-field procedure with the van Leeuwen–Baerends, Umezawa, Slater, and Becke–Johnson model potentials	36
3.1	Ingredients ρ , s , q , and u of functional derivatives of generalized gradient approximations	51
3.2	Components $\rho^{1/3}R(s)$, $\rho^{1/3}Q(s)q$, and $\rho^{1/3}U(s)u$ of functional derivatives of the B88, PBE, and G96 exchange functionals	55
3.3	Component $\rho^{1/3}R(s)$ of functional derivatives of the B88, PBE, and G96 exchange functionals compared with the scaled semilocal part of the LB94 model potential	56
3.4	Stray model potential LB94 compared with integrable model potentials fd-LB94 and fd-revLB94 derived from the LB94	58
5.1	Exchange part of the LB94 potential and functional derivatives of the Λ -LB94 and Q-LB94 exchange functionals	78
5.2	Exchange part of the LB94 model potential and functional derivatives of the Q-revLB94, B88, and PBE exchange functionals	83
5.3	The LB94, Q-revLB94, B88, and PBE exchange potentials multiplied by r to emphasize their asymptotic behavior	83
6.1	Hartree and LDA exchange-correlation potentials for the H atom	92
6.2	Hartree and LDA exchange-correlation potentials for the Ne atom	92
6.3	HOMO ($1s$) eigenvalue for the H atom as a function of the HOMO depopulation	94
6.4	HOMO ($2p_z$) eigenvalue for the Ne atom as a function of the HOMO depopulation	94
6.5	The sum of Hartree and PBE exchange-correlation potentials for a series of partially ionized hydrogen ions $H^{+\delta}$	95
6.6	PBE exchange-correlation potential for the Ne atom with and without fractional depopulation of the HOMO	96
6.7	LDA orbital energies in a Be atom as functions of the HOMO depopulation	101

List of Tables

2.1	Exchange energies from various exchange potentials obtained as line integrals along the Q-, Λ - and Z-paths	38
2.2	Atomic total energies from various model exchange potentials computed using the exact-exchange energy functional and the virial relation	40
2.3	Molecular total energies from various model exchange potentials computed using the exact-exchange energy functional and the virial relation	41
2.4	Magnitudes of the exchange-correlation force and torque vectors evaluated for various model potentials	43
3.1	Exchange energies from the LB94, fd-LB94, fd-revLB94 potentials, and the PBE functional	59
5.1	Tests of translational invariance of the Λ -LB94 and Q-LB94 functionals	79
5.2	Atomic total energies computed using Λ -LB94, Q-LB94, Q-revLB94, B88, and PBE exchange-only approximations	81
5.3	Negative of the HOMO energy obtained using the Λ -LB94, Q-revLB94, B88, and PBE exchange-only approximations	84
6.1	Vertical ionization energies computed using standard and self-interaction-corrected LDA and PBE potentials	98
6.2	Kohn–Sham eigenvalue differences and TDDFT excitation energies for a Be atom computed using LDA and self-interaction-corrected LDA .	101
6.3	Mean absolute errors relative to experiment for 104 vertical excitation energies calculated using TDDFT with various density functionals . .	104
6.4	Vertical excitation energies for the Be atom (1S)	105
6.5	Vertical excitation energies for the Mg atom (1S)	106
6.6	Vertical excitation energies for the Zn atom (1S)	107
6.7	Vertical excitation energies for the CO molecule ($X\ ^1\Sigma^+$)	108
6.8	Vertical excitation energies for the CH ₂ O molecule ($\tilde{X}\ ^1A_1$)	109
6.9	Vertical excitation energies for the C ₂ H ₂ molecule ($\tilde{X}\ ^1\Sigma_g^+$)	110
6.10	Vertical excitation energies for the C ₂ H ₄ molecule ($\tilde{X}\ ^1A_g$)	111
6.11	Vertical excitation energies for the H ₂ O molecule ($\tilde{X}\ ^1A_1$)	112
6.12	Vertical excitation energies for the N ₂ molecule ($X\ ^1\Sigma_g^+$)	113

List of Abbreviations

B3LYP	—	Becke–Lee–Yang–Parr hybrid
B88	—	Becke-88
BJ	—	Becke–Johnson
BLYP	—	Becke–Lee–Yang–Parr
C	—	correlation
DFT	—	density functional theory
DGE	—	density-gradient expansion
DIIS	—	direct inversion in the iterative subspace
EXX	—	exact exchange
FA	—	Fermi–Amaldi
G96	—	Gill-96
GC	—	gradient-corrected
GGA	—	generalized gradient approximation
HF	—	Hartree–Fock
H	—	Hartree
HOMO	—	highest occupied molecular orbital
HXC	—	Hartree-exchange-correlation
KLI	—	Krieger–Li–Iafrate
LB94	—	van Leeuwen–Baerends-94
LDA	—	local density approximation
LHF	—	localized Hartree–Fock
MAE	—	mean absolute error
MAPE	—	mean absolute percentage error
OEP	—	optimized effective potential
PBE0	—	Perdew–Burke–Ernzerhof hybrid
PBE	—	Perdew–Burke–Ernzerhof
RPP	—	Räsänen–Pittalis–Proetto
SCF	—	self-consistent field
SIC	—	self-interaction correction
SIE	—	self-interaction error
S	—	Slater
TDDFT	—	time-dependent density functional theory
TPSS	—	Tao–Perdew–Staroverov–Scuseria
U06	—	Umezawa-06
UGBS	—	universal Gaussian basis set
VIE	—	vertical ionization energy
W	—	Wigner
XC	—	exchange-correlation
X	—	exchange

List of Symbols

E_h	—	atomic unit of energy (1 hartree = 2625.50 kJ mol ⁻¹ = 27.2114 eV)
a_0	—	atomic unit of length (1 bohr = 0.529177 Å)
N	—	number of electrons
Z	—	nuclear charge
\mathbf{r}	—	position vector
ρ	—	electron density
ρ_q	—	magnitude-scaled density
ρ_λ	—	coordinate-scaled density
ρ_ζ	—	magnitude- and coordinate-scaled density
$\tilde{\rho}$	—	electron-deficient density
$\gamma(\mathbf{r}, \mathbf{r}')$	—	density matrix
$F[\rho]$	—	general density functional
f	—	general energy density
E	—	total energy
E_{XC}	—	exchange-correlation energy
E_X	—	exchange energy
V	—	energy of electrons in external field
V_{ee}	—	energy of electron-electron interaction
v	—	external potential
v_s	—	Kohn–Sham potential
v_{HXC}	—	Hartree-exchange-correlation (electronic) potential
v_H	—	Hartree (electrostatic) potential
v_{XC}	—	exchange-correlation potential
v_X	—	exchange potential
ϕ_i	—	Kohn–Sham orbitals
ϵ_i	—	Kohn–Sham eigenvalues
g	—	norm of the density gradient
s	—	reduced density gradient
l	—	Laplacian of the density
q	—	reduced density Laplacian
w	—	Hessian-dependent density variable
u	—	reduced Hessian-dependent density variable
β	—	empirical parameter in the LB94, fd-LB94, and Q-LB94 models
R, Q, U	—	components of a GGA exchange potential
δ	—	highest occupied molecular level depopulation

Chapter 1

Introduction

1.1 Density functional theory

In 1964, Pierre Hohenberg and Walter Kohn proved [1] that the energy and electronic properties of atoms and molecules are uniquely determined by the electron density $\rho(\mathbf{r}) \equiv \rho(x, y, z)$. The work of Hohenberg and Kohn has become the beginning of what is now called density functional theory (DFT), one of the most successful and widely used methods of electronic structure calculations.

Density functional theory is an attractive alternative to conventional wavefunction-based methods. The electronic wavefunction Ψ of a system with N electrons depends on $3N$ spatial coordinates, while the density depends only on three coordinates, x , y and z . This makes calculations involving the electron density faster than calculations with wavefunctions. In fact, density functional theory makes it possible to study systems with hundreds and even thousands of atoms [2].

In DFT, the total electronic energy is expressed as a functional of the density $E[\rho]$. This functional can be written as a sum of several terms: The kinetic energy of electrons, $T[\rho]$, the energy of electrons in the external field, $V[\rho]$, and the energy of electron-electron interaction, $V_{ee}[\rho]$,

$$E[\rho] = T[\rho] + V[\rho] + V_{ee}[\rho]. \quad (1.1)$$

Of these terms, only $V[\rho]$ is known as an explicit functional of the density,

$$V[\rho] = \int v(\mathbf{r})\rho(\mathbf{r}) d\mathbf{r}, \quad (1.2)$$

where $v(\mathbf{r})$ is a multiplicative external potential acting on the electrons. For atoms,

molecules and solids, $v(\mathbf{r})$ is simply the Coulombic potential of the nuclei with charges Z_A at positions \mathbf{R}_A ,

$$v(\mathbf{r}) = - \sum_A \frac{Z_A}{|\mathbf{r} - \mathbf{R}_A|}. \quad (1.3)$$

Using Eq. (1.2), the total energy functional of Eq. (1.1) can be expressed as

$$E[\rho] = F[\rho] + \int v(\mathbf{r})\rho(\mathbf{r}) d\mathbf{r}, \quad (1.4)$$

where the functional $F[\rho] = T[\rho] + V_{\text{ee}}[\rho]$. The leading contribution to the term $V_{\text{ee}}[\rho]$ is the classical Coulomb electron-electron repulsion

$$J[\rho] = \frac{1}{2} \int d\mathbf{r} \int \frac{\rho(\mathbf{r})\rho(\mathbf{r}')}{|\mathbf{r} - \mathbf{r}'|} d\mathbf{r}'. \quad (1.5)$$

Using Eq. (1.5), the functional $F[\rho]$ may be rewritten as

$$F[\rho] = T[\rho] + J[\rho] + \text{a non-classical term}, \quad (1.6)$$

where the non-classical term describes the quantum-mechanical effects of electronic exchange and correlation [3]. The functional $F[\rho]$ is *universal* in that it is the same for any chemical system. All system-specific information is contained in the external potential $v(\mathbf{r})$, provided that the number of electrons N is fixed.

Hohenberg and Kohn also proved [1] that the total energy functional $E[\rho]$ of Eq. (1.4) is variational, that is, for any trial N -electron density $\tilde{\rho}$ it gives an energy that is above the exact ground-state energy E_0 , or $E[\tilde{\rho}] \geq E_0$. Therefore, the trial density that minimizes the value of the functional $E[\rho]$ is the true ground-state density. In order to make this result practical, we need to know the functional $F[\rho]$.

1.2 Kohn–Sham method

The crucial part of the functional $F[\rho]$ is the electron-electron interaction energy $V_{\text{ee}}[\rho]$. Suppose we want to apply the Hohenberg–Kohn theory to a system of *non-interacting* electrons moving in a field of external potential $v(\mathbf{r})$. For this system (denoted by a symbol “ s ”), the many-electron Schrödinger equation can be solved exactly; the solution is an antisymmetrized product of orbitals ϕ_i determined from

the single-particle Schrödinger equations

$$\left[-\frac{1}{2}\nabla^2 + v(\mathbf{r}) \right] \phi_i(\mathbf{r}) = \epsilon_i \phi_i(\mathbf{r}). \quad (1.7)$$

Because the electrons in this fictitious system do not interact, the term $V_{\text{ee}}[\rho]$ vanishes, so the functional $F_s[\rho]$ becomes simply

$$F_s[\rho] = -\frac{1}{2} \sum_{i=1}^N \langle \phi_i | \nabla^2 | \phi_i \rangle \equiv T_s[\rho], \quad (1.8)$$

with the electron density given by

$$\rho(\mathbf{r}) = \sum_{i=1}^N |\phi_i(\mathbf{r})|^2. \quad (1.9)$$

Formally, $T_s[\rho]$ is a functional of the orbitals ϕ_i . However, for non-interacting systems, $T_s[\rho] = F_s[\rho]$, which means that $T_s[\rho]$ is a universal functional of the density ρ alone. For the real (interacting) system, the functional $F[\rho]$ can now be written as

$$F[\rho] = T_s[\rho] + J[\rho] + E_{\text{XC}}[\rho], \quad (1.10)$$

where the term $E_{\text{XC}}[\rho]$ includes the effects of exchange and correlation. The functional $E_{\text{XC}}[\rho]$ is unknown; formally, it is defined as $E_{\text{XC}}[\rho] = F[\rho] - T_s[\rho] - J[\rho]$.

Minimization of the total energy functional

$$E[\rho] = T_s[\rho] + \int v(\mathbf{r})\rho(\mathbf{r}) d\mathbf{r} + \frac{1}{2} \int d\mathbf{r} \int \frac{\rho(\mathbf{r})\rho(\mathbf{r}')}{|\mathbf{r} - \mathbf{r}'|} d\mathbf{r}' + E_{\text{XC}}[\rho] \quad (1.11)$$

with respect to ρ yields a set of one-electron Hartree-like equations known as the Kohn–Sham equations,

$$\left[-\frac{1}{2}\nabla^2 + v_s(\mathbf{r}) \right] \phi_i(\mathbf{r}) = \epsilon_i \phi_i(\mathbf{r}). \quad (1.12)$$

The Kohn–Sham potential $v_s(\mathbf{r})$ is the effective potential energy operator defined as a functional derivative of the functional $E[\rho] - T_s[\rho]$. It can be written as

$$v_s(\mathbf{r}) = v(\mathbf{r}) + v_{\text{HXC}}(\mathbf{r}), \quad (1.13)$$

where v is the potential of the nuclei and v_{HXC} is the effective electronic Hartree–

exchange-correlation potential. The v_{HXC} subsumes all electron-electron interactions of the real system and is itself partitioned as

$$v_{\text{HXC}}(\mathbf{r}) = v_{\text{H}}(\mathbf{r}) + v_{\text{XC}}(\mathbf{r}), \quad (1.14)$$

where the Hartree potential v_{H} is the functional derivative of the electrostatic repulsion functional $J[\rho]$,

$$v_{\text{H}}(\mathbf{r}) = \int \frac{\rho(\mathbf{r}')}{|\mathbf{r}' - \mathbf{r}|} d\mathbf{r}', \quad (1.15)$$

and the exchange-correlation potential v_{XC} is the functional derivative of the exchange-correlation functional $E_{\text{XC}}[\rho]$,

$$v_{\text{XC}}(\mathbf{r}) = \frac{\delta E_{\text{XC}}[\rho]}{\delta \rho(\mathbf{r})}. \quad (1.16)$$

Comparison between Eqs. (1.7) and (1.12) suggests the following interpretation of the potential $v_s(\mathbf{r})$: It is the external potential of a fictitious system of non-interacting electrons that has the same density $\rho(\mathbf{r})$ as the real (interacting) system [4]. The density constructed by Eq. (1.9) from the orbitals obtained by solving the Kohn–Sham equations *is* the density that minimizes the total energy functional $E[\rho]$ of the system of interacting electrons. But the potential v_s itself depends on the electron density, so the Kohn–Sham equations need to be solved iteratively. The self-consistent procedure involves the following steps: (i) start with an initial guess for the density; (ii) construct v_{H} and v_{XC} , and solve the Kohn–Sham equations; (iii) update the density using the new orbitals ϕ_i . This procedure is repeated until self-consistency, i.e., until the Kohn–Sham equations return the input density.

The simplicity and formal exactness of the Kohn–Sham density functional theory come with a price. The exact exchange-correlation functional $E_{\text{XC}}[\rho]$ is unknown and must be approximated for any practical application. There is no systematic procedure for the improvement of density-functional approximations, and developers often include empirical parameters to achieve good agreement with experiments. As a result, most density-functional methods existing today occupy an intermediate position between semiempirical and *ab initio* theories.

1.3 Functionals and functional derivatives

1.3.1 Definition of functionals and functional derivatives

In this section we present a brief discussion of the properties of functionals and functional derivatives by comparing them to the familiar concepts from the ordinary calculus. Recall that a *function* is a rule assigning a number to another number. A *functional* is a rule assigning a number to a function,

$$f(\mathbf{r}) \xrightarrow{\text{rule}} F[f]. \quad (1.17)$$

In simple terms, a functional can be thought of as a function whose argument is a function. Examples of functionals include:

- A definite integral over a continuous function $f(x)$:

$$F[f] = \int_{x_1}^{x_2} f(x) dx. \quad (1.18)$$

- A prescription which associates a function with the value of this function at a particular point x_0 :

$$F[f] = f(x_0). \quad (1.19)$$

This functional can be represented as an integral with the Dirac delta function (refer to Appendix A for details):

$$F[f] = \int_{x_1}^{x_2} f(x) \delta(x - x_0) dx, \quad x_1 < x_0 < x_2. \quad (1.20)$$

Approximate density functionals often depend on the density ρ and its first and sometimes second derivatives through the gradient $\nabla\rho$ and the Laplacian $\nabla^2\rho$, respectively,

$$F[\rho] = \iiint_V f(\rho, \nabla\rho, \nabla^2\rho) d\mathbf{r}, \quad (1.21)$$

where the integration volume V is the entire coordinate space. Usually the triple integral sign \iiint_V is reduced to a single \int with the implied integration limits. Functionals of the type of Eq. (1.21) are called *explicit* because they are constructed from the density-dependent ingredients alone. By contrast, *orbital-dependent* functionals such as $T_s[\rho]$ of Eq. (1.8) include the Kohn–Sham orbitals and are thus *implicit* functionals of ρ . The simplest explicit functionals are the Coulomb repulsion of the density

given by Eq. (1.5) and the local-density approximation (LDA) for exchange energy of the uniform electron gas,

$$E_X^{\text{LDA}}[\rho] = -C_X \int \rho^{4/3}(\mathbf{r}) d\mathbf{r}, \quad (1.22)$$

where $C_X = (3/4)(3/\pi)^{1/3}$ is a non-empirical constant.

Similar to the ordinary calculus, there exists calculus dealing with the functionals [5–7]. The central quantity to the calculus of variations is the concept of a functional derivative. Let $F[\rho]$ be a density-functional approximation for some kind of electronic energy. For a given $\rho(\mathbf{r})$ and an arbitrary integrable function $h(\mathbf{r})$, consider the functional defined by

$$DF[\rho, h] = \lim_{t \rightarrow 0} \frac{F[\rho + th] - F[\rho]}{t} = \left\{ \frac{d}{dt} F[\rho + th] \right\}_{t=0} \quad (1.23)$$

If this functional exists and is linear in h , then it is called the Gâteaux differential at ρ in the direction h . Usually, it may be written as a linear (in h) integral operator

$$DF[\rho, h] = \int v([\rho]; \mathbf{r}) h(\mathbf{r}) d\mathbf{r}, \quad (1.24)$$

where $v([\rho]; \mathbf{r})$ is a function independent of $h(\mathbf{r})$. The distribution $v([\rho]; \mathbf{r})$ is called the *functional derivative* of $F[\rho]$, and it is itself a functional of ρ at every point \mathbf{r} ,

$$v([\rho]; \mathbf{r}) \equiv \frac{\delta F[\rho]}{\delta \rho(\mathbf{r})}. \quad (1.25)$$

For a particular choice of $h = \delta\rho$, the differential $DF[\rho, h]$ becomes the classical variation of the functional $F[\rho]$,

$$\delta F[\rho] = \int \frac{\delta F[\rho]}{\delta \rho(\mathbf{r})} \delta \rho(\mathbf{r}) d\mathbf{r}, \quad (1.26)$$

which implies that the total change in F upon variation of the function $\rho(\mathbf{r})$ is a linear superposition of the local changes summed over the entire range of \mathbf{r} values. In light of this discussion, Eq. (1.26) can be interpreted as an extension of the total differential of a function of several variables

$$f(x_1, x_2, \dots, x_N) \quad \rightarrow \quad df = \sum_{n=1}^N \frac{\partial f}{\partial x_n} dx_n. \quad (1.27)$$

to the case of an infinite number of variables [5, 7].

1.3.2 Calculation of functional derivatives

In order to calculate the functional derivative of $F[\rho]$, one has to evaluate the differential $DF[\rho, h]$ using Eq. (1.23), convert the result into the form of Eq. (1.24) and then identify the functional derivative $\delta F[\rho]/\delta\rho(\mathbf{r})$. As an example, consider the local density approximation for exchange energy defined by Eq. (1.22). The first differential of that functional is given by

$$DE_X^{\text{LDA}}[\rho, h] = -C_X \left\{ \frac{d}{dt} \int [\rho(\mathbf{r}) + th(\mathbf{r})]^{4/3} d\mathbf{r} \right\}_{t=0} = -\frac{4}{3} C_X \int \rho^{1/3}(\mathbf{r}) h(\mathbf{r}) d\mathbf{r}. \quad (1.28)$$

Comparing this expression with Eq. (1.24) we conclude that the functional derivative of the LDA exchange functional, called the LDA potential for exchange v_X^{LDA} , is

$$v_X^{\text{LDA}}(\mathbf{r}) \equiv \frac{\delta E_X^{\text{LDA}}[\rho]}{\delta\rho(\mathbf{r})} = -\frac{4}{3} C_X \rho^{1/3}(\mathbf{r}). \quad (1.29)$$

Before we proceed further, let us show how the calculation of functional derivatives can be simplified with the help of Dirac's delta function (Appendix A). Let $h(\mathbf{r}) = \delta(\mathbf{r} - \mathbf{r}')$. Substituting $\delta(\mathbf{r} - \mathbf{r}')$ into Eq. (1.24) and employing the definition of the delta function, we obtain

$$DE[\rho, \delta] = \int \frac{\delta E[\rho]}{\delta\rho(\mathbf{r})} \delta(\mathbf{r} - \mathbf{r}') d\mathbf{r} = \frac{\delta E[\rho]}{\delta\rho(\mathbf{r}')}, \quad (1.30)$$

and the functional derivative is simply equal to the first differential $DE[\rho, \delta]$,

$$\frac{\delta E[\rho]}{\delta\rho(\mathbf{r}')} = \left\{ \frac{d}{dt} E[\rho(\mathbf{r}) + t\delta(\mathbf{r} - \mathbf{r}')] \right\}_{t=0} \quad (1.31)$$

Let us illustrate this by differentiating the electrostatic repulsion functional $J[\rho]$ given by Eq. (1.5). We can rewrite $J[\rho]$ as

$$J[\rho] = \frac{1}{2} \int d\mathbf{r}' \int \frac{\rho(\mathbf{r}')\rho(\mathbf{r}'')}{|\mathbf{r}' - \mathbf{r}''|} d\mathbf{r}''. \quad (1.32)$$

Application of Eq. (1.31) yields

$$\begin{aligned} \frac{\delta J[\rho]}{\delta \rho(\mathbf{r})} &= \frac{1}{2} \left\{ \frac{d}{dt} \int d\mathbf{r}' \int \frac{[\rho(\mathbf{r}') + t\delta(\mathbf{r}' - \mathbf{r})][\rho(\mathbf{r}'') + t\delta(\mathbf{r}'' - \mathbf{r})]}{|\mathbf{r}' - \mathbf{r}''|} d\mathbf{r}'' \right\}_{t=0} \\ &= \frac{1}{2} \int \frac{\rho(\mathbf{r}')}{|\mathbf{r}' - \mathbf{r}|} d\mathbf{r}' + \frac{1}{2} \int \frac{\rho(\mathbf{r}'')}{|\mathbf{r} - \mathbf{r}''|} d\mathbf{r}'' = \int \frac{\rho(\mathbf{r}')}{|\mathbf{r}' - \mathbf{r}|} d\mathbf{r}', \end{aligned} \quad (1.33)$$

where we have used the fact that $|\mathbf{r} - \mathbf{r}''| = |\mathbf{r}'' - \mathbf{r}|$ and changed the dummy integration variable from \mathbf{r}'' to \mathbf{r}' .

In a similar fashion one can derive a general functional differentiation formula for explicitly density-dependent functionals of the type of Eq. (1.21):

$$\frac{\delta F[\rho]}{\delta \rho(\mathbf{r})} = \frac{\partial f}{\partial \rho} - \nabla \cdot \left(\frac{\partial f}{\partial \nabla \rho} \right) + \nabla^2 \left(\frac{\partial f}{\partial \nabla^2 \rho} \right), \quad (1.34)$$

where $\partial f / \partial \nabla \rho$ is a shorthand for a vector with three components $\partial f / \partial \rho'_\alpha$, in which $\rho'_\alpha \equiv \partial \rho / \partial \alpha$ and $\alpha = x, y, z$.

Finally, let us derive a useful expression for the derivative of a functional with respect to a parameter. Consider the functional $F[\rho]$, in which the function $\rho(\mathbf{r}, t)$ in turn depends on a parameter t . The variation of $F[\rho]$ is defined by

$$\delta F[\rho] = \int \frac{\delta F[\rho]}{\delta \rho(\mathbf{r}, t)} \delta \rho(\mathbf{r}, t) d\mathbf{r}. \quad (1.35)$$

Suppose the function $\rho(\mathbf{r}, t)$ is varied by changing the parameter t only. Then

$$\delta \rho(\mathbf{r}, t) = \frac{\partial \rho(\mathbf{r}, t)}{\partial t} dt, \quad (1.36)$$

and

$$\delta F[\rho] = \int \frac{\delta F[\rho]}{\delta \rho(\mathbf{r}, t)} \frac{\partial \rho(\mathbf{r}, t)}{\partial t} d\mathbf{r} dt. \quad (1.37)$$

Observe that F does not involve integration over t , and may thus be treated as a *function* of t . The variation of $F(t)$ is then simply equal to $\delta F(t) = (\partial F / \partial t) dt$. Comparing this equality with Eq. (1.37), we arrive at

$$\frac{\partial F}{\partial t} = \int \frac{\delta F[\rho]}{\delta \rho(\mathbf{r}, t)} \frac{\partial \rho(\mathbf{r}, t)}{\partial t} d\mathbf{r}. \quad (1.38)$$

With the shorthand $\rho_t(\mathbf{r}) \equiv \rho(\mathbf{r}, t)$, this last expression becomes

$$\frac{\partial F[\rho_t]}{\partial t} = \int \frac{\delta F[\rho_t]}{\delta \rho_t(\mathbf{r})} \frac{\partial \rho_t(\mathbf{r})}{\partial t} d\mathbf{r}. \quad (1.39)$$

We will employ this formula in the following Section.

1.4 Potential-driven density functional theory

In order to perform density-functional-theory calculations, one needs an approximation for the exchange-correlation functional $E_{\text{XC}}[\rho]$. The potential v_{XC} is then obtained as a functional derivative of $E_{\text{XC}}[\rho]$ using the techniques discussed in the previous Section. Dozens of approximate exchange-correlation functionals have been proposed to date [3, 8–10], some of them closely approaching the chemical level of accuracy of 1 kcal mol⁻¹. Unfortunately, functional derivatives of most existing density functionals lack essential properties of the exact potential [11]. For example, all density-functional approximations fail to reproduce the exact Coulombic $-1/r$ asymptotic decay of the potential. The result is a wrong description of molecular response properties such as ionization, electronic excitation energies, and hyperpolarizabilities. A possible solution is to approximate the exchange-correlation potential v_{XC} directly.

1.4.1 Model potentials

Model exchange-correlation potentials are usually designed to mimic the asymptotic behavior [12–14], shell structure [15–18], and derivatives discontinuities [19, 20] of the exact potential. Compared to common density functionals, potential approximations predict very accurate molecular response properties [19–22]. In this section, we will review some of the model potentials existing today and explain how they work.

Fermi–Amaldi potential

The Fermi–Amaldi (FA) potential is defined by

$$v_{\text{X}}^{\text{FA}}(\mathbf{r}) = -\frac{1}{N}v_{\text{H}}(\mathbf{r}), \quad (1.40)$$

where $v_{\text{H}}(\mathbf{r})$ is the electrostatic potential of Eq. (1.15) and N is the number of electrons. Formally, the potential of Eq. (1.40) is a functional derivative of the Fermi–Amaldi density functional [23–25] obtained under the assumption that N is a constant.

The Fermi–Amaldi model has the correct $-1/r$ asymptotic decay due to the presence of the electrostatic kernel $|\mathbf{r}' - \mathbf{r}|^{-1}$. This follows from the multipole expansion [25, 26] of $v_X^{\text{FA}}(\mathbf{r})$,

$$v_X^{\text{FA}}(\mathbf{r}) = -\frac{1}{N} \int \frac{\rho(\mathbf{r}')}{|\mathbf{r}' - \mathbf{r}|} d\mathbf{r}' \rightarrow -\frac{1}{r} \quad (r \rightarrow \infty). \quad (1.41)$$

Taken by itself, the Fermi–Amaldi potential is a poor representation of the true v_{XC} . Still, it has the correct Coulombic decay and therefore can be used to tailor the long-range behavior of other model potentials [19, 25, 27]. One of the models that involves the Fermi–Amaldi term as an ingredient is the Umezawa potential [14].

Umezawa potential

Umezawa [14] used the Fermi–Amaldi potential to refine the asymptotic behavior of the LDA potential. The exchange-like part of the Umezawa model (U06) is given by

$$v_X^{\text{U06}}(\mathbf{r}) = g_1(\mathbf{r})v_X^{\text{LDA}}(\mathbf{r}) + g_2(\mathbf{r})v_X^{\text{FA}}(\mathbf{r}). \quad (1.42)$$

The switching functions $g_1(\mathbf{r})$ and $g_2(\mathbf{r})$ are defined as

$$g_1(\mathbf{r}) = \frac{1}{\ln(1 + \gamma^5 \xi^5 s^5) + 1} \quad \text{and} \quad g_2(\mathbf{r}) = 1 - e^{-\gamma^2 \xi^2 s^2}, \quad (1.43)$$

where $\xi = 2^{1/3}$ is the factor arising in the transition to the spin-unpolarized form and $\gamma = 0.125$ is the empirical parameter chosen to fit the U06 potential (combined with the Perdew–Zunger approximation for correlation [28]) to the true v_{XC} of the helium atom. The quantity s is a dimensionless reduced-density gradient, a ubiquitous component of gradient-dependent approximations [29],

$$s = \frac{|\nabla\rho|}{\rho^{4/3}}. \quad (1.44)$$

The Umezawa potential employs the switching functions g_1 and g_2 to adjust the weights of the LDA and Fermi–Amaldi terms in different physical regions of the density. The asymptotic regions of atoms and molecules ($r \rightarrow \infty$) are characterized by the large reduced-density gradient ($s \rightarrow \infty$), so the functions g_1 and g_2 approach 0 and 1 respectively. As a result, the U06 model acquires the proper long-range decay of the Fermi–Amaldi potential.

Model potential of van Leeuwen and Baerends

Another strategy for developing model exchange-correlation potentials is to specifically design analytic expressions with the correct asymptotic behavior [12, 30]. Consider, for example, the model potential of van Leeuwen and Baerends (LB94) [12]. This approximation is defined as a sum of the LDA potential and a semilocal gradient correction term. The exchange-like part of the LB94 is given by

$$v_X^{\text{LB94}} = v_X^{\text{LDA}} - \rho^{1/3} \frac{\beta \xi s^2}{1 + 3\beta \xi s \sinh^{-1}(\xi s)}. \quad (1.45)$$

Here, s is the reduced-density gradient of Eq. (1.44), $\xi = 2^{1/3}$, and β is an empirical parameter. The value of $\beta = 0.05$ was determined by fitting the LB94 potential (combined with the LDA correlation potential of Ref. 31) to the exact exchange-correlation potential of the Be atom.

The gradient correction term of Eq. (1.45) has the analytic form of the Becke exchange energy density [8]. To understand why this correction exhibits the Coulombic decay, consider its behavior in the limit of large s . Asymptotic expansion of the semilocal part of LB94 yields, up to the leading term,

$$-\frac{\rho^{1/3} \beta \xi s^2}{1 + 3\beta \xi s \sinh^{-1}(\xi s)} \sim -\frac{1}{3} \frac{\rho^{1/3} s}{\ln s} \quad (s \rightarrow \infty). \quad (1.46)$$

Upon substitution of the exponential density $\rho(r) = Ne^{-ar}$ into the expression above, its right-hand side becomes exactly $-1/r$.

Because of the proper long-range decay, well-defined shell structure, and the computational simplicity, LB94 to this day remains one of the most popular model exchange-correlation potentials.

Slater, Becke–Johnson and related models

So far we considered approximations to the total exchange-correlation potential. There also exist a number of approximations to the exact exchange-only potential. Consider the conventional exact-exchange (EXX) energy functional,

$$E_X^{\text{EXX}} = -\frac{1}{4} \int d\mathbf{r} \int \frac{|\gamma(\mathbf{r}, \mathbf{r}')|^2}{|\mathbf{r} - \mathbf{r}'|} d\mathbf{r}', \quad (1.47)$$

where

$$\gamma(\mathbf{r}, \mathbf{r}') = \sum_{i=1}^N \phi_i(\mathbf{r})\phi_i^*(\mathbf{r}') \quad (1.48)$$

is the density matrix of the Kohn–Sham non-interacting system. The exact-exchange functional of Eq. (1.47) is defined as the Hartree–Fock exchange energy formula written in terms of the Kohn–Sham orbitals. Because the exact-exchange functional explicitly depends on the Kohn–Sham orbitals, its functional derivative cannot be obtained by techniques described in the Section 1.3.2. It can be, however, evaluated numerically using the optimized effective potential (OEP) method [32, 33]. Due to the ill-posed nature of the OEP problem in a finite basis set [34, 35], attempts have been made to model the functional derivative of Eq. (1.47) directly [13, 15–18, 36].

The averaged exchange-charge potential of Slater [13] arises as a leading term in the expression for a functional derivative of the exact-exchange functional [16]. For closed-shell systems, this potential can be written as

$$v_X^S(\mathbf{r}) = -\frac{1}{2\rho(\mathbf{r})} \int \frac{|\gamma(\mathbf{r}, \mathbf{r}')|^2}{|\mathbf{r} - \mathbf{r}'|} d\mathbf{r}', \quad (1.49)$$

where $\gamma(\mathbf{r}, \mathbf{r}')$ is given by Eq. (1.48). Like the model potentials we discussed before, v_X^S possesses the proper Coulombic asymptotic decay. But unfortunately, for a uniform electron gas, the Slater potential is deeper than the exact-exchange potential by a factor of 3/2 and is not a good approximation if taken alone.

The Slater potential is a starting point for many other approximations. In the Becke–Johnson model [17], for example, the exchange potential is represented as the sum of the Slater potential and a correction term,

$$v_X^{BJ} = v_X^S + \frac{k_{BJ}}{2\pi}, \quad (1.50)$$

where

$$k_{BJ} = \left(\frac{10}{3} \frac{\tau}{\rho} \right)^{1/2} \quad (1.51)$$

and $\tau(\mathbf{r}) = \frac{1}{2} \sum_{i=1}^N |\nabla\phi_i(\mathbf{r})|^2$ is the Kohn–Sham kinetic energy density. Inclusion of the τ -dependent term brings the Becke–Johnson model closer to the exact-exchange potential [17]. At the same time, $k_{BJ}/2\pi$ becomes a constant for exponential densities, and the resulting potential has a wrong $-1/r + C$ asymptotic decay, where C is a system-dependent constant.

The Becke–Johnson potential can be improved by adding to it a term that depends

on the derivatives of $\tau(\mathbf{r})$ and $\rho(\mathbf{r})$. The result is the gradient-corrected (GC) potential of Staroverov [18],

$$v_X^{\text{GC}} = v_X^{\text{BJ}} - \frac{7}{288\pi} \frac{|\nabla k_{\text{BJ}}^2|^2}{k_{\text{BJ}}^5}. \quad (1.52)$$

This correction refines the shell structure of the potential but inherits the incorrect $-1/r + C$ behavior of the Becke–Johnson model.

Another improvement of the Becke–Johnson potential was proposed by Räsänen, Pittalis and Proetto [36]. For real Kohn–Sham orbitals, their potential is given by the same formula as the Becke–Johnson model of Eq. (1.50) but with k_{BJ} replaced by k_{RPP} defined as

$$k_{\text{RPP}} = \left(\frac{10}{3} \frac{\tau - \tau_W}{\rho} \right)^{1/2} \quad (1.53)$$

where $\tau_W = |\nabla\rho|/8\rho$ is the von Weizsäcker correction to the Thomas–Fermi kinetic energy density [37]. The correction of Räsänen and co-workers vanishes at each point \mathbf{r} for one- and two-electron densities and has the exact $-1/r$ asymptotic decay.

Potentials of the localized Hartree–Fock family

A further improvement of the Slater potential is provided by the model potentials of the localized Hartree–Fock (LHF) family [38]. The members of this family can be represented as the Slater potential v_X^{S} plus a correction,

$$v_X(\mathbf{r}) = v_X^{\text{S}}(\mathbf{r}) + \frac{1}{\rho(\mathbf{r})} \sum_{i=1}^N \sum_{j=1}^N \omega_{ij} \phi_i^*(\mathbf{r}) \phi_j(\mathbf{r}). \quad (1.54)$$

Different choices of ω_{ij} correspond to different models. The potentials defined by Eq. (1.54) include the approximations of Krieger, Li, and Iafrate (KLI) [15], Della Sala and Görling [38], Grüning, Gritsenko, and Baerends [39], and Staroverov, Scuseria, and Davidson [40]. Very recently, the author in collaboration with Kananenka, Kohut, Ryabinkin, and Staroverov designed a new accurate model potential [41] of the same family. This potential was constructed with the aid of the Kohn–Sham inversion procedure [12, 42, 43] for the Hartree–Fock equations, and is given by

$$v_X(\mathbf{r}) = v_X^{\text{S}}([\rho^{\text{HF}}]; \mathbf{r}) + \frac{1}{\rho^{\text{HF}}(\mathbf{r})} \sum_{i=1}^N (\epsilon_i - \epsilon_i^{\text{HF}}) |\phi_i^{\text{HF}}(\mathbf{r})|^2. \quad (1.55)$$

The whole expression, including the Slater potential $v_X^{\text{S}}([\rho^{\text{HF}}]; \mathbf{r})$, is constructed using the Hartree–Fock orbitals ϕ_i^{HF} and the density ρ^{HF} . Our model is a special case of

Eq. (1.54) with $\omega_{ij} = (\epsilon_i - \epsilon_i^{\text{HF}})\delta_{ij}$, where ϵ_i are the eigenvalues of the potential v_X and ϵ_i^{HF} are the Hartree–Fock orbital energies. Since a potential is always determined up to an arbitrary constant, we fixed it by requiring $\omega_{\text{HOMO}} = 0$. This choice eliminated the HOMO from the last term of Eq. (1.55) and ensured that the potential inherits the correct $-1/r$ decay of the Slater model. The potential of Eq. (1.55) is computed iteratively starting with the Hartree–Fock orbitals until the eigenvalues ϵ_i become consistent between iterations. For this reason, the model of Eq. (1.55) was termed the ‘ ϵ -consistent potential’.

Let us analyze the relation between the ϵ -consistent potential and two potentials proposed in Ref. 38, TLHF and TKLI. TLHF and TKLI approximations are equivalent to the LHF [38] and KLI [15] but, similar to our model, are defined using the Hartree–Fock orbitals. The parameters ω_{ij} that generate these potentials are:

$$\begin{aligned} \text{TLHF: } \omega_{ij} &= \langle \phi_j^{\text{HF}} | v_X^{\text{TLHF}} - \hat{K} | \phi_i^{\text{HF}} \rangle \\ \text{TKLI: } \omega_{ij} &= \langle \phi_i^{\text{HF}} | v_X^{\text{TKLI}} - \hat{K} | \phi_i^{\text{HF}} \rangle \delta_{ij} \\ \text{Eq. (1.55): } \omega_{ij} &= (\epsilon_i - \epsilon_i^{\text{HF}}) \delta_{ij} \end{aligned}$$

In these equations, \hat{K} is the non-local Hartree–Fock exchange energy operator [44]. The TLHF model depends on the full matrix ω_{ij} , while TKLI and Eq. (1.55) neglect its off-diagonal part. Furthermore, ω_{ij} for the TKLI and the ϵ -consistent models can be brought to a similar form [41] as

$$\begin{aligned} \text{TKLI: } \omega_{ij} &\approx \langle \phi_i^{\text{HF}} | \hat{h} | \phi_i^{\text{HF}} \rangle \delta_{ij} - \epsilon_i^{\text{HF}} \delta_{ij} \\ \text{Eq. (1.55): } \omega_{ij} &= \epsilon_i \delta_{ij} - \epsilon_i^{\text{HF}} \delta_{ij}, \end{aligned}$$

where \hat{h} is the local Kohn–Sham operator with TKLI exchange potential. Thus, the model potential defined by Eq. (1.55) amounts to a replacement of expectation values $\langle \phi_i^{\text{HF}} | \hat{h} | \phi_i^{\text{HF}} \rangle$ in TKLI with eigenvalues ϵ_i . It has similar performance to other potentials from the family, and is more accurate than the Slater and Becke–Johnson models [41].

1.4.2 Reconstruction of density functionals¹

Application of the potential-driven DFT has long been hindered by several methodological difficulties. One of the problems is that the energy functional, corresponding to a given model potential, is usually unknown. This means that one needs to find a way to compute the energy corresponding to a model potential. Furthermore, the parent functional for a model potential may not exist at all. We are going to address these issues in more detail in the present and the following Sections.

Assume that a model potential v_{XC} has a parent functional $E_{\text{XC}}[\rho]$. Since the explicit form of $E_{\text{XC}}[\rho]$ is unknown, one needs some sort of functional “integration” procedure to compute the energy. Many texts discuss functional differentiation at length [7, 26, 37], but very few consider the inverse problem [45].

On the basis of Eq. (1.34) it is obvious that for any *local* exchange-correlation potential (that is, a potential that depends only on ρ but not on $\nabla\rho$ or higher derivatives of ρ), the exchange-correlation energy density can be found simply as an indefinite integral (antiderivative) of v_{XC} with respect to ρ . For *semilocal* exchange-correlation potentials, which also depend on $\nabla\rho$ and higher derivatives of ρ , a more general method is required. Such a method was developed by van Leeuwen and Baerends [46], who essentially reincarnated Volterra’s result from the general theory of functional calculus [5]. The idea of van Leeuwen and Baerends was to introduce an additional parameter t into the density $\rho(\mathbf{r})$ to create a path of densities $\rho_t(\mathbf{r})$. As explained at the end of Section 1.3.2, the *functional* $E_{\text{XC}}[\rho]$ then becomes a *function* of the variable t , $E_{\text{XC}}[\rho_t] = E_{\text{XC}}(t)$. The derivative of this function is given by Eq. (1.39):

$$\frac{\partial E_{\text{XC}}(t)}{\partial t} = \int \frac{\delta E_{\text{XC}}[\rho_t]}{\delta \rho_t(\mathbf{r})} \frac{\partial \rho_t(\mathbf{r})}{\partial t} d\mathbf{r} = \int v_{\text{XC}}([\rho_t]; \mathbf{r}) \frac{\partial \rho_t(\mathbf{r})}{\partial t} d\mathbf{r}. \quad (1.56)$$

Integrating this derivative from $t = A$ to $t = B$, we arrive at the following energy difference:

$$E_{\text{XC}}[\rho_B] - E_{\text{XC}}[\rho_A] = \int_A^B \frac{\partial E_{\text{XC}}(t)}{\partial t} dt = \int_A^B dt \int v_{\text{XC}}([\rho_t]; \mathbf{r}) \frac{\partial \rho_t(\mathbf{r})}{\partial t} d\mathbf{r}, \quad (1.57)$$

which holds for an arbitrary path connecting ρ_A and ρ_B [46]. Equation (1.57) is the most general form of the van Leeuwen–Baerends line integral. In particular, if the parametrization $\rho_t(\mathbf{r})$ is such that $E_{\text{XC}}[\rho_A] = 0$ and $\rho_B(\mathbf{r}) = \rho(\mathbf{r})$, then Eq. (1.57)

¹Reproduced in part with permission from **A. P. Gaiduk**, S. K. Chulkov, and V. N. Staroverov, “Reconstruction of density functionals from Kohn–Sham potentials by integration along density scaling paths”, *J. Chem. Theory Comput.* **5**, 699 (2009). Copyright 2009, American Chemical Society.

reduces to

$$E_{\text{XC}}[\rho] = \int_A^B dt \int v_{\text{XC}}([\rho_t]; \mathbf{r}) \frac{\partial \rho_t(\mathbf{r})}{\partial t} d\mathbf{r}. \quad (1.58)$$

This last expression can be used to assign an energy to a given model potential without prior knowledge of the functional $E_{\text{XC}}[\rho]$.

Any reasonable parametrization ρ_t can be used with the line-integral formula of Eq. (1.58). The word “reasonable” means that the derivative $\partial \rho_t / \partial t$ exists for all values of t . In practice, it is convenient to perform line integration along paths of magnitude- or coordinate-scaled density. This allows one to have $v_{\text{XC}}([\rho_t]; \mathbf{r})$ in a closed form at any point along the integration path. We will now give several examples of such density transformations. The first example is the *linear* density scaling explored by Liu and Parr [47], Chan and Handy [48], and Nagy *et al.* [49]. We will call it the q -scaling,

$$\rho_q(\mathbf{r}) = q\rho(\mathbf{r}). \quad (1.59)$$

Another example is the *uniform* density scaling, which we will call the λ -scaling. This transformation, extensively studied by Levy [50], is defined by

$$\rho_\lambda(\mathbf{r}) = \lambda^3 \rho(\lambda \mathbf{r}). \quad (1.60)$$

Under the λ -scaling of the density, any valid *exchange* potential is homogeneous of degree one [51, 52]:

$$v_{\text{X}}([\rho_\lambda]; \mathbf{r}) = \lambda v_{\text{X}}([\rho]; \lambda \mathbf{r}). \quad (1.61)$$

The line integral of Eq. (1.58) expressed in terms of the λ -scaled exchange potential can be evaluated in closed form; the result is the Levy–Perdew virial relation [46, 53]

$$E_{\text{X}}[\rho] = \int v_{\text{X}}(\mathbf{r}) [3\rho(\mathbf{r}) + \mathbf{r} \cdot \nabla \rho(\mathbf{r})] d\mathbf{r}. \quad (1.62)$$

Finally, consider the density scaling proposed by Perdew and co-workers [54]. We will refer to it as the ζ -scaling,

$$\rho_\zeta(\mathbf{r}) = \zeta^2 \rho(\zeta^{1/3} \mathbf{r}). \quad (1.63)$$

The paths connecting the points $A = 0$ and $B = 1$ along the q -, λ -, and ζ -scaled densities are called, respectively, the Q-, Λ -, and Z-paths. Among these paths, only the Λ -path conserves the electron number. The number of electrons along the Q- and Z-paths changes as qN and ζN , respectively, where N is number of electrons in $\rho(\mathbf{r})$. Note that the condition $E_{\text{XC}}[\rho_A] = 0$ is trivially satisfied for the Q-path. For the Λ -path, $\rho_\lambda(\mathbf{r})$ becomes infinitely dilute (vanishes locally) as $\lambda \rightarrow 0$, so that

$\lim_{\lambda \rightarrow 0} E_{\text{XC}}[\rho_\lambda] = 0$ [50, 55, 56]. For the Z-path, both $\rho_\zeta(\mathbf{r})$ and $E_{\text{XC}}[\rho_\zeta]$ vanish in the $\zeta \rightarrow 0$ limit.

Partial derivatives of these scaled densities with respect to their scaling parameters are readily obtained by applying the chain rule of differentiation. For future reference, we write out the results:

$$\frac{\partial \rho_q(\mathbf{r})}{\partial q} = \rho(\mathbf{r}), \quad (1.64)$$

$$\frac{\partial \rho_\lambda(\mathbf{r})}{\partial \lambda} = \lambda^2 [3\rho(\lambda\mathbf{r}) + (\lambda\mathbf{r}) \cdot \nabla_{\lambda\mathbf{r}}\rho(\lambda\mathbf{r})], \quad (1.65)$$

$$\frac{\partial \rho_\zeta(\mathbf{r})}{\partial \zeta} = \zeta \left[2\rho(\zeta^{1/3}\mathbf{r}) + \frac{\zeta^{1/3}\mathbf{r}}{3} \cdot \nabla_{\zeta^{1/3}\mathbf{r}}\rho(\zeta^{1/3}\mathbf{r}) \right]. \quad (1.66)$$

We will now illustrate how Eq. (1.58) can be used to reconstruct exchange and correlation density functionals from the corresponding functional derivatives.

Local density approximation for exchange

According to Eq. (1.29), the LDA potential for exchange is given by

$$v_{\text{X}}^{\text{LDA}}([\rho]; \mathbf{r}) = -\frac{4}{3}C_{\text{X}}\rho^{1/3}(\mathbf{r}). \quad (1.67)$$

Suppose we did not know what functional generated this potential. Let us employ the line integral method to reconstruct this “unknown” functional.

Under the q -scaling of the density, the LDA exchange potential transforms as

$$v_{\text{X}}^{\text{LDA}}([\rho_q]; \mathbf{r}) = q^{1/3}v_{\text{X}}^{\text{LDA}}([\rho]; \mathbf{r}). \quad (1.68)$$

Multiplying this potential by $\partial \rho_q(\mathbf{r})/\partial q = \rho(\mathbf{r})$ and integrating over q we obtain the Q-reconstruction

$$E_{\text{X,Q}}^{\text{LDA}}[\rho] = \frac{3}{4} \int \rho(\mathbf{r})v_{\text{X}}^{\text{LDA}}([\rho]; \mathbf{r}) d\mathbf{r}, \quad (1.69)$$

which, in view of Eq. (1.67), is identical with $E_{\text{X}}^{\text{LDA}}[\rho]$ of Eq. (1.22).

Under the uniform density scaling, the LDA exchange potential transforms as

$$v_{\text{X}}^{\text{LDA}}([\rho_\lambda]; \mathbf{r}) = \lambda v_{\text{X}}^{\text{LDA}}([\rho]; \lambda\mathbf{r}). \quad (1.70)$$

Inserting the λ -scaled LDA potential into Eq. (1.58) we obtain the Λ -reconstruction:

$$E_{\text{X,\Lambda}}^{\text{LDA}}[\rho] = \int v_{\text{X}}^{\text{LDA}}([\rho]; \mathbf{r})[3\rho(\mathbf{r}) + \mathbf{r} \cdot \nabla\rho(\mathbf{r})] d\mathbf{r}, \quad (1.71)$$

which is just the Levy–Perdew relation of Eq. (1.62). It is not obvious, but can be proved by invoking the divergence theorem, that the value of $E_{X,\Lambda}^{\text{LDA}}[\rho]$ is equal to $E_{X,Q}^{\text{LDA}}[\rho]$ for any ρ vanishing at infinity. Numerical evaluation of the integrals of Eqs. (1.69) and (1.71) for test densities also confirms their equivalence [57].

Consider now the ζ -scaling of the LDA exchange potential

$$v_X^{\text{LDA}}([\rho_\zeta]; \mathbf{r}) = \zeta^{2/3} v_X^{\text{LDA}}([\rho]; \zeta^{1/3} \mathbf{r}). \quad (1.72)$$

Substitution of the ζ -scaled LDA exchange potential into the line integral formula yields

$$E_{X,Z}^{\text{LDA}}[\rho] = \int_0^1 d\zeta \int \zeta^{2/3} v_X^{\text{LDA}}([\rho]; \zeta^{1/3} \mathbf{r}) \zeta \left[2\rho(\zeta^{1/3} \mathbf{r}) + \frac{\zeta^{1/3} \mathbf{r}}{3} \cdot \nabla_{\zeta^{1/3} \mathbf{r}} \rho(\zeta^{1/3} \mathbf{r}) \right] d\mathbf{r}. \quad (1.73)$$

After the substitution $\zeta^{1/3} \mathbf{r} \rightarrow \mathbf{r}$ and integration over ζ we obtain the Z-reconstruction of the LDA:

$$E_{X,Z}^{\text{LDA}}[\rho] = \frac{3}{5} \int v_X^{\text{LDA}}([\rho]; \mathbf{r}) \left[2\rho(\mathbf{r}) + \frac{\mathbf{r}}{3} \cdot \nabla \rho(\mathbf{r}) \right] d\mathbf{r}. \quad (1.74)$$

This functional is actually a linear combination of the Q- and Λ -reconstructions, namely, $\frac{4}{5} E_{X,Q}^{\text{LDA}}[\rho] + \frac{1}{5} E_{X,\Lambda}^{\text{LDA}}[\rho]$, as can be seen by combining Eqs. (1.69) and (1.71). Since each of the Q- and Λ -reconstructions is numerically equivalent to $E_X^{\text{LDA}}[\rho]$, the value of $E_{X,Z}^{\text{LDA}}[\rho]$ is also equal to $E_X^{\text{LDA}}[\rho]$. Thus, Eqs. (1.69), (1.71), and (1.74) are different but equivalent representations of the same functional.

Local density approximation for correlation

Consider now the Wigner correlation functional

$$E_C^{\text{W}}[\rho] = - \int \frac{a\rho}{b + r_s} d\mathbf{r}, \quad (1.75)$$

where $r_s = (3/4\pi\rho)^{1/3}$ and $a = 0.44$ and $b = 7.8$ are constants. The functional derivative of $E_C^{\text{W}}[\rho]$ is

$$v_C^{\text{W}}([\rho]; \mathbf{r}) = -a \frac{b + (4/3)r_s(\mathbf{r})}{[b + r_s(\mathbf{r})]^2}, \quad (1.76)$$

where we have used the fact that $dr_s/d\rho = -r_s/3\rho$. Let us reconstruct the Wigner correlation functional from $v_C^{\text{W}}([\rho]; \mathbf{r})$ by using Eq. (1.58) and integrating the potential along three distinct density scaling paths.

The q -scaled Wigner correlation potential is

$$v_C^W([\rho_q]; \mathbf{r}) = -a \frac{b + (4/3)q^{-1/3}r_s(\mathbf{r})}{[b + q^{-1/3}r_s(\mathbf{r})]^2}. \quad (1.77)$$

The Q-reconstruction is, therefore,

$$E_{C,Q}^W[\rho] = -a \int d\mathbf{r} \rho(\mathbf{r}) \int_0^1 \frac{b + (4/3)q^{-1/3}r_s}{(b + q^{-1/3}r_s)^2} dq = - \int \frac{a\rho(\mathbf{r})}{b + r_s(\mathbf{r})} d\mathbf{r}, \quad (1.78)$$

which is precisely the original functional $E_C^W[\rho]$.

Under the uniform density scaling, the Wigner correlation potential transforms as

$$v_C^W([\rho_\lambda]; \mathbf{r}) = -a \frac{b + (4/3)\lambda^{-1}r_s(\lambda\mathbf{r})}{[b + \lambda^{-1}r_s(\lambda\mathbf{r})]^2}. \quad (1.79)$$

The line integral along the Λ -path can be written as

$$E_{C,\Lambda}^W[\rho] = -a \int_0^1 d\lambda \int \frac{b + (4/3)\lambda^{-1}r_s(\lambda\mathbf{r})}{[b + \lambda^{-1}r_s(\lambda\mathbf{r})]^2} [3\rho(\lambda\mathbf{r}) + (\lambda\mathbf{r}) \cdot \nabla_{\lambda\mathbf{r}}\rho(\lambda\mathbf{r})] \frac{d(\lambda\mathbf{r})}{\lambda}. \quad (1.80)$$

Changing the real-space integration variable $\lambda\mathbf{r} \rightarrow \mathbf{r}$ and integrating over λ we obtain the Λ -reconstruction of the Wigner functional

$$E_{C,\Lambda}^W[\rho] = -a \int \left[\frac{1}{b} \ln \frac{b + r_s}{r_s} + \frac{1}{3(b + r_s)} \right] [3\rho(\mathbf{r}) + \mathbf{r} \cdot \nabla\rho(\mathbf{r})] d\mathbf{r}. \quad (1.81)$$

Similarly, we have derived the Z-reconstruction

$$E_{C,Z}^W[\rho] = -a \int \left[\frac{1 - r_s/b - (3/2)(r_s/b)^2}{b + r_s} + \frac{3r_s^{3/2} \tan^{-1} \sqrt{b/r_s}}{2b^{5/2}} \right] \left[2\rho(\mathbf{r}) + \frac{\mathbf{r}}{3} \cdot \nabla\rho(\mathbf{r}) \right] d\mathbf{r}, \quad (1.82)$$

which, unlike the exchange functionals above, does not appear to be a linear combination of the Q- and Λ -reconstructions. However, numerical calculation [57] proves that the correlation energies obtained by Eqs. (1.81) and (1.82) are exactly the same as those obtained by Eq. (1.75).

1.4.3 Potentials that are not functional derivatives

Equation (1.58) was derived under the assumption that the parent functional $E_{XC}[\rho]$ for the potential v_{XC} actually exists. For any such potential, the line integration recovers the parent functional $E_{XC}[\rho]$ in which the energy density may have been

transformed to a new gauge determined by the choice of the integration path. It may happen, however, that a model potential does not have a parent functional, that is, it is not a functional derivative. In such a case, the energy obtained using Eq. (1.58) will in general depend on the particular integration path [46].

Consider, for example, the following model potential:

$$v_M([\rho]; \mathbf{r}) = \frac{|\nabla\rho(\mathbf{r})|}{\rho(\mathbf{r})}. \quad (1.83)$$

Is there a functional that generates this potential? We will show that the answer to this question is “no”.

Under the q -scaling, this potential is unchanged:

$$v_M([\rho_q]; \mathbf{r}) = \frac{|\nabla\rho_q|}{\rho_q} = v_M([\rho]; \mathbf{r}), \quad (1.84)$$

Therefore, the line integral along the Q-path is

$$I_Q = \int_0^1 dq \int v_M([\rho_q]; \mathbf{r}) \frac{\partial\rho_q(\mathbf{r})}{\partial q} d\mathbf{r} = \int |\nabla\rho(\mathbf{r})| d\mathbf{r}. \quad (1.85)$$

Under the uniform density scaling,

$$v_M([\rho_\lambda]; \mathbf{r}) = \frac{|\nabla\rho_\lambda|}{\rho_\lambda} = \lambda v_M([\rho]; \lambda\mathbf{r}), \quad (1.86)$$

so the line integral along the Λ -path is

$$I_\Lambda = \int_0^1 d\lambda \int v_M([\rho_\lambda]; \mathbf{r}) \frac{\partial\rho_\lambda(\mathbf{r})}{\partial\lambda} d\mathbf{r} = \int \frac{|\nabla\rho(\mathbf{r})|}{\rho(\mathbf{r})} [3\rho(\mathbf{r}) + \mathbf{r} \cdot \nabla\rho(\mathbf{r})] d\mathbf{r}. \quad (1.87)$$

Finally, under the ζ -scaling

$$v_M([\rho_\zeta]; \mathbf{r}) = \frac{|\nabla\rho_\zeta(\mathbf{r})|}{\rho_\zeta(\mathbf{r})} = \zeta^{1/3} v_M([\rho]; \zeta^{1/3}\mathbf{r}), \quad (1.88)$$

and the line integral along the Z-path is

$$I_Z = \int_0^1 d\zeta \int v_M([\rho_\zeta]; \mathbf{r}) \frac{\partial\rho_\zeta(\mathbf{r})}{\partial\zeta} d\mathbf{r} = \frac{3}{4} \int \frac{|\nabla\rho(\mathbf{r})|}{\rho(\mathbf{r})} \left[2\rho(\mathbf{r}) + \frac{\mathbf{r}}{3} \cdot \nabla\rho(\mathbf{r}) \right] d\mathbf{r}. \quad (1.89)$$

It is easy to see that the three reconstructions are related to each other: $I_Z = \frac{3}{4}I_Q + \frac{1}{4}I_\Lambda$. Numerical evaluation of the three integrals given by Eqs. (1.85), (1.87), and (1.89)

yields different values [57]. Therefore, the quantity defined by Eq. (1.83) is not a functional derivative of any density functional with respect to $\rho(\mathbf{r})$.

Let us introduce new terminology. We will call the model potential *integrable* if it has a parent functional. If a model potential is not a functional derivative of any density functional, we will call it *non-integrable* or *stray*. The outcome of line integration depends on whether the potential is integrable or not. If $v_{\text{XC}}(\mathbf{r})$ is integrable, the line integration recovers the parent functional E_{XC} . If $v_{\text{XC}}(\mathbf{r})$ is stray, then the line integral is path-dependent, which means that the energy assigned to that potential is not unique.

The issue of stray potentials is closely related to the problem of incomplete differentials from the ordinary calculus [58]. Consider a well-behaved function $f(x, y)$. The total differential of f has the form

$$df = P(x, y) dx + Q(x, y) dy, \quad (1.90)$$

where

$$P(x, y) \equiv \frac{\partial f(x, y)}{\partial x} \quad \text{and} \quad Q(x, y) \equiv \frac{\partial f(x, y)}{\partial y}. \quad (1.91)$$

According to the theorem on the symmetry of second mixed derivatives, the functions $P(x, y)$ and $Q(x, y)$ are related to each other via the condition

$$\frac{\partial P(x, y)}{\partial y} \equiv \frac{\partial^2 f(x, y)}{\partial x \partial y} = \frac{\partial^2 f(x, y)}{\partial y \partial x} \equiv \frac{\partial Q(x, y)}{\partial x}. \quad (1.92)$$

The complete differential df of Eq. (1.90) has a special property: Line integration of df along an arbitrary path C from (x_1, y_1) to (x_2, y_2) *always* yields [58]

$$\int_C df = \int_C P(x, y) dx + \int_C Q(x, y) dy = f(x_2, y_2) - f(x_1, y_1). \quad (1.93)$$

Assume for a while that we have not derived the functions P and Q using Eq. (1.91) but rather, approximated them directly. If the model functions P and Q are such that Eq. (1.92) does not hold, the sum $P(x, y) dx + Q(x, y) dy$ is not a complete differential. Line integration of this sum will depend on the particular choice of the path C [58].

The situation described above is analogous to what happens when the model Kohn–Sham potential is stray. Recall that the differential of a functional [Eq. (1.26)] is a generalization of a differential of a multivariable function [Eq. (1.27)]. In this light, the potential $v(\mathbf{r}) \equiv \delta F[\rho]/\delta \rho(\mathbf{r})$ is equivalent to a *set* of partial derivatives $\partial f/\partial x_i$. In calculus of variations, there exists a condition for integrability similar to

Eq. (1.92),

$$\frac{\delta v([\rho]; \mathbf{r})}{\delta \rho(\mathbf{r}')} = \frac{\delta v([\rho]; \mathbf{r}')}{\delta \rho(\mathbf{r})}. \quad (1.94)$$

This relation was first stated by Volterra [5] and subsequently introduced into density functional theory by Ou-Yang and Levy [52]. Stray model potentials do not satisfy Eq. (1.94). As a result, expression for $\delta F[\rho]$ of Eq. (1.26) evaluated with stray potentials is *not* a complete differential, and the line integral of Eq. (1.58) depends on an integration path.

1.4.4 Problems of non-integrable model potentials

Path-dependence of the line integral is not the only problem of stray model potentials. Recall that the Kohn–Sham equations (1.12) minimize the total energy functional $E[\rho]$ given by Eq. (1.11). If the exchange–correlation potential in Eq. (1.12) is not a functional derivative, the Kohn–Sham equations do not represent a solution to any implied energy minimization problem. As a result, the density constructed from the converged Kohn–Sham orbitals $\phi_i(\mathbf{r})$ does not correspond to the true minimum of the energy. This means that stray potentials cannot be used for molecular geometry optimizations [59–61] because the point where the forces acting on the nuclei vanish will not coincide with the energy minimum [59].

Furthermore, energies assigned to model potentials often lack translational and rotational invariance. Consider the Levy–Perdew virial relation of Eq. (1.62), the usual energy expression used for model exchange potentials. Integration of the virial relation by parts yields an equivalent form

$$E_X[\rho] = - \int \rho(\mathbf{r}) \mathbf{r} \cdot \nabla v_X([\rho]; \mathbf{r}) d\mathbf{r}. \quad (1.95)$$

Suppose we displace a molecule from its original position by $-\mathbf{R}$, so that the density $\rho(\mathbf{r})$ becomes $\rho'(\mathbf{r}) = \rho(\mathbf{r} + \mathbf{R})$. Exchange energy evaluated for a displaced molecule using Eq. (1.95) is

$$E_X[\rho'] = - \int \rho(\mathbf{r} + \mathbf{R}) \mathbf{r} \cdot \nabla_{\mathbf{r}} v_X([\rho]; \mathbf{r} + \mathbf{R}) d\mathbf{r}. \quad (1.96)$$

After the variable substitution $\mathbf{r}' = \mathbf{r} + \mathbf{R} \rightarrow \mathbf{r}$, we can rewrite the expression above as

$$E_X[\rho'] = E_X[\rho] + \mathbf{R} \cdot \int \rho(\mathbf{r}) \nabla v_X([\rho]; \mathbf{r}) d\mathbf{r}. \quad (1.97)$$

Translational invariance requires that the second term on the right-hand side of Eq. (1.97) vanish for an arbitrary \mathbf{R} . This is possible only if, for every ρ ,

$$\int \rho(\mathbf{r}) \nabla v_X([\rho]; \mathbf{r}) d\mathbf{r} = 0, \quad (1.98)$$

or, after integration by parts,

$$\int v_X([\rho]; \mathbf{r}) \nabla \rho(\mathbf{r}) d\mathbf{r} = 0. \quad (1.99)$$

Similar expression also exists for the invariance of the virial energy with respect to arbitrary rotations of the molecule,

$$\int v_X([\rho]; \mathbf{r}) \mathbf{r} \times \nabla \rho(\mathbf{r}) d\mathbf{r} = 0. \quad (1.100)$$

The relations (1.98)–(1.100) are known in the literature as the “zero-force” and “zero-torque” conditions on the density [53]. They are automatically satisfied if $v_X([\rho]; \mathbf{r})$ is a functional derivative of some translationally and rotationally invariant energy functional, but are violated if the potential is stray. As a result, the virial energies corresponding to stray model potentials depend on the position of the molecule with respect to the coordinate axes. No such problems exist for integrable potentials that originate from some density functional.

Finally, even when the total energy is not needed (e.g., in time-dependent density functional theory), use of stray potentials can still result in artifacts such as spurious self-excitations of the system [62]. Other response properties, e.g. molecular polarizabilities, are also affected by the integrability of model potentials [63]. All this means that one needs to have reliable methods to detect stray potentials and to construct integrable model potentials directly.

1.5 Objectives of the study

The purpose of my graduate research was twofold. First, we wanted to develop a method to identify and “repair” stray model potentials (i.e., make them integrable), and be able to construct integrable potentials directly. Second, we wanted to design accurate potential approximations and using them, improve prediction of molecular response properties. This thesis describes some of our results achieved to this end.

In Chapter 2, we propose a set of numerical tests to identify stray potentials. In

Chapter 3, we investigate the structure of functional derivatives of density-dependent approximations and, guided by this information, propose a practical procedure for constructing integrable model potentials. Chapter 4 discusses a modification of this approach to avoid the explicit reference to the density functional. In Chapter 5, we propose a novel application of the line-integration technique for the development of density functionals from stray model potentials. Finally, in Chapter 6, we develop a correction scheme for functional derivatives of standard density functionals. Our correction scheme effectively generates model potentials *on the fly*.

Bibliography

- [1] P. Hohenberg and W. Kohn, “Inhomogeneous electron gas”, *Phys. Rev.* **136**, B864 (1964).
- [2] W. Koch and M. C. Holthausen, *A Chemist’s Guide to Density Functional Theory*, Wiley, New York, 2nd ed. (2001).
- [3] G. E. Scuseria and V. N. Staroverov, “Progress in the development of exchange-correlation functionals”, in *Theory and Applications of Computational Chemistry: The First Forty Years*, edited by C. E. Dykstra, G. Frenking, K. S. Kim, and G. E. Scuseria, Elsevier, Amsterdam (2005).
- [4] W. Kohn and L. J. Sham, “Self-consistent equations including exchange and correlation effects”, *Phys. Rev.* **140**, A1133 (1965).
- [5] V. Volterra, *Theory of Functionals and of Integral and Integro-Differential Equations*, Dover Publications, Inc., New York (1959).
- [6] M. M. Vainberg, *Variational Methods for the Study of Nonlinear Operators*, Holden-Day, San Francisco (1964).
- [7] E. Engel and R. M. Dreizler, *Density Functional Theory: An Advanced Course*, Springer, Berlin (2011).
- [8] A. D. Becke, “Density-functional exchange-energy approximation with correct asymptotic behavior”, *Phys. Rev. A* **38**, 3098 (1988).
- [9] J. P. Perdew, K. Burke, and M. Ernzerhof, “Generalized gradient approximation made simple”, *Phys. Rev. Lett.* **77**, 3865 (1996).
- [10] J. Tao, J. P. Perdew, V. N. Staroverov, and G. E. Scuseria, “Climbing the density functional ladder: Nonempirical meta-generalized gradient approximation designed for molecules and solids”, *Phys. Rev. Lett.* **91**, 146401 (2003).

- [11] C. Filippi, X. Gonze, and C. J. Umrigar, “Generalized gradient approximations to density functional theory: Comparison with exact results”, in *Recent Developments and Applications of Modern Density Functional Theory, Theoretical and Computational Chemistry*, Vol. 4, edited by J. M. Seminario, Elsevier, pp. 295–326 (1996).
- [12] R. van Leeuwen and E. J. Baerends, “Exchange-correlation potential with correct asymptotic behavior”, *Phys. Rev. A* **49**, 2421 (1994).
- [13] J. C. Slater, “A simplification of the Hartree–Fock method”, *Phys. Rev.* **81**, 385 (1951).
- [14] N. Umezawa, “Explicit density-functional exchange potential with correct asymptotic behavior”, *Phys. Rev. A* **74**, 032505 (2006).
- [15] J. B. Krieger, Y. Li, and G. J. Iafrate, “Construction and application of an accurate local spin-polarized Kohn–Sham potential with integer discontinuity: Exchange-only theory”, *Phys. Rev. A* **45**, 101 (1992).
- [16] O. Gritsenko, R. van Leeuwen, E. van Lenthe, and E. J. Baerends, “Self-consistent approximation to the Kohn–Sham exchange potential”, *Phys. Rev. A* **51**, 1944 (1995).
- [17] A. D. Becke and E. R. Johnson, “A simple effective potential for exchange”, *J. Chem. Phys.* **124**, 221101 (2006).
- [18] V. N. Staroverov, “A family of model Kohn–Sham potentials for exact exchange”, *J. Chem. Phys.* **129**, 134103 (2008).
- [19] D. J. Tozer and N. C. Handy, “Improving virtual Kohn–Sham orbitals and eigenvalues: Application to excitation energies and static polarizabilities”, *J. Chem. Phys.* **109**, 10180 (1998).
- [20] M. E. Casida and D. R. Salahub, “Asymptotic correction approach to improving approximate exchange-correlation potentials: Time-dependent density-functional theory calculations of molecular excitation spectra”, *J. Chem. Phys.* **113**, 8918 (2000).
- [21] M. E. Casida, C. Jamorski, K. C. Casida, and D. R. Salahub, “Molecular excitation energies to high-lying bound states from time-dependent density-functional

- response theory: Characterization and correction of the time-dependent local density approximation ionization threshold”, *J. Chem. Phys.* **108**, 4439 (1998).
- [22] P. R. T. Schipper, O. V. Gritsenko, S. J. A. van Gisbergen, and E. J. Baerends, “Molecular calculations of excitation energies and (hyper)polarizabilities with a statistical average of orbital model exchange-correlation potentials”, *J. Chem. Phys.* **112**, 1344 (2000).
- [23] E. Fermi and E. Amaldi, *Acad. Ital. Rome* **6**, 117 (1934).
- [24] R. Parr and S. Ghosh, “Toward understanding the exchange-correlation energy and total-energy density functionals”, *Phys. Rev. A* **51**, 3564 (1995).
- [25] P. W. Ayers, R. C. Morrison, and R. G. Parr, “Fermi–Amaldi model for exchange-correlation: atomic excitation energies from orbital energy differences”, *Mol. Phys.* **103**, 2061 (2005).
- [26] G. B. Arfken and H. J. Weber, *Mathematical Methods for Physicists*, Academic Press, San Diego, 6th ed. (2005).
- [27] M. Grüning, O. V. Gritsenko, S. J. A. van Gisbergen, and E. J. Baerends, “Shape corrections to exchange-correlation potentials by gradient-regulated seamless connection of model potentials for inner and outer region”, *J. Chem. Phys.* **114**, 652 (2001).
- [28] J. P. Perdew and A. Zunger, “Self-interaction correction to density-functional approximations for many-electron systems”, *Phys. Rev. B* **23**, 5048 (1981).
- [29] J. P. Perdew and S. Kurth, “Density functionals for non-relativistic Coulomb systems in the new century”, in *A Primer in Density Functional Theory*, edited by C. Fiolhais, F. Nogueira, and M. Marques, Springer, Berlin (2003).
- [30] A. Lembarki, F. Rogemond, and H. Chermette, “Gradient-corrected exchange potential with the correct asymptotic behavior and the corresponding exchange-energy functional obtained from the virial theorem”, *Phys. Rev. A* **52**, 3704 (1995).
- [31] S. H. Vosko, L. Wilk, and M. Nusair, “Accurate spin-dependent electron liquid correlation energies for local spin density calculations: A critical analysis”, *Can. J. Phys.* **58**, 1200 (1980).

- [32] J. D. Talman and W. F. Shadwick, “Optimized effective atomic central potential”, *Phys. Rev. A* **14**, 36 (1976).
- [33] W. Yang and Q. Wu, “Direct method for optimized effective potentials in density-functional theory”, *Phys. Rev. Lett.* **89**, 143002 (2002).
- [34] S. Ivanov, S. Hirata, and R. J. Bartlett, “Finite-basis-set optimized effective potential exchange-only method”, *J. Chem. Phys.* **116**, 1269 (2002).
- [35] V. N. Staroverov, G. E. Scuseria, and E. R. Davidson, “Optimized effective potentials yielding Hartree–Fock energies and densities”, *J. Chem. Phys.* **124**, 141103 (2006).
- [36] E. Räsänen, S. Pittalis, and C. R. Proetto, “Universal correction for the Becke–Johnson exchange potential”, *J. Chem. Phys.* **132**, 044112 (2010).
- [37] R. G. Parr and W. Yang, *Density–Functional Theory of Atoms and Molecules*, Oxford University Press, New York (1989).
- [38] F. Della Sala and A. Görling, “Efficient localized Hartree–Fock methods as effective exact-exchange Kohn–Sham methods for molecules”, *J. Chem. Phys.* **115**, 5718 (2001).
- [39] M. Grüning, O. V. Gritsenko, and E. J. Baerends, “Exchange potential from the common energy denominator approximation for the Kohn–Sham Green’s function: Application to (hyper)polarizabilities of molecular chains”, *J. Chem. Phys.* **116**, 6435 (2002).
- [40] V. N. Staroverov, G. E. Scuseria, and E. R. Davidson, “Effective local potentials for orbital-dependent density functionals”, *J. Chem. Phys.* **125**, 081104 (2006).
- [41] A. Kananenka, S. V. Kohut, A. P. Gaiduk, I. G. Ryabinkin, and V. N. Staroverov, “Generation of model potentials using the Kohn–Sham inversion procedure”, manuscript in preparation.
- [42] O. V. Gritsenko, R. van Leeuwen, and E. J. Baerends, “Molecular exchange-correlation Kohn–Sham potential and energy density from *ab initio* first- and second-order density matrices: Examples for XH (X=Li, B, F)”, *J. Chem. Phys.* **104**, 8535 (1996).
- [43] R. A. King and N. C. Handy, “Kinetic energy functionals from the Kohn–Sham potential”, *Phys. Chem. Chem. Phys.* **2**, 5049 (2000).

- [44] A. Szabo and N. S. Ostlund, *Modern Quantum Chemistry: Introduction to Advanced Electronic Structure Theory*, Macmillan Publishing Co., Inc., New York (1982).
- [45] R. van Leeuwen, *Kohn–Sham Potentials in Density Functional Theory*, Ph.D. thesis, Vrije Universiteit Amsterdam (1994).
- [46] R. van Leeuwen and E. J. Baerends, “Energy expressions in density-functional theory using line integrals”, *Phys. Rev. A* **51**, 170 (1995).
- [47] S. Liu and R. G. Parr, “Expansion of the correlation-energy density functional $E_c[\rho]$ and its kinetic-energy component $T_c[\rho]$ in terms of homogeneous functionals”, *Phys. Rev. A* **53**, 2211 (1996).
- [48] G. K.-L. Chan and N. C. Handy, “Kinetic-energy systems, density scaling, and homogeneity relations in density-functional theory”, *Phys. Rev. A* **59**, 2670 (1999).
- [49] Á. Nagy, “Density scaling and exchange-correlation energy”, *J. Chem. Phys.* **123**, 044105 (2005).
- [50] M. Levy, “Coordinate scaling requirements for approximating exchange and correlation”, in *Density Functional Theory*, edited by E. K. U. Gross and R. M. Dreizler, Plenum Press, New York, pp. 11–31 (1995).
- [51] H. Ou-Yang and M. Levy, “Theorem for exact local exchange potential”, *Phys. Rev. Lett.* **65**, 1036 (1990).
- [52] H. Ou-Yang and M. Levy, “Theorem for functional derivatives in density-functional theory”, *Phys. Rev. A* **44**, 54 (1991).
- [53] M. Levy and J. P. Perdew, “Hellmann–Feynman, virial, and scaling requisites for the exact universal density functionals. Shape of the correlation potential and diamagnetic susceptibility for atoms”, *Phys. Rev. A* **32**, 2010 (1985).
- [54] J. P. Perdew, L. A. Constantin, and E. Sagvolden, “Relevance of the slowly varying electron gas to atoms, molecules, and solids”, *Phys. Rev. Lett.* **97**, 223002 (2006).
- [55] M. Levy, “Density-functional exchange correlation through coordinate scaling in adiabatic connection and correlation hole”, *Phys. Rev. A* **43**, 4637 (1991).

- [56] R. van Leeuwen, O. V. Gritsenko, and E. J. Baerends, “Analysis and modelling of atomic and molecular Kohn–Sham potentials”, *Top. Curr. Chem.* **180**, 107 (1996).
- [57] A. P. Gaiduk, S. K. Chulkov, and V. N. Staroverov, “Reconstruction of density functionals from Kohn–Sham potentials by integration along density scaling paths”, *J. Chem. Theory Comput.* **5**, 699 (2009).
- [58] H. Margenau and G. M. Murphy, *The Mathematics of Physics and Chemistry*, D. Van Nostrand Company, Inc., New York, 2nd ed. (1943).
- [59] R. Neumann, R. H. Nobes, and N. C. Handy, “Exchange functionals and potentials”, *Mol. Phys.* **87**, 1 (1996).
- [60] D. J. Tozer, “The asymptotic exchange potential in Kohn–Sham theory”, *J. Chem. Phys.* **112**, 3507 (2000).
- [61] H. Chermette, A. Lembarki, H. Razafinjanahary, and F. Rogemond, “Gradient-corrected exchange potential functional with the correct asymptotic behaviour”, *Adv. Quantum Chem.* **33**, 105 (1999).
- [62] M. Mundt, S. Kümmel, R. van Leeuwen, and P.-G. Reinhard, “Violation of the zero-force theorem in the time-dependent Krieger–Li–Iafrate approximation”, *Phys. Rev. A* **75**, 050501(R) (2007).
- [63] A. Karolewski, R. Armiento, and S. Kümmel, “Polarizabilities of polyacetylene from a field-counteracting semilocal functional”, *J. Chem. Theory Comput.* **5**, 712 (2009).

Chapter 2

Tests for functional derivatives

2.1 Introduction

An attractive alternative to pursuing the functional $E_{XC}[\rho]$ of Eq. (1.11) is to approximate the potential $v_{XC}([\rho]; \mathbf{r})$ of Eq. (1.16) directly with the Kohn–Sham orbitals, which gives rise to the potential-driven density functional theory. However, a model exchange–correlation potential may be stray, that is, not a functional derivative of any functional. Stray model potentials produce a number of unphysical artifacts discussed in Sec. 1.4.4.

Several workers have devised analytical and numerical criteria [1–4] to test the integrability of model potentials. For example, Ou–Yang and Levy examined translation symmetry properties of the Slater potential [5] and found that it is not a functional derivative [2], while Karolewski *et al.* [4] demonstrated that the Becke–Johnson potential [6] is stray by comparing the polarizabilities of polyacetylene fragments computed using different methods. More generally, it has been remarked that approximate potentials are usually not functional derivatives [7].

The present work is a concentrated effort to address the problem of stray potentials in a general way. Our approach is to identify a few necessary conditions for a functional derivative that can be turned into straightforward numerical tests and then to apply these tests to actual model Kohn–Sham potentials.

Reprinted in part with permission from **A. P. Gaiduk** and V. N. Staroverov, “Virial exchange energies from model exact-exchange potentials”, *J. Chem. Phys.* **128**, 204101 (2008). Copyright 2008, American Institute of Physics.

Reprinted in part with permission from **A. P. Gaiduk** and V. N. Staroverov, “How to tell when a model Kohn–Sham potential is not a functional derivative”, *J. Chem. Phys.* **131**, 044107 (2009). Copyright 2009, American Institute of Physics.

2.2 Methodology

In this section, we discuss analytic properties that distinguish functional derivatives from stray potentials and formulate three numerical tests for stray potentials.

2.2.1 Self-consistent-field convergence test

In the functional-driven approach, the functional $E_{\text{XC}}[\rho]$ is known from the outset while the potential $v_{\text{XC}}(\mathbf{r})$ is determined as the functional derivative of $E_{\text{XC}}[\rho]$. The iterative solution of the Kohn–Sham equations with integrable $v_{\text{XC}}(\mathbf{r})$ is variational, and the self-consistent-field (SCF) energy is strictly lower than any intermediate energy. If, by contrast, the exchange–correlation potential is stray, then the Kohn–Sham equations do not solve any implied energy minimization problem and the orbitals $\phi_i(\mathbf{r})$ do not necessarily yield the lowest energy. In practice, this means that some intermediate values of $E[\rho]$ during the iterative solution of Eq. (1.12) could be below the energy at convergence.

These arguments lead us to our first test for stray potentials: If in any iteration of the SCF procedure the total energy obtained from a Kohn–Sham potential is lower than at convergence, the potential is not a functional derivative. Of course, an abnormal convergence pattern may simply indicate that the energy converges to an excited state (i.e., a local minimum). However, if this abnormality is not a remediable SCF convergence problem, then the trial potential $v_{\text{XC}}(\mathbf{r})$ does not have a parent functional.

2.2.2 Line-integral test

The line-integral method provides a solution to the inverse problem of functional differentiation [3]. In this method, the difference between two values of $E_{\text{XC}}[\rho]$ at arbitrary densities ρ_A and ρ_B is obtained as a line integral along a path of parametrized densities ρ_t connecting ρ_A and ρ_B . If the parametrization is such that $E_{\text{XC}}[\rho_A] = 0$ and $\rho_B = \rho$, then the line integral can be written as Eq. (1.58).

The value of the line integral can be easily evaluated for a given model potential $v_{\text{XC}}([\rho]; \mathbf{r})$, which provides a convenient way to calculate the exchange–correlation energy corresponding to the unknown functional. If the model potential is a functional derivative, then any reconstruction of the functional yields the same value. If, however, the potential is stray, then the line integrals along different paths yield different energies. In this work, we employ the line-integral method as a test for stray po-

tentials. We recover density functionals from model potentials using the formula of Eq. (1.58) along the Q-, Λ - and Z-paths given by Eqs. (1.59), (1.60), and (1.63), and compare the integrals. If the values of the integrals are not the same, the potential is stray.

The line-integral test is limited only to the potentials that explicitly depend on the electron density and its derivatives. This leaves out a wide and important class of potentials constructed from the Kohn–Sham orbitals and eigenvalues [8, 9]. We address this problem and propose a similar test applicable to orbital-dependent potentials in the following subsection.

2.2.3 Virial-energy test for exact-exchange potentials

Almost all approximate exact-exchange potentials (Sec. 1.4.1) depend on the Kohn–Sham orbitals, and it is not possible to assign the line-integral energy to them along an arbitrary path. Luckily, under the λ -scaling of the density [Eq. (1.60)], exchange potentials satisfy the relation of Eq. (1.61), and the line integration can be accomplished analytically to give the Levy–Perdew virial relation of Eq. (1.62).

This means that there are at least two energy expressions for model exact-exchange potentials at our disposal: (i) the “parent” EXX functional given by Eq. (1.47) and (ii) the Levy–Perdew formula of Eq. (1.62). This suggests another straightforward test for functional derivatives: Compare the energies assigned to a model potential using the conventional exact-exchange functional and the Levy–Perdew virial relation. If a model potential $v_X(\mathbf{r})$ descends from the functional of Eq. (1.47), the energies evaluated using these two methods will be the same. Of course, the virial-energy test is useful only for approximate exchange potentials but not for the full exchange-correlation potential. This does not matter in practice because the few exchange-correlation model potentials existing today [10–12] are density-dependent, and can be examined using the line-integral test. From our experience, virial-energy and line-integral tests complement each other.

2.2.4 Zero-force and zero-torque tests

Any physically reasonable approximation to the exchange-correlation functional must be invariant with respect to translation and rotation of the density. Levy and Perdew [13] and, independently, van Leeuwen and Baerends [3] found that functional derivatives of invariant functionals satisfy two static-equilibrium conditions of “no net external force” and “no net external torque” on the density. These conditions, also

referred to as the “zero-force” and “zero-torque” theorems [14], are formulated as two vector identities, $\int \rho(\mathbf{r}) \nabla v_{\text{XC}}(\mathbf{r}) d\mathbf{r} = 0$ and $\int \rho(\mathbf{r}) \mathbf{r} \times \nabla v_{\text{XC}}(\mathbf{r}) d\mathbf{r} = 0$. Integration by parts yields more convenient Eqs. (1.99) and (1.100). The zero-force and zero-torque conditions can be derived either by invoking the Hellmann–Feynman theorem [13] or by evaluating the line integral along the path taken as a simple translation or rotation of the density [3].

The identities of Eqs. (1.99) and (1.100) can also be used to examine the properties of a potential v_{XC} . It follows from the careful analysis of van Leeuwen and Baerends that if the zero-force and zero-torque theorems do not hold for an approximate v_{XC} , then either (i) the potential does not have the translational and rotational invariance or (ii) it is not a functional derivative [3]. In fact, if v_{XC} does not explicitly depend on the position vector \mathbf{r} , then the possibility (i) can be safely rejected, which in turn means that the potential is not a functional derivative.

Using these arguments, we employ the zero-force and zero-torque theorems as a test for stray potentials. We evaluate the integrals of Eqs. (1.99) and (1.100) with a model potential, and if they do not vanish, we conclude that the model potential is not a functional derivative.

2.3 Results and discussion

From the tests described in Sec. 2.2, only the zero-force theorem has been used to identify stray potentials [2, 7] prior to this study. The other tests have been formulated and developed in our work. We have applied our tests to the Fermi–Amaldi, Umezawa, van Leeuwen–Baerends, Slater, Becke–Johnson, Staroverov, and the ϵ -consistent potentials described in Sec. 1.4.1. For simplicity, we did not include the LDA for correlation (which *is* a functional derivative) in the Umezawa and the van Leeuwen–Baerends models.

For comparison purposes, we also tested several potentials that are *a priori* known to be functional derivatives. The integrable potentials were derived from the LDA, Gill (G96) [15], and Becke (B88) [16] exchange functionals using the expression of Eq. (1.34) for a functional derivative of explicitly density-dependent functionals.

All calculations were performed in an appropriately modified development version of the GAUSSIAN program [17]. In all occurrences, the Slater potential was obtained by the finite-basis-set resolution-of-the-identity technique of Ref. 18 as described in Ref. 19. Because this method is exact only in the complete basis set limit, large uncontracted basis sets were used to minimize numerical errors [19]. In addition,

the potential of Staroverov required special handling because it involves a highly oscillatory gradient $\nabla\tau$ from $|\nabla k_{\text{BJ}}^2|^2$. These oscillations are large enough to cause a noticeable error in the potential and in the exchange energy. To reduce this error, we used the prescription of Ref. 20 and set

$$\frac{|\nabla k_{\text{BJ}}^2|^2}{k_{\text{BJ}}^5} = 0 \quad \text{if} \quad r < \frac{1}{10Z}, \quad (2.1)$$

where Z is the charge of the nucleus. This cutoff introduces only a negligible error and would be unnecessary in codes employing Slater-type basis functions.

2.3.1 SCF convergence pattern

The self-consistent-field convergence test can be applied to any potential for which one can easily obtain the energy. In the potential-driven approach to DFT, the parent functional is not known, so the exchange-correlation contribution to the total energy should be evaluated as a line integral. When a potential scales like Eq. (1.61), which is the case for the Fermi–Amaldi potential and the exchange parts of the Umezawa and van Leeuwen–Baerends models, the line integral along the Λ -path reduces to the Levy–Perdew relation of Eq. (1.62). We used Levy–Perdew relation to compute the energy from these and other (exact-exchange) model potentials. For consistency, we initialized all SCF calculations with converged Hartree–Fock orbitals.

Fig. 2.1 shows typical SCF convergence patterns observed during an iterative solution of the Kohn–Sham equations in which the exchange-correlation potentials are functional derivatives. The total energy approaches the minimum strictly from above and the convergence behavior is generally monotonic. We note that monotonicity is not a requirement for a functional derivative. It is essential that the total energy is never below its lowest (converged) value. Conversely, Fig. 2.2 shows that the total energies obtained from the model potentials of van Leeuwen and Baerends, Umezawa, Slater, Becke and Johnson oscillate during the convergence and at some points are actually *below* the converged values. The SCF solutions obtained with these model potentials do not appear to be excited states because all our attempts to obtain a lower energy and tweak the SCF procedure into the same convergence behavior as in Fig. 2.1 (by using different initial guesses, turning on and off the DIIS, applying level shifting and other SCF convergence controls) have been unsuccessful. The dipping below the minimum in each of the panels of Fig. 2.2 strongly suggests that the van Leeuwen–Baerends, Umezawa, Slater, and Becke–Johnson potentials are stray.

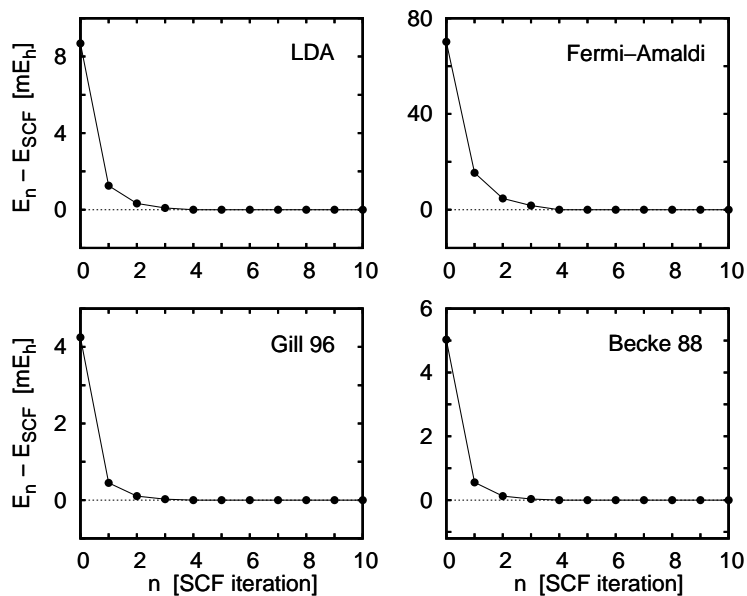


Figure 2.1: Convergence of the total energy during the iterative self-consistent-field solution of the Kohn–Sham equations with the functional derivatives of the LDA, Gill, Becke exchange functionals, and Fermi–Amaldi model potential. All calculations are performed for a Mg atom in the cc-pVQZ basis set starting from the HF/cc-pVQZ density. The direct inversion in the iterative subspace (DIIS) [21] is turned off. The convergence pattern “from above” is consistent with the fact that the potentials are functional derivatives.

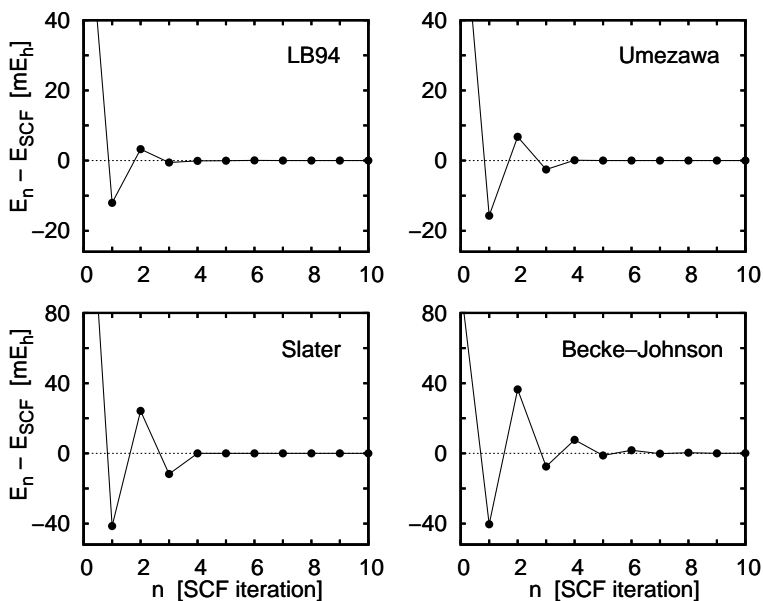


Figure 2.2: Same as Fig. 2.1 but for the model potentials of van Leeuwen–Baerends, Umezawa, Slater, and Becke–Johnson. The oscillatory convergence pattern indicates that the tested potentials are not functional derivatives.

2.3.2 Path dependence of the line integral

As explained in Sec. 2.2.2, the line-integral test cannot be easily applied to orbital-dependent models such as that of Slater, Becke–Johnson, etc. For this reason, we shall use this test only with the Fermi–Amaldi, and the exchange parts of the van Leeuwen–Baerends and Umezawa potentials.

First, let us write out general formulas for the line integrals along the Q-, Λ - and Z-paths, which hold for all three potentials. For the Q-path, we have

$$E_{X,Q}[\rho] = \int d\mathbf{r} \rho(\mathbf{r}) \int_0^1 dq v_X([\rho_q]; \mathbf{r}). \quad (2.2)$$

Under the uniform scaling of the density, all the potentials tested transform as Eq. (1.61), so the integral over the parameter λ in the expression

$$E_{X,\Lambda}[\rho] = \int d\mathbf{r} [3\rho(\mathbf{r}) + \mathbf{r} \cdot \nabla\rho(\mathbf{r})] \int_0^1 \frac{d\lambda}{\lambda} v_X([\rho_\lambda]; \frac{\mathbf{r}}{\lambda}) \quad (2.3)$$

becomes the Levy–Perdew virial relation of Eq. (1.62). Finally, the line integral along the Z-path can be written as

$$E_{X,Z}[\rho] = \int d\mathbf{r} \left[2\rho(\mathbf{r}) + \frac{\mathbf{r}}{3} \cdot \nabla\rho(\mathbf{r}) \right] \int_0^1 d\zeta v_X \left([\rho_\zeta]; \frac{\mathbf{r}}{\zeta^{1/3}} \right), \quad (2.4)$$

where the quantity $v_X([\rho_\zeta]; \zeta^{-1/3}\mathbf{r})$ means the original potential v_X written in terms of the density $\zeta^2\rho(\mathbf{r})$.

Fermi–Amaldi potential has a simple dependence on the density $\rho(\mathbf{r})$, so the integrals over the scaling parameters in Eqs. (2.2) and (2.4) can be evaluated analytically. Assuming that N is fixed, we get for the Q-path

$$E_{X,Q}^{\text{FA}}[\rho] = \frac{1}{2} \int \rho(\mathbf{r}) v_X^{\text{FA}}(\mathbf{r}) d\mathbf{r} \quad (2.5)$$

and for the Z-path,

$$E_{X,Z}^{\text{FA}}[\rho] = \frac{3}{7} \int \left[2\rho(\mathbf{r}) + \frac{\mathbf{r}}{3} \cdot \nabla\rho(\mathbf{r}) \right] v_X^{\text{FA}}(\mathbf{r}) d\mathbf{r}. \quad (2.6)$$

We calculated these line integrals with the Fermi–Amaldi, van Leeuwen–Baerends, and Umezawa potentials for several atoms and molecules. The results of our calculations are presented in Table 2.1. The line integrals evaluated with the Fermi–Amaldi potential along different paths all have the same energy. This happens because the

Table 2.1: Exchange energies (in hartrees) obtained from various exchange potentials as line integrals along the Q-, Λ - and Z-paths. The energies are evaluated at the HF/UGBS densities for atoms and the HF/cc-pVQZ densities for molecules.

System	Fermi-Amaldi			Umezawa			van Leeuwen-Baerends		
	$E_X^Q = E_X^\Lambda = E_X^Z$	E_X^Q	E_X^Λ	E_X^Q	E_X^Λ	E_X^Z	E_X^Q	E_X^Λ	E_X^Z
Atoms:									
H	-0.3125	-0.3181	-0.1823	-0.3070	-0.4435	-0.2789	-0.4048		
He	-1.0258	-1.1650	-0.8743	-1.1530	-1.4780	-0.9847	-1.3621		
Li	-1.3541	-1.7461	-1.4894	-1.7587	-2.5455	-1.7044	-2.3479		
Be	-1.7890	-2.4987	-2.3055	-2.5439	-3.8006	-2.6363	-3.5273		
N	-3.7369	-5.7956	-5.6647	-5.9344	-9.1683	-6.7985	-8.6111		
Ne	-6.6147	-11.0107	-10.8445	-11.2596	-16.6147	-12.9909	-15.7623		
Na	-7.2759	-12.6328	-12.5969	-12.9435	-19.1439	-15.0178	-18.1732		
Mg	-7.9842	-14.3649	-14.5300	-14.7448	-21.7825	-17.2787	-20.7231		
P	-10.2286	-20.0268	-20.5498	-20.6018	-30.5182	-24.3291	-29.0606		
Ar	-12.8671	-26.8037	-27.6394	-27.5845	-40.3898	-32.5402	-38.5398		
Ca	-14.2447	-31.1884	-32.5169	-32.1426	-46.9983	-38.2234	-44.9293		
Zn	-25.8630	-63.4147	-65.1354	-64.8930	-91.0614	-77.2639	-87.7929		
Kr	-32.5646	-85.7400	-88.0939	-87.6517	-121.2443	-103.7220	-117.0872		
Cd	-46.5422	-137.2004	-140.4224	-139.9671	-189.5924	-163.9985	-183.5032		
Molecules: ^a									
N ₂	-5.3415	-10.7709	-11.7032	-11.2382	-18.2396	-13.5633	-17.1382		
H ₂ O	-4.6782	-7.9424	-7.8996	-8.1558	-12.3686	-9.3289	-11.6533		
NH ₃	-3.9139	-6.7033	-6.6309	-6.8975	-10.5967	-7.6616	-9.9053		
CH ₄	-3.2716	-5.6631	-5.5503	-5.8461	-9.1038	-6.1672	-8.4114		
CH ₃	-3.1722	-5.3483	-5.2721	-5.5152	-8.6292	-5.9643	-8.0013		

^aExperimental geometries: N₂, $r(\text{NN})=1.09769$ Å; H₂O, $r(\text{OH})=0.9575$ Å, $\theta(\text{HOH})=104.51^\circ$; NH₃, $r(\text{NH})=1.012$ Å, $\theta(\text{HNH})=106.70^\circ$; CH₄, $r(\text{CH})=1.087$ Å; CH₃ (²A₂'), $r(\text{CH})=1.080$ Å.

Fermi–Amaldi potential is a functional derivative of the scaled electrostatic repulsion energy functional. We note that if the number of electrons N in the denominator of the Fermi–Amaldi potential is treated as a functional of the density rather than a constant, then the potential is not a functional derivative and the line integral becomes path-dependent.

For the Umezawa and van Leeuwen–Baerends potentials, the line integrals over the scaling parameters q and ζ in Eqs. (2.2) and (2.4) do not lend themselves to analytical evaluation but can be easily computed with one-dimensional quadratures at every real-space grid point \mathbf{r} . We have done so using 256-node Gauss–Legendre quadratures [22]. The real-space integration was then completed using a tight GAUSSIAN three-dimensional grid with 299 radial shells and 974 angular points per shell. Table 2.1 shows that line integrals along Q-, Λ -, and Z-paths all yield different exchange energies for the van Leeuwen–Baerends and Umezawa potentials, and that the difference between the values is significant. This suggests that these two model potentials are stray.

We note that in the previously published assessments of the van Leeuwen–Baerends and Umezawa potentials [10, 12, 23–25], the exchange energies were invariably obtained by the Levy–Perdew virial relation which corresponds to our Λ -path, one of many paths possible.

2.3.3 Virial energies from exact-exchange potentials

We apply this test only to approximate exact-exchange potentials of Slater, Becke–Johnson, Staroverov, and to the ϵ -consistent model given by Eq. (1.55). For each potential, we solve Kohn–Sham equations self-consistently and compare two values of the exact-exchange-only total energy E : one in which E_X is found via Eq. (1.47) and the other in which E_X is found via Eq. (1.62). The resulting *total* energies are denoted by E_{EXX} and E_{virial} , respectively.

Table 2.2 compares conventional and virial exact-exchange-only total energies of 14 selected atoms obtained using self-consistent potentials constructed in the universal Gaussian basis set (UGBS) of Ref. 26. The optimized effective potentials yield almost identical energies when using the exact and the virial functionals. This is an expected result because the OEP *is* a functional derivative of the exact-exchange energy functional. The Slater potential is a zeroth-order approximation to the OEP, and it gives the largest deviations of virial energies from the exact values. The virial energies are too negative because the Slater potential is too deep in the energetically important region near a nucleus [27].

Table 2.2: Total energies (in E_h) computed using various self-consistent model exchange potentials via the conventional exact-exchange energy functional (E_{EXX}) and the virial relation ($E_{\text{virial}} = E_{\text{EXX}} + \Delta E_{\text{virial}}$) for selected atoms. Calculations use the UGBS basis set.

Atoms	Slater		Becke-Johnson		Staroverov		Eq. (1.55)		OEP ^a	
	E_{EXX}	ΔE_{virial}	E_{EXX}	ΔE_{virial}	E_{EXX}	ΔE_{virial}	E_{EXX}	ΔE_{virial}	E_{EXX}	ΔE_{virial}
H	-0.50000	0.0000	-0.50000	0.0000	-0.50000	0.0000	-0.50000	0.0000	-0.50000	0.0000
He	-2.86168	0.0000	-2.86094	0.0825	-2.86096	0.0817	-2.86168	0.0000	-2.86168	0.0000
Li	-7.42690	-0.1324	-7.43130	0.0504	-7.42740	0.0048	-7.43244	-0.0025	-7.43249	0.0000
Be	-14.56141	-0.3900	-14.57168	0.0317	-14.56710	-0.0771	-14.57231	-0.0104	-14.57243	-0.0001
N	-54.37589	-1.4399	-54.39926	0.2506	-54.39854	0.0758	-54.40308	0.0292	-54.40339	0.0000
Ne	-128.5007	-3.199	-128.5358	0.782	-128.5399	0.553	-128.5449	0.146	-128.5454	0.000
Na	-161.7938	-3.955	-161.8489	0.806	-161.8507	0.532	-161.8560	0.178	-161.8566	0.000
Mg	-199.5330	-4.909	-199.6057	0.799	-199.6067	0.481	-199.6108	0.196	-199.6116	0.001
P	-340.6224	-7.300	-340.7110	0.904	-340.7119	0.400	-340.7140	0.237	-340.7150	-0.001
Ar	-526.7030	-10.144	-526.8089	1.182	-526.8101	0.447	-526.8108	0.284	-526.8121	-0.003
Ca	-676.6062	-12.599	-676.7484	1.127	-676.7477	0.258	-676.7502	0.275	-676.7520	0.002
Zn	-1777.5762	-27.764	-1777.8240	2.130	-1777.8263	0.905	-1777.8314	0.977	-1777.8344	0.001
Kr	-2751.7558	-37.804	-2752.0364	3.129	-2752.0383	1.546	-2752.0400	1.502	-2752.0427	-0.008
Cd	-5464.6959	-62.823	-5465.1080	3.618	-5465.1080	1.194	-5465.1092	2.193	-5465.1135	0.004
m.a.v. ^b	—	12.319	—	1.064	—	0.468	—	0.431	—	0.001

^aOptimized effective potential energies are from Ref. 1.

^bMean absolute value.

Table 2.3: Same as Table 2.2 but for molecules. Calculations use the completely uncontracted 6-311++G(3df, 3pd) basis set.

Molecules ^b	Slater			Becke-Johnson			Eq. (1.55)			OEP ^a		
	E_{EXX}	ΔE_{virial}		E_{EXX}	ΔE_{virial}		E_{EXX}	ΔE_{virial}		E_{EXX}	ΔE_{virial}	
N ₂	-108.89950	-3.483		-108.97329	0.232		-108.97470	0.307		-108.97744	-0.005	
H ₂ O	-76.01137	-2.334		-76.05117	0.242		-76.05594	0.142		-76.05713	-0.006	
NH ₃	-56.17399	-1.889		-56.21285	-0.028		-56.21579	0.113		-56.21691	-0.006	
CH ₄	-40.17161	-1.418		-40.20789	-0.265		-40.20907	0.099		-40.21005	0.002	
CH ₃	-39.53999	-1.331		-39.57150	-0.182		-39.57407	0.071		-39.57489	-0.002	
m.a.v.	—	2.091		—	0.190		—	0.146		—	0.004	

^aOptimized effective potential energies are from Ref. 1.

^bExperimental geometries: N₂, $r(\text{NN})=1.09769$ Å; H₂O, $r(\text{OH})=0.9575$ Å, $\theta(\text{HOH})=104.51^\circ$; NH₃, $r(\text{NH})=1.012$ Å; $\theta(\text{HNN})=106.70^\circ$; CH₄, $r(\text{CH})=1.087$ Å; CH₃ (²A₂'), $r(\text{CH})=1.080$ Å.

The model of Becke and Johnson yields significantly smaller discrepancies between E_{EXX} and E_{virial} than the Slater potential. Nevertheless, the differences ΔE_{virial} are still appreciable. Note that the Slater potential is exact for both the H and He atoms, but $v_{\text{X}}^{\text{BJ}}(\mathbf{r})$ is exact only for the H atom. This is because the Becke–Johnson correction term $k_{\text{BJ}}/2\pi$ reduces to a constant only for *exponential* one-electron spin-densities which occur in the H atom but not in He (nor in H_2^+).

The gradient-corrected potential of Staroverov is significantly closer to the OEP potential than the approximation of Becke and Johnson. Still, it is exact only for the H atom, but not for He. The ϵ -consistent model of Eq. (1.55) yields even smaller energy differences and in addition, is exact for two-electron systems. This property of the ϵ -consistent model comes from the Slater potential and is missing in both the Becke–Johnson and Staroverov approximations.

Table 2.3 makes similar comparisons for molecules. Here, discrepancies between E_{EXX} and E_{virial} follow similar trends, although less systematically than in atoms, possibly because the uncontracted 6-311++G(3df, 3pd) basis set used for molecules is not large enough for accurate resolution of the identity. The Staroverov potential is not included in this comparison because the oscillations from $\nabla\tau$ near the nuclei distort the results. Unfortunately, it is more difficult to remove the oscillations from the molecules than from the individual atoms.

The results in this section indicate that the Slater, Becke–Johnson, Staroverov, and the ϵ -consistent potentials are not functional derivatives of the exact-exchange energy functional. As the quality of potentials increases from the Slater to the ϵ -consistent model, the difference between the virial and the exact-exchange energy ΔE_{virial} decreases. This gradual improvement of the virial energies indicates that the model potentials in the row Slater < Becke–Johnson < Staroverov < ϵ -consistent indeed become closer to the functional derivative of the exact-exchange energy functional.

2.3.4 Exchange-correlation force and torque on the density

In applying the net zero-force and zero-torque tests it is necessary to keep in mind that the integrals of Eqs. (1.99) and (1.100) may vanish by symmetry [7]. It is always the case for atoms and symmetric molecules. In order to avoid false positives, the integrals of Eqs. (1.99) and (1.100) should be evaluated using molecular densities, preferably of low symmetry.

In Table 2.4, we compare the values of the net force and net torque for two molecules: H_2O , which belongs to the C_{2v} group, and HSOH (oxadisulfane), which has no high-order symmetry elements [28]. The zero-force test is failed by all potentials

Table 2.4: Magnitudes of the net force and net torque vectors of Eqs. (1.99) and (1.100) evaluated for various model potentials using the HF densities. Completely uncontracted 6-311++G(3df,3pd) basis set was used for fair comparison with the Slater (v_X^S) and Becke–Johnson (v_X^{BJ}) potentials constructed by the finite-basis-set resolution of the identity. The molecules are in the standard orientation as defined in the GAUSSIAN [17] program.

Molecule ^a	v_X^{LDA}	v_X^{FA}	v_X^{G96}	v_X^{U06}	v_X^{LB94}	v_X^S	v_X^{BJ}
Net exchange force (in hartrees/bohr)							
H ₂ O (C_{2v})	0.0000	0.0000	0.0000	0.0755	0.0605	0.0256	0.0152
HSOH (C_1)	0.0000	0.0000	0.0000	0.0565	0.1432	0.1337	0.0393
Net exchange torque (in hartrees/bohr)							
H ₂ O (C_{2v})	0.0000	0.0000	0.0000	0.0000	0.0000	0.0000	0.0000
HSOH (C_1)	0.0000	0.0000	0.0000	0.0830	0.0785	0.0498	0.0487

^aGeometries: H₂O, $r(\text{OH})=0.9575$ Å, $\theta(\text{HOH})=104.51^\circ$; HSOH, equilibrium MP2/6-31G* geometry.

except v_X^{LDA} , v_X^{FA} , and v_X^{G96} , which are functional derivatives. The zero-torque test gives a false positive for all model potentials in the case of H₂O molecule. The reason is that H₂O has two perpendicular mirror planes and the components of the vector $\mathbf{r} \times \nabla\rho(\mathbf{r})$ vanish by symmetry. When the asymmetric molecular density of HSOH is used, the net torque vanishes only for the LDA, Fermi–Amaldi, and Gill potentials. Based on our results, we conclude that the model potentials of van Leeuwen and Baerends, Umezawa, Slater, and Becke and Johnson are not functional derivatives.

2.4 Conclusion

Model Kohn–Sham potentials are usually designed to have at least a few basic properties of the exact potential such as proper scaling behavior, atomic shell structure, correct asymptotic decay, recovery of the gradient expansion to some order, and so on. The property of being a functional derivative may be more difficult to impose but it is actually very important for practical calculations with model potentials.

First, if a potential does not have a parent functional, then the energy assigned to it by the van Leeuwen and Baerends line integral formula is path-dependent and, therefore, ambiguous. Differences between energies evaluated along different integration paths may be as large as several hartrees. Next, stray potentials generate spurious forces and torques on the density. Energies obtained from such potentials are not invariant with respect to translation of the density and may depend on the

orientation of the molecule. Finally, if the potential is not a functional derivative, the Kohn–Sham equations do not represent a solution to any implied energy-minimization problem. This is relevant to geometry optimizations, because the point where the energy gradient is zero will not coincide with the energy minimum [24].

In this work, we have selected three properties of functional derivatives that are especially convenient for detecting stray potentials. Of these, the SCF convergence test is the most straightforward but also the least rigorous because the “dipping below the minimum” may indicate that the energy converges to an excited state, which is a local minimum. The line-integral test is more reliable, but it can only be applied to the potentials expressed exclusively in terms of the density. The virial-energy test complements the line-integral test, but is useful only for approximations to the exact-exchange potential. The zero-force and zero-torque tests appear to be the most general and useful, because they are very easy to implement and can be applied to any potential. Passing all our tests, however, is not sufficient to guarantee that the trial potential is a functional derivative, although in practice a false positive would be extremely unlikely.

Using these tests, we have demonstrated that the model potentials of van Leeuwen and Baerends, Umezawa, Slater, Becke and Johnson, and Staroverov, as well as the ϵ -consistent potential, are not functional derivatives. Some of these approximations, namely, the Slater, Becke–Johnson, and van Leeuwen–Baerends potentials have been identified as stray by other workers [2, 4, 24] prior to this study. Our results fully support those conclusions.

Bibliography

- [1] A. P. Gaiduk and V. N. Staroverov, “Virial exchange energies from model exact-exchange potentials”, *J. Chem. Phys.* **128**, 204101 (2008).
- [2] H. Ou-Yang and M. Levy, “Theorem for exact local exchange potential”, *Phys. Rev. Lett.* **65**, 1036 (1990).
- [3] R. van Leeuwen and E. J. Baerends, “Energy expressions in density-functional theory using line integrals”, *Phys. Rev. A* **51**, 170 (1995).
- [4] A. Karolewski, R. Armiento, and S. Kümmel, “Polarizabilities of polyacetylene from a field-counteracting semilocal functional”, *J. Chem. Theory Comput.* **5**, 712 (2009).
- [5] J. C. Slater, “A simplification of the Hartree–Fock method”, *Phys. Rev.* **81**, 385 (1951).
- [6] A. D. Becke and E. R. Johnson, “A simple effective potential for exchange”, *J. Chem. Phys.* **124**, 221101 (2006).
- [7] R. van Leeuwen, O. V. Gritsenko, and E. J. Baerends, “Analysis and modelling of atomic and molecular Kohn–Sham potentials”, *Top. Curr. Chem.* **180**, 107 (1996).
- [8] A. Görling, “Orbital- and state-dependent functionals in density-functional theory”, *J. Chem. Phys.* **123**, 062203 (2005).
- [9] S. Kümmel and L. Kronik, “Orbital-dependent density functionals: Theory and applications”, *Rev. Mod. Phys.* **80**, 3 (2008).
- [10] R. van Leeuwen and E. J. Baerends, “Exchange-correlation potential with correct asymptotic behavior”, *Phys. Rev. A* **49**, 2421 (1994).

- [11] A. Lembarki, F. Rogemond, and H. Chermette, “Gradient-corrected exchange potential with the correct asymptotic behavior and the corresponding exchange-energy functional obtained from the virial theorem”, *Phys. Rev. A* **52**, 3704 (1995).
- [12] N. Umezawa, “Explicit density-functional exchange potential with correct asymptotic behavior”, *Phys. Rev. A* **74**, 032505 (2006).
- [13] M. Levy and J. P. Perdew, “Hellmann–Feynman, virial, and scaling requisites for the exact universal density functionals. Shape of the correlation potential and diamagnetic susceptibility for atoms”, *Phys. Rev. A* **32**, 2010 (1985).
- [14] M. Mundt, S. Kümmel, R. van Leeuwen, and P.-G. Reinhard, “Violation of the zero-force theorem in the time-dependent Krieger–Li–Iafrate approximation”, *Phys. Rev. A* **75**, 050501(R) (2007).
- [15] P. M. W. Gill, “A new gradient-corrected exchange functional”, *Mol. Phys.* **89**, 433 (1996).
- [16] A. D. Becke, “Density-functional exchange-energy approximation with correct asymptotic behavior”, *Phys. Rev. A* **38**, 3098 (1988).
- [17] M. J. Frisch, G. W. Trucks, H. B. Schlegel, G. E. Scuseria, M. A. Robb, J. R. Cheeseman, J. J. A. Montgomery, T. Vreven, G. Scalmani, B. Mennucci, V. Barone, G. A. Petersson, M. Caricato, H. Nakatsuji, M. Hada, M. Ehara, K. Toyota, R. Fukuda, J. Hasegawa, M. Ishida, T. Nakajima, Y. Honda, O. Kitao, H. Nakai, X. Li, H. P. Hratchian, J. E. Peralta, A. F. Izmaylov, K. N. Kudin, J. J. Heyd, E. Brothers, V. Staroverov, G. Zheng, R. Kobayashi, J. Normand, J. L. Sonnenberg, S. S. Iyengar, J. Tomasi, M. Cossi, N. Rega, J. C. Burant, J. M. Millam, M. Klene, J. E. Knox, J. B. Cross, V. Bakken, C. Adamo, J. Jaramillo, R. Gomperts, R. E. Stratmann, O. Yazyev, A. J. Austin, R. Cammi, C. Pomelli, J. W. Ochterski, P. Y. Ayala, K. Morokuma, G. A. Voth, P. Salvador, J. J. Dannenberg, V. G. Zakrzewski, S. Dapprich, A. D. Daniels, M. C. Strain, Ö. Farkas, D. K. Malick, A. D. Rabuck, K. Raghavachari, J. B. Foresman, J. V. Ortiz, Q. Cui, A. G. Baboul, S. Clifford, J. Cioslowski, B. B. Stefanov, G. Liu, A. Liashenko, P. Piskorz, I. Komaromi, R. L. Martin, D. J. Fox, T. Keith, M. A. Al-Laham, C. Y. Peng, A. Nanayakkara, M. Challacombe, W. Chen, M. W. Wong, and J. A. Pople, “Gaussian Development Version, Revision F.02”, Gaussian Inc., Wallingford, CT (2006).

- [18] F. Della Sala and A. Görling, “Efficient localized Hartree–Fock methods as effective exact-exchange Kohn–Sham methods for molecules”, *J. Chem. Phys.* **115**, 5718 (2001).
- [19] J. Tao, V. N. Staroverov, G. E. Scuseria, and J. P. Perdew, “Exact-exchange energy density in the gauge of a semilocal density-functional approximation”, *Phys. Rev. A* **77**, 012509 (2008).
- [20] V. N. Staroverov, “A family of model Kohn–Sham potentials for exact exchange”, *J. Chem. Phys.* **129**, 134103 (2008).
- [21] P. Pulay, “Improved SCF convergence acceleration”, *J. Comp. Chem.* **3**, 556 (1982).
- [22] W. H. Press, S. A. Teukolsky, W. T. Vetterling, and B. P. Flannery, *Numerical Recipes. The Art of Scientific Computing*, Cambridge University Press, Cambridge, 3rd ed. (2007).
- [23] A. Banerjee and M. K. Harbola, “Density-functional-theory calculations of the total energies, ionization potentials, and optical response properties with the van Leeuwen–Baerends potential”, *Phys. Rev. A* **60**, 3599 (1999).
- [24] R. Neumann, R. H. Nobes, and N. C. Handy, “Exchange functionals and potentials”, *Mol. Phys.* **87**, 1 (1996).
- [25] O. V. Gritsenko, P. R. T. Schipper, and E. J. Baerends, “Approximation of the exchange-correlation Kohn–Sham potential with a statistical average of different orbital model potentials”, *Chem. Phys. Lett.* **302**, 199 (1999).
- [26] E. V. R. de Castro and F. E. Jorge, “Accurate universal Gaussian basis set for all atoms of the periodic table”, *J. Chem. Phys.* **108**, 5225 (1998).
- [27] O. Gritsenko, R. van Leeuwen, E. van Lenthe, and E. J. Baerends, “Self-consistent approximation to the Kohn–Sham exchange potential”, *Phys. Rev. A* **51**, 1944 (1995).
- [28] G. Winnewisser, F. Lewen, S. Thorwirth, M. Behnke, J. Hahn, J. Gauss, and E. Herbst, “Gas-phase detection of HSOH: Synthesis by flash vacuum pyrolysis of di-tert-butyl sulfoxide and rotational-torsional spectrum”, *Chem. Eur. J.* **9**, 5501 (2003).

Chapter 3

Analytic structure of functional derivatives

3.1 Introduction

An attractive alternative to development of density-functional approximations is to model the exchange-correlation potential v_{XC} without recourse to functional differentiation [1–4]. This approach makes it easier to impart v_{XC} with essential analytic properties such as Coulombic ($-1/r$) asymptotic decay, shell structure, and derivative discontinuity [1, 5–9]. Unfortunately, potentials approximated directly are not likely to be functional derivatives of some density functionals on their own accord, which leads to numerous problems in density-functional calculations [3, 4]. To make the potential-driven DFT a viable alternative to the functional-driven approach, one needs to be able to directly construct integrable model potentials.

In this Chapter, we propose such a method based on direct examination of the analytic structure of functional derivatives. We start by deriving a suitable analytic representation for functional derivatives of generalized gradient approximations (GGA), the simplest class of semilocal density functionals. Using this expression we demonstrate that the functional derivative of every GGA consists of a few simple terms such that the knowledge of any one of these terms is usually sufficient to reconstruct the entire functional derivative. After presenting the working equations of our method we illustrate their use by constructing a first integrable semilocal model exchange potential.

Reprinted in part with permission from **A. P. Gaiduk** and V. N. Staroverov, “Construction of integrable model Kohn–Sham potentials by analysis of the structure of functional derivatives”, *Phys. Rev. A* **83**, 012509 (2011). Copyright 2011, American Physical Society.

3.2 Methodology

3.2.1 Functional derivatives of GGAs

The term GGA refers to density-functional approximations of the form

$$F[\rho] = \int f(\rho, g) d\mathbf{r}, \quad (3.1)$$

where g is the norm of the density gradient,

$$g \equiv |\nabla\rho| = (\rho_x^2 + \rho_y^2 + \rho_z^2)^{1/2}, \quad (3.2)$$

in which $\rho_x \equiv \partial\rho/\partial x$, $\rho_y \equiv \partial\rho/\partial y$, and $\rho_z \equiv \partial\rho/\partial z$. Functional derivatives of GGAs can be evaluated using a standard formula of calculus of variations [10, 11], a special case of Eq. (1.34) with no dependence on the Laplacian of the density $\nabla^2\rho$:

$$v(\mathbf{r}) \equiv \frac{\delta F[\rho]}{\delta\rho(\mathbf{r})} = \frac{\partial f}{\partial\rho} - \nabla \cdot \left(\frac{\partial f}{\partial\nabla\rho} \right), \quad (3.3)$$

where $\partial f/\partial\nabla\rho$ is a shorthand for a vector with the components $\partial f/\partial\rho_x$, $\partial f/\partial\rho_y$, and $\partial f/\partial\rho_z$. Taken alone, Eq. (3.3) does not provide much insight into the structure of functional derivatives. The scalar product of the operator ∇ and $\partial f/\partial\nabla\rho$ in Eq. (3.3) needs to be evaluated for every particular functional, which makes this formula not very convenient for practical applications.

Let us obtain a more revealing representation of $v(\mathbf{r})$. Using the chain rule of differentiation and the fact that $\partial g/\partial\nabla\rho = \nabla\rho/g$, we cast the second term of Eq. (3.3) as

$$\nabla \cdot \left(\frac{\partial f}{\partial\nabla\rho} \right) = \left(\nabla \frac{\partial f}{\partial g} \right) \cdot \frac{\nabla\rho}{g} - \frac{\partial f}{\partial g} \left(\nabla \cdot \frac{\nabla\rho}{g} \right). \quad (3.4)$$

Further differentiation on the right-hand side yields

$$\nabla \cdot \left(\frac{\partial f}{\partial\nabla\rho} \right) = \frac{\partial^2 f}{\partial\rho\partial g} g + \frac{\partial^2 f}{\partial g^2} \frac{\nabla\rho \cdot \nabla g}{g} + \frac{\partial f}{\partial g} \left(\frac{l}{g} - \frac{\nabla\rho \cdot \nabla g}{g^2} \right), \quad (3.5)$$

where $l \equiv \nabla^2\rho$. Observe that the three Cartesian components of the vector $\nabla g \equiv (g_x, g_y, g_z)$ can be written as $g_i = g^{-1} \sum_j \rho_{ij} \rho_j$, where $i, j = x, y, z$ and ρ_{ij} are the components of the Hessian tensor of the density. This permits us to write

$$\nabla\rho \cdot \nabla g = \frac{1}{g} \sum_{ij} \rho_i \rho_{ij} \rho_j = \frac{w}{g}, \quad (3.6)$$

where we define w as

$$w = \sum_{ij} \rho_i \rho_{ij} \rho_j \quad (i, j = x, y, z). \quad (3.7)$$

The quantity w is identical to the density-dependent function $(\nabla\rho)^\dagger(\nabla\nabla^\dagger\rho)(\nabla\rho)$ discussed earlier by Jemmer and Knowles [12–14]. Combining Eqs. (3.3)–(3.7), we write the result as

$$v = \frac{\partial f}{\partial \rho} - \frac{\partial^2 f}{\partial \rho \partial g} g - \frac{\partial f}{\partial g} \frac{l}{g} + \left(\frac{\partial f}{\partial g} - g \frac{\partial^2 f}{\partial g^2} \right) \frac{w}{g^3}. \quad (3.8)$$

Note that this formula is given completely in terms of density-dependent ingredients ρ , g , l , and w , and does not involve explicit differentiation with respect to the real-space coordinates, so it is more practical than the original Eq. (3.3). We refer to the quantities ρ , g , l , and w as the variables of functional derivatives of GGAs.

For the purpose of development of model Kohn–Sham potentials with the proper scaling behavior, it is more convenient to use dimensionless derivatives of the density. The dimensionless counterparts of g , l , and w are

$$s = \frac{g}{\rho^{4/3}}, \quad q = \frac{l}{\rho^{5/3}}, \quad u = \frac{w}{\rho^{13/3}}. \quad (3.9)$$

To obtain a formula similar to Eq. (3.8) for the functional

$$F[\rho] = \int f(\rho, s) \, d\mathbf{r}, \quad (3.10)$$

we use Eq. (3.9) and the following transformation rules

$$\frac{\partial}{\partial \rho} \rightarrow \frac{\partial}{\partial \rho} + \frac{\partial s}{\partial \rho} \frac{\partial}{\partial s} = \frac{\partial}{\partial \rho} - \frac{4}{3} \frac{s}{\rho} \frac{\partial}{\partial s}, \quad (3.11)$$

$$\frac{\partial}{\partial g} \rightarrow \frac{\partial s}{\partial g} \frac{\partial}{\partial s} = \frac{s}{g} \frac{\partial}{\partial s}. \quad (3.12)$$

After some manipulations we arrive at the final result

$$v = \frac{\partial f}{\partial \rho} + \frac{4}{3} \frac{\partial^2 f}{\partial s^2} \frac{s^2}{\rho} - \frac{\partial^2 f}{\partial \rho \partial s} s - \frac{\partial f}{\partial s} \frac{q}{\rho s} + \left(\frac{\partial f}{\partial s} - s \frac{\partial^2 f}{\partial s^2} \right) \frac{u}{\rho s^3}. \quad (3.13)$$

Note that in this formula, the variables ρ and s are formally independent, and the derivative of f with respect to ρ refers *only* to the explicit dependence of f on ρ . The implicit dependence on ρ through s is taken into account by Eq. (3.11).

Expressions similar to Eqs. (3.8) and (3.13) have been derived earlier by other

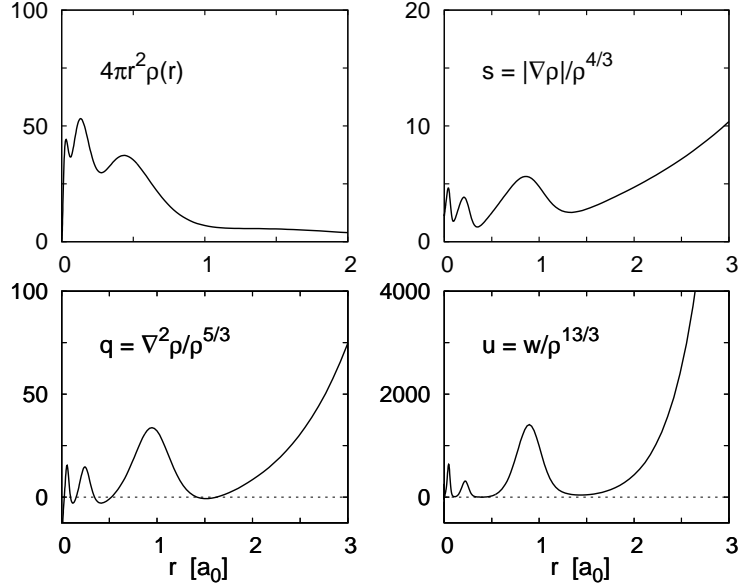


Figure 3.1: The four ingredients of functional derivatives of GGAs evaluated at the HF/UGBS density of the Kr atom.

workers [1, 3, 15, 16] and used for analyzing the capabilities and limitations of GGAs. In the present work, we emphasize a different perspective in which Eqs. (3.8) and (3.13) are viewed as a means of constructing integrable model potentials.

3.2.2 Ingredients of functional derivatives of GGAs

Equation (3.13) tells us that the functional derivative of any GGA depends on at most four ingredients: ρ , s , q , and u , and that the dependence on q and u is *linear*. Figure 3.1 compares the plots of these quantities for the electron density of the Kr atom computed by the Hartree–Fock (HF) method using the universal Gaussian basis set (UGBS) of Ref. 17. In order to rationalize these plots we make use of the fact that atomic densities are approximately piecewise exponential [18]. Consider a spherically symmetric N -electron exponential density

$$\rho = \frac{N}{8\pi} a^3 e^{-ar}. \quad (3.14)$$

For this ρ it is straightforward to show that

$$s = \left(\frac{8\pi}{N}\right)^{1/3} e^{ar/3} = a\rho^{-1/3}, \quad (3.15)$$

$$q = \left(\frac{8\pi}{N}\right)^{2/3} \left(1 - \frac{2}{ar}\right) e^{2ar/3} = s^2 - \frac{2s^2}{ar}, \quad (3.16)$$

$$u = \left(\frac{8\pi}{N}\right)^{4/3} e^{4ar/3} = s^4. \quad (3.17)$$

These equations reveal that the shell structure of exponential densities is transferred to s , q , and u , and that the maxima of s , q , and u for such densities occur simultaneously at the same values of r . Eqs. (3.14)–(3.17) also show that s , q , and u diverge at large r because these quantities are proportional to negative powers of the density, and that q diverges at the nucleus because it contains a term proportional to $1/r$. One can even estimate the value of s at the nucleus. In a many-electron atom, the density near $r = 0$ is essentially two-electron exponential [19]. For $N = 2$, Eq. (3.15) gives $s(r = 0) = (4\pi)^{1/3} \approx 2.325$ regardless of the value of the exponent. This result is in excellent agreement with Fig. 3.1.

It is appropriate to remark here that the dimensionless quantities q and u are more well-behaved than their dimensional counterparts l and w . In particular, plots of l and w (not shown here) would exhibit spurious oscillations near the nucleus which are well-known artifacts of cusplless Gaussian-type basis functions [20, 21].

Equation (3.13) tells us that any model potential constructed only from ρ and s is not a functional derivative. According to Eq. (3.13), the only way to avoid q - and u -dependence of the potential is to have $\partial f / \partial s = 0$, a requirement that no GGA can satisfy by definition. However, dependence on u is not necessary. The potential v does not involve u when

$$s \frac{\partial^2 f}{\partial s^2} - \frac{\partial f}{\partial s} = 0. \quad (3.18)$$

Integrating this equation twice, we find the energy-density function that satisfies this condition:

$$f(\rho, s) = s^2 \epsilon_1(\rho) + \epsilon_2(\rho), \quad (3.19)$$

where $\epsilon_1(\rho)$ and $\epsilon_2(\rho)$ are arbitrary functions of ρ . We conclude that the functional derivative of a GGA does not depend on u only if the energy density is of the form of Eq. (3.19). Functionals of this type include second-order density gradient expansions for exchange and correlation, as well as the Thomas–Fermi–Weizsäcker kinetic energy functional [11].

3.2.3 Analytic structure of functional derivatives of exchange GGAs

Let us now focus on functional derivatives of GGAs for exchange. The energy-density function $f(\rho, s)$ of exchange functionals can be written as a sum of the local-density approximation term and a gradient-dependent correction,

$$f_X(\rho, s) = f_X^{\text{LDA}}(\rho) + \rho^{4/3}G(s), \quad (3.20)$$

where $f_X^{\text{LDA}}(\rho) = -C_X\rho^{4/3}$ with $C_X = (3/4)(3/\pi)^{1/3}$ [cf. Eq. (1.22)] and $G(s)$ is a function of the reduced density gradient s only. Such analytic form of energy density ensures that the exchange energy has correct scaling behavior $E_X[\rho_\lambda] = \lambda E_X[\rho]$ under the uniform transformation of the density of Eq. (1.60). Substituting f from Eq. (3.20) into Eq. (3.13), we arrive at the following formula for functional derivatives of exchange-only GGA functionals,

$$v_X = v_X^{\text{LDA}} + \rho^{1/3} [R(s) + Q(s)q + U(s)u], \quad (3.21)$$

where

$$v_X^{\text{LDA}} = \frac{\partial f_X^{\text{LDA}}}{\partial \rho} = -\frac{4}{3}C_X\rho^{1/3} \quad (3.22)$$

and

$$R(s) = \frac{4}{3} \left(\frac{d^2G}{ds^2}s^2 - \frac{dG}{ds}s + G \right), \quad (3.23)$$

$$Q(s) = -\frac{1}{s} \frac{dG}{ds}, \quad (3.24)$$

$$U(s) = \frac{1}{s^3} \left(\frac{dG}{ds} - s \frac{d^2G}{ds^2} \right). \quad (3.25)$$

These equations show that each of the functions $R(s)$, $Q(s)$, and $U(s)$ uniquely determines $G(s)$ and, hence, the entire functional derivative v_X . Let us elaborate.

Suppose that we know $R(s)$. Then $G(s)$ can be obtained by solving Eq. (3.23) using the method described in sections 9.5 and 9.6 of Ref. 10. The general solution is

$$G(s) = s I_0(s) \ln s - s I_1(s), \quad (3.26)$$

where $I_0(s)$ and $I_1(s)$ are antiderivatives given by

$$I_n(s) = \frac{3}{4} \int \frac{R(s)}{s^2} \ln^n s ds + C_n, \quad n = 0, 1, \quad (3.27)$$

and C_n are integration constants. Once $R(s)$ is known, the components $Q(s)$ and $U(s)$ of the functional derivative immediately follow from Eqs. (3.24) and (3.25). Similarly, if we know the function $Q(s)$, then $G(s)$ is given by

$$G(s) = - \int sQ(s) ds + C. \quad (3.28)$$

Finally, if we start with the function $U(s)$, then $G(s)$ may be obtained by integrating Eq. (3.25) using the method of section 9.2 of Ref. 10 to give

$$G(s) = - \int \left[s \left(\int sU(s) ds + C_1 \right) \right] ds + C_2. \quad (3.29)$$

Thus, the problem of developing an integrable exchange potential reduces to constructing any of its components $\rho^{1/3}R(s)$, $\rho^{1/3}Q(s)q$, or $\rho^{1/3}U(s)u$. To devise such functions, we need to know what they may look like. We take some clues from standard exchange GGAs. As an example, consider the functional derivative of Becke (B88) [22], Perdew, Burke and Ernzerhof (PBE) [23], and Gill (G96) [24] exchange functionals. Factors $G(s)$ corresponding to these functionals are as follows:

$$G^{\text{B88}}(s) = - \frac{b\xi s^2}{1 + 6b\xi s \sinh^{-1}(\xi s)}, \quad (3.30)$$

where $b = 0.0042$ and $\xi = 2^{1/3}$ is a factor which arises in the conversion to the non-spin-polarized form;

$$G^{\text{PBE}}(s) = - \frac{C_X \mu s^2}{1 + \mu s^2 / \kappa}, \quad (3.31)$$

where $\mu = 0.21951/4(3\pi^2)^{2/3}$ and $\kappa = 0.804$; and

$$G^{\text{G96}}(s) = -\gamma s^{3/2}, \quad (3.32)$$

where $\gamma = 2^{1/6}/137$.

We evaluated functional derivatives of the above functionals using Eq. (3.21) and plotted their components in Fig. 3.2. The figure shows that distinct GGA exchange potentials have very similar composition: The shell structure almost entirely comes from the terms $\rho^{1/3}Q(s)q$ and $\rho^{1/3}U(s)u$, whereas the term $\rho^{1/3}R(s)$ is relatively small. Overall, the shape of the contributions to v_X is very similar for different approximations.

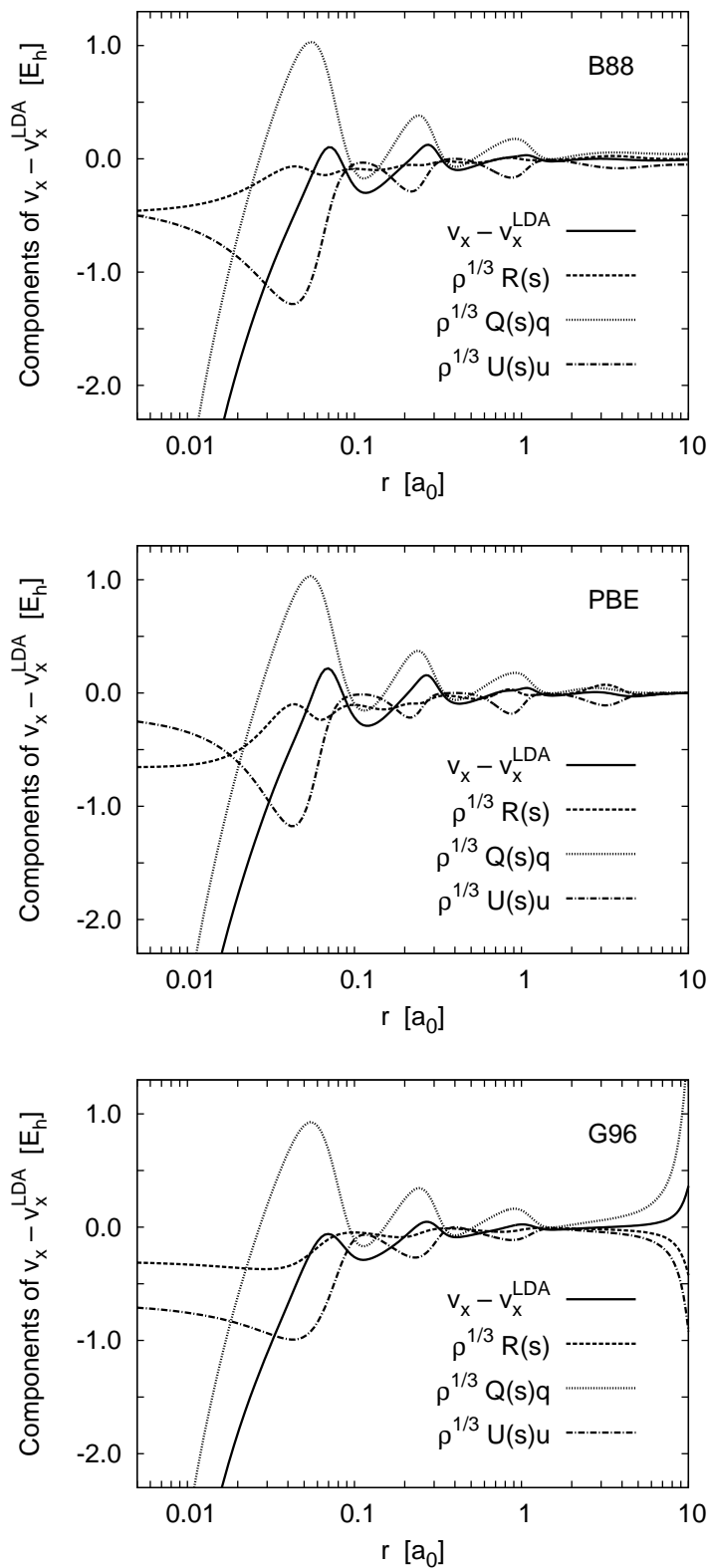


Figure 3.2: Decomposition of $v_x - v_x^{\text{LDA}}$, the semilocal part of functional derivatives of the B88, PBE, and G96 exchange functionals. The components are defined by Eqs. (3.21)–(3.25) and evaluated at the HF/UGBS density of a Kr atom.

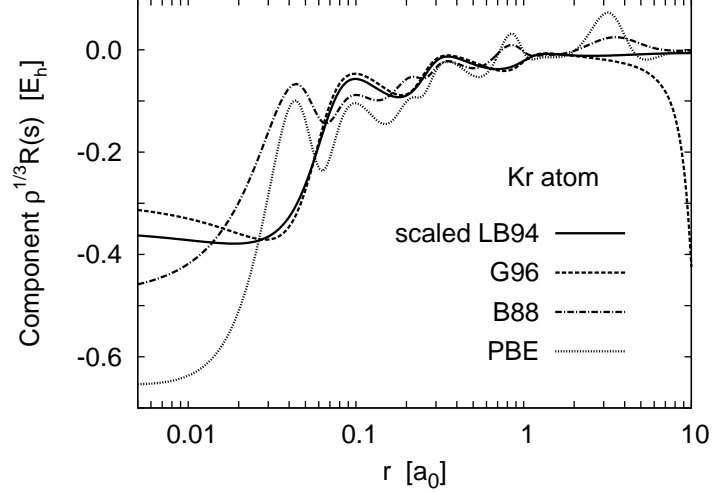


Figure 3.3: Component $\rho^{1/3}R(s)$ defined by Eq. (3.23) for functional derivatives of the B88, PBE, and G96 exchange functionals, and the semilocal part of the LB94 model potential scaled by 0.06. All quantities are evaluated at the HF/UGBS density of a Kr atom.

3.3 Application

It follows from our discussion that to develop an integrable model potential of the GGA type, one needs to approximate any of the terms of v_X identified in the previous section. Let us take a closer look at the terms v_X^{LDA} and $\rho^{1/3}R(s)$ of Eq. (3.21). Their sum has the same analytic structure as the exchange part of the van Leeuwen–Baerends model potential defined by Eq. (1.45). Our idea is to use the LB94 model to construct an integrable potential v_X . Observe that the semilocal part of LB94 must be scaled by approximately 0.06 to be a valid representation of the $\rho^{1/3}R(s)$ term (Fig. 3.3). But for now, let us use the *unscaled* LB94 potential.

Having identified the $R(s)$ function as the gradient correction of the LB94 potential, we use Eq. (3.26) to recover the function $G(s)$ and then set $C_0 = C_1 = 0$. Finally, we insert $G(s)$ into Eqs. (3.24) and (3.25) to obtain $Q(s)$ and $U(s)$. This leads to the following functional derivative, called fd-LB94, recovered from the stray LB94 potential:

$$v_X^{\text{fd-LB94}} = v_X^{\text{LB94}} - \frac{\rho^{1/3}}{s} \left(J_0 \ln s - J_1 + J_0 \right) q + \frac{\rho^{1/3}}{s^3} \left(J_0 \ln s - J_1 - s \frac{dJ_0}{ds} \right) u, \quad (3.33)$$

where $J_0(s)$ and $J_1(s)$ are given by

$$J_n(s) = -\frac{3}{4} \int_0^s \frac{\beta \xi \ln^n t}{1 + 3\beta \xi t \sinh^{-1}(\xi t)} dt, \quad n = 0, 1. \quad (3.34)$$

The corresponding energy functional is

$$E_X^{\text{fd-LB94}}[\rho] = E_X^{\text{LDA}}[\rho] + \int \rho^{4/3} s [J_0(s) \ln s - J_1(s)] d\mathbf{r}. \quad (3.35)$$

The fd-LB94 potential of Eq. (3.33) and the associated density functional of Eq. (3.35) are unusual in that they involve nonelementary functions $J_0(s)$ and $J_1(s)$ defined by Eq. (3.34). These functions do not pose any difficulty in numerical calculations and may be readily evaluated using one-dimensional quadratures for every value of s . In this paper, we computed the integrals $J_n(s)$ using Gauss–Legendre quadratures with 100 nodes per integral. The added computational cost of these integrals is very small.

To verify that the fd-LB94 potential is indeed a functional derivative, we used the zero-force and zero-torque tests discussed in Chapter 2. We calculated the net exchange force $\int v_X(\mathbf{r}) \nabla \rho(\mathbf{r}) d\mathbf{r}$ and torque $\int v_X(\mathbf{r}) \mathbf{r} \times \nabla \rho(\mathbf{r}) d\mathbf{r}$ with the LB94 and fd-LB94 potentials and found that the integrals vanish for asymmetric density of HSOH molecule [25] for the fd-LB94, but not for the LB94 potential. This confirms that the repaired potential is indeed a functional derivative (for details, see Sec. 2.3.4).

As seen in Fig. 3.4, the LB94 and fd-LB94 potentials differ considerably. Compared to LB94, the fd-LB94 potential is too negative near the nucleus. Whereas the LB94 potential has an underdeveloped shell structure, the fd-LB94 potential exaggerates it. In addition, the fd-LB94 potential has a singularity at $r = 0$ introduced through the Laplacian-dependent term—a feature common to GGA-based potentials (see Fig. 3.2). Also, although Fig. 3.4 does not show this, the LB94 potential decays asymptotically as $-1/r$, whereas the fd-LB94 potential increases without bound as $r \rightarrow \infty$. This behavior hardly matters in practice because it occurs well outside the energetically important region and is much slower than that of the G96 potential.

It is easy to see why the fd-LB94 potential is too negative and exaggerates the shell structure. According to Fig. 3.3, the gradient correction in the LB94 is a valid representation of the term $\rho^{1/3} R(s)$ of GGA potentials only when it is scaled down roughly by a factor of 0.06. The fd-LB94 approximation, however, uses the *unscaled* LB94 potential as a source. In other words, although the term $\rho^{1/3} R(s)$ in the fd-LB94 potential has a qualitatively correct shape, it is about an order of magnitude larger than it should be. The possible remedies are (i) to scale down the semilocal part of

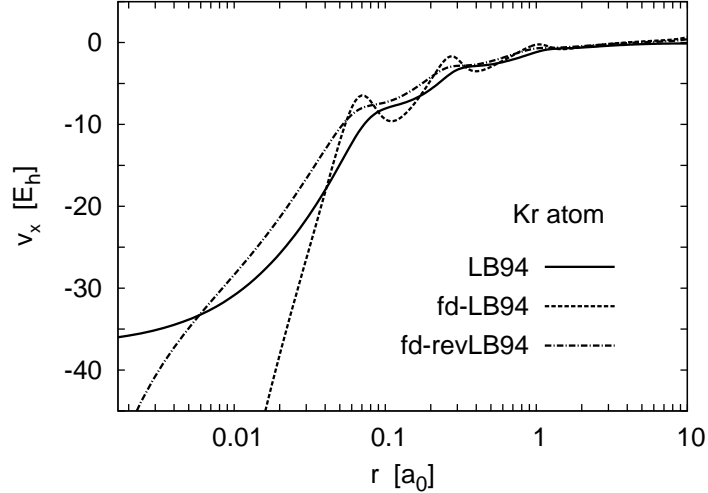


Figure 3.4: Stray model potential LB94 and integrable model potentials fd-LB94 and fd-revLB94. The latter are given by Eq. (3.33) with $\beta = 0.05$ and $\beta = 0.004$, respectively. All potentials are constructed using the HF/UGBS density of a Kr atom. Fully self-consistent LB94 and fd-revLB94 potentials are not shown but are very similar.

LB94 potential or (ii) to vary the empirical parameter β . We found that changing β from 0.05 to 0.004 gives a realistic integrable potential. The functional derivative recovered from the revised LB94 potential (revLB94), in which $\beta = 0.004$, is called here fd-revLB94 and is depicted in Fig. 3.4. Its shape between $r = 0$ and 10 bohr is very similar to that of the PBE and B88 potentials.

To extract exchange energies from our model potentials we employed the Levy–Perdew virial relation [26] of Eq. (1.62). For the functional derivatives fd-LB94 and fd-revLB94, the Levy–Perdew formula yields the same energy as the density functional given by Eq. (3.35). As follows from Table 3.1, the fd-revLB94 potential predicts very accurate exchange energies. The energies from fd-revLB94 are significantly closer to the exact values than the LB94 results and are on par with other exchange functionals such as PBE. The fd-LB94 energies are too low due to the reasons discussed above.

There is one property of the LB94 potential which has not been passed to the fd-revLB94 model. The function $R(s)$ of the LB94 model is such that the complete functional derivative “grown” from it no longer has the $-1/r$ decay. Conceivably, the asymptotic behavior of fd-revLB94 might be improved by fine-tuning the integration constants C_0 and C_1 appearing in Eq. (3.27).

Table 3.1: Exchange energies obtained from the LB94, fd-LB94, fd-revLB94 potentials, and the PBE functional. The fd-LB94 and fd-revLB94 are both given by Eq. (3.33) with $\beta = 0.05$ and $\beta = 0.004$, respectively. All energies are evaluated by the Levy–Perdew relation of Eq. (1.62) at the HF/UGBS densities. Fully self-consistent values are not shown but are within 1.9% for LB94 and within 0.4% for fd-revLB94.

Atom	E_X (units of E_h)				
	LB94	fd-LB94	fd-revLB94	PBE	Exact ^a
He	-0.9847	-2.4390	-1.0602	-1.0136	-1.0258
Be	-2.6363	-5.9871	-2.7113	-2.6358	-2.6669
Ne	-12.9909	-22.1584	-12.1579	-12.0667	-12.1083
Mg	-17.2787	-28.4425	-15.9862	-15.9147	-15.9943
Ar	-32.5402	-50.3845	-30.0590	-29.9960	-30.1850
Ca	-38.2234	-58.0148	-35.0470	-35.0156	-35.2112
Zn	-77.2639	-106.2587	-69.4627	-69.5280	-69.6413
Kr	-103.7220	-138.9071	-93.3204	-93.4250	-93.8560

^aHF/UGBS values.

3.4 Conclusion

We have shown that functional derivatives of generalized gradient approximations have a strong inner structure which can be exploited for designing integrable model Kohn–Sham potentials. We have identified several characteristic terms present in every functional derivative of a GGA and derived the equations which relate these terms to one another. Using these relations one can take any particular term and reconstruct the entire functional derivative along with the associated density functional. Existing model potentials such as LB94 may be used as sources of the component $\rho^{1/3}R(s)$, but they need to be modified to ensure that the resulting approximation yields accurate properties.

The method outlined in this Chapter represents a distinct approach to developing density functional approximations via model Kohn–Sham potentials. It goes beyond conventional GGA construction in the sense that it naturally leads to potentials and functionals involving unconventional integral expressions such as those appearing in Eq. (3.33). We expect that by putting the emphasis on the potential it should be easier to incorporate into density-functional approximations the important exact constraints such as the proper asymptotic behavior and the shell structure.

Bibliography

- [1] R. van Leeuwen and E. J. Baerends, “Exchange-correlation potential with correct asymptotic behavior”, *Phys. Rev. A* **49**, 2421 (1994).
- [2] R. van Leeuwen and E. J. Baerends, “Energy expressions in density-functional theory using line integrals”, *Phys. Rev. A* **51**, 170 (1995).
- [3] R. van Leeuwen, O. V. Gritsenko, and E. J. Baerends, “Analysis and modelling of atomic and molecular Kohn–Sham potentials”, *Top. Curr. Chem.* **180**, 107 (1996).
- [4] R. Neumann, R. H. Nobes, and N. C. Handy, “Exchange functionals and potentials”, *Mol. Phys.* **87**, 1 (1996).
- [5] O. Gritsenko, R. van Leeuwen, E. van Lenthe, and E. J. Baerends, “Self-consistent approximation to the Kohn–Sham exchange potential”, *Phys. Rev. A* **51**, 1944 (1995).
- [6] M. Grüning, O. V. Gritsenko, S. J. A. van Gisbergen, and E. J. Baerends, “Shape corrections to exchange-correlation potentials by gradient-regulated seamless connection of model potentials for inner and outer region”, *J. Chem. Phys.* **114**, 652 (2001).
- [7] P. R. T. Schipper, O. V. Gritsenko, S. J. A. van Gisbergen, and E. J. Baerends, “Molecular calculations of excitation energies and (hyper)polarizabilities with a statistical average of orbital model exchange-correlation potentials”, *J. Chem. Phys.* **112**, 1344 (2000).
- [8] A. D. Becke and E. R. Johnson, “A simple effective potential for exchange”, *J. Chem. Phys.* **124**, 221101 (2006).
- [9] E. Räsänen, S. Pittalis, and C. R. Proetto, “Universal correction for the Becke–Johnson exchange potential”, *J. Chem. Phys.* **132**, 044112 (2010).

- [10] G. B. Arfken and H. J. Weber, *Mathematical Methods for Physicists*, Academic Press, San Diego, 6th ed. (2005).
- [11] R. G. Parr and W. Yang, *Density-Functional Theory of Atoms and Molecules*, Oxford University Press, New York (1989).
- [12] P. Jemmer and P. J. Knowles, "Generation of functional derivatives in Kohn-Sham density-functional theory", *Comput. Phys. Commun.* **100**, 93 (1997).
- [13] P. Jemmer and P. J. Knowles, "Erratum to *Generation of functional derivatives in Kohn-Sham density-functional theory*", *Comput. Phys. Commun.* **103**, 95 (1997).
- [14] P. Jemmer and P. J. Knowles, "Symbolic algebra in functional derivative potential calculations", *J. Comput. Chem.* **19**, 300 (1998).
- [15] P. M. W. Gill and J. A. Pople, "Exact exchange functional for the hydrogen atom", *Phys. Rev. A* **47**, 2383 (1993).
- [16] J. P. Perdew and W. Yue, "Accurate and simple density functional for the electronic exchange energy: Generalized gradient approximation", *Phys. Rev. B* **33**, 8800 (1986).
- [17] E. V. R. de Castro and F. E. Jorge, "Accurate universal Gaussian basis set for all atoms of the periodic table", *J. Chem. Phys.* **108**, 5225 (1998).
- [18] W.-P. Wang and R. Parr, "Statistical atomic models with piecewise exponentially decaying electron densities", *Phys. Rev. A* **16**, 891 (1977).
- [19] P. Politzer, "Separation of core and valence regions in atoms", *J. Chem. Phys.* **64**, 4634 (1976).
- [20] M. E. Mura, P. J. Knowles, and C. A. Reynolds, "Accurate numerical determination of Kohn-Sham potentials from electronic densities: I. Two-electron systems", *J. Chem. Phys.* **106**, 9659 (1997).
- [21] P. R. T. Schipper, O. V. Gritsenko, and E. J. Baerends, "Kohn-Sham potentials corresponding to Slater and Gaussian basis set densities", *Theor. Chem. Acc.* **98**, 16 (1997).
- [22] A. D. Becke, "Density-functional exchange-energy approximation with correct asymptotic behavior", *Phys. Rev. A* **38**, 3098 (1988).

- [23] J. P. Perdew, K. Burke, and M. Ernzerhof, “Generalized gradient approximation made simple”, *Phys. Rev. Lett.* **77**, 3865 (1996).
- [24] P. M. W. Gill, “A new gradient-corrected exchange functional”, *Mol. Phys.* **89**, 433 (1996).
- [25] G. Winnewisser, F. Lewen, S. Thorwirth, M. Behnke, J. Hahn, J. Gauss, and E. Herbst, “Gas-phase detection of HSOH: Synthesis by flash vacuum pyrolysis of di-tert-butyl sulfoxide and rotational-torsional spectrum”, *Chem. Eur. J.* **9**, 5501 (2003).
- [26] M. Levy and J. P. Perdew, “Hellmann–Feynman, virial, and scaling requisites for the exact universal density functionals. Shape of the correlation potential and diamagnetic susceptibility for atoms”, *Phys. Rev. A* **32**, 2010 (1985).

Chapter 4

Integrability conditions for model potentials

4.1 Introduction

Development of practical exchange-correlation potential approximations has long been hindered by two methodological challenges: (i) how to obtain the energy from a Kohn–Sham potential and (ii) how to ensure that a model potential actually corresponds to some density functional. The first problem was addressed by the line integral method of van Leeuwen and Baerends [1]. The second problem has not been tackled so far in general (a special case of the exchange-only GGAs has been solved in Chapter 3), but it cannot be ignored if one wants to use model potentials to calculate observable physical properties. Given that a model potential is not likely to be integrable by itself, one must find a way to impose this property as a constraint.

The basic condition of integrability for model potentials based on the symmetry of second functional derivative was derived by Ou-Yang and Levy [2] and by van Leeuwen and Baerends [1]:

$$\frac{\delta v([\rho]; \mathbf{r})}{\delta \rho(\mathbf{r}')} = \frac{\delta v([\rho]; \mathbf{r}')}{\delta \rho(\mathbf{r})}. \quad (4.1)$$

(For more detail, refer to Chapter 1.) Although this condition is both necessary and sufficient, it is too general to be exploited as a constraint or even to serve as a convenient test. Here we transform Eq. (4.1) into a set of convenient analytic

Reprinted in part with permission from **A. P. Gaiduk** and V. N. Staroverov, “Explicit construction of functional derivatives in potential-driven density-functional theory”, *J. Chem. Phys.* **133**, 101104 (2010). Copyright 2010, American Institute of Physics.

integrability conditions which enable one not only to identify, but also to construct functional derivatives. This method complements and generalizes the approach of the previous Chapter exploiting the structure of functional derivatives.

4.2 Methodology

In this section, we will obtain a practical equivalent of Eq. (4.1) in terms of second differentials. Consider the second differential $D^2F[\rho, h, k]$ obtained in a similar way to $DF[\rho, h]$ of Eq. (1.23). For fixed ρ and h ,

$$D^2F[\rho, h, k] = \left\{ \frac{d}{dt} DF[\rho + tk, h] \right\}_{t=0} \quad (4.2)$$

where $k(\mathbf{r})$ is an arbitrary normed function. The second differential is a bilinear functional of h and k , so it may be written as [3]

$$D^2F[\rho, h, k] = \int d\mathbf{r} \int d\mathbf{r}' K([\rho]; \mathbf{r}, \mathbf{r}') h(\mathbf{r}) k(\mathbf{r}'). \quad (4.3)$$

The kernel of this operator is called the second functional derivative of $F[\rho]$, and it is customary to write

$$K([\rho]; \mathbf{r}, \mathbf{r}') \equiv \frac{\delta^2 F}{\delta\rho(\mathbf{r})\delta\rho(\mathbf{r}')} = \frac{\delta v([\rho]; \mathbf{r})}{\delta\rho(\mathbf{r}')}. \quad (4.4)$$

According to the condition (4.1), the proper kernel $K([\rho]; \mathbf{r}, \mathbf{r}')$ is symmetric in \mathbf{r} and \mathbf{r}' . Referring to Eq. (4.3), this implies that the second differential $D^2F[\rho, h, k]$ is symmetric in h and k . As we will see, this leads to an integrability condition equivalent to Eq. (4.1).

Let us express the second differential of $F[\rho]$ in Eq. (4.3) using the Gâteaux differential of the potential v . The potential $v([\rho]; \mathbf{r})$ is a functional of ρ at each point \mathbf{r} , so its first differential along an arbitrary direction k is given by

$$Dv([\rho, k]; \mathbf{r}) = \left\{ \frac{d}{dt} v([\rho + tk]; \mathbf{r}) \right\}_{t=0} \quad (4.5)$$

Let us rewrite Eq. (4.2) by casting the first Gâteaux differential in the form of Eq. (1.24), moving the d/dt operator inside the integral, and invoking Eq. (4.5). The result is

$$D^2F[\rho, h, k] = \int Dv([\rho, k]; \mathbf{r}) h(\mathbf{r}) d\mathbf{r}. \quad (4.6)$$

Relating this equality to the symmetric kernel condition, we see that for a trial potential $v([\rho]; \mathbf{r})$ to be integrable, it is necessary and sufficient that the right-hand side of Eq. (4.6) be symmetric in h and k for every h , k , and ρ :

$$\int Dv([\rho, k]; \mathbf{r})h(\mathbf{r}) d\mathbf{r} = \int Dv([\rho, h]; \mathbf{r})k(\mathbf{r}) d\mathbf{r}. \quad (4.7)$$

A complete formal proof of this result may be found in Ref. 4 as Theorem 5.1. Condition (4.7) is equivalent to Eq. (4.1).

We thus have two alternative ways to check the integrability of a potential $v([\rho]; \mathbf{r})$: (i) directly through the symmetry of the kernel [Eq. (4.1)]; (ii) using the symmetry condition on the second differential [Eq. (4.7)]. We will now show that the second approach is more practical by applying these two methods to a simple case of explicitly density-dependent potential $v([\rho], \mathbf{r})$ of the form

$$v = v(\rho, \nabla\rho, \nabla^2\rho). \quad (4.8)$$

4.2.1 Integrability from the symmetry of the kernel

Let us evaluate both sides of Eq. (4.1) using the Dirac delta function $\delta(\mathbf{r} - \mathbf{r}')$ as prescribed by Eq. (1.31). For the left-hand side $\delta v([\rho]; \mathbf{r})/\delta\rho(\mathbf{r}')$ we have

$$\frac{\delta v([\rho], \mathbf{r})}{\delta\rho(\mathbf{r}')} = Dv([\rho, \delta]; \mathbf{r}). \quad (4.9)$$

With the particular choice of density-dependent ingredients of v given by Eq. (4.8), the differential $Dv([\rho, \delta]; \mathbf{r})$ can be computed simply as the differential of a *function*,

$$Dv([\rho, \delta]; \mathbf{r}) = \left. \left\{ \frac{d}{dt} v(\rho(\mathbf{r}) + t\delta(\mathbf{r} - \mathbf{r}'), \nabla\rho(\mathbf{r}) + t\nabla\delta(\mathbf{r} - \mathbf{r}'), \nabla^2\rho(\mathbf{r}) + t\nabla^2\delta(\mathbf{r} - \mathbf{r}')) \right\} \right|_{t=0} \quad (4.10)$$

where all the gradients ∇ are with respect to \mathbf{r} . Taking the derivative d/dt and setting $t = 0$, we obtain the left-hand side of Eq. (4.1):

$$\frac{\delta v([\rho], \mathbf{r})}{\delta\rho(\mathbf{r}')} = \frac{\partial v}{\partial\rho}(\mathbf{r})\delta(\mathbf{r} - \mathbf{r}') + \frac{\partial v}{\partial\nabla\rho}(\mathbf{r})\nabla_{\mathbf{r}}\delta(\mathbf{r} - \mathbf{r}') + \frac{\partial v}{\partial\nabla^2\rho}(\mathbf{r})\nabla_{\mathbf{r}}^2\delta(\mathbf{r} - \mathbf{r}'). \quad (4.11)$$

The right-hand side of Eq. (4.1) has all the variables \mathbf{r} and \mathbf{r}' interchanged:

$$\frac{\delta v([\rho], \mathbf{r}')}{\delta\rho(\mathbf{r})} = \frac{\partial v}{\partial\rho}(\mathbf{r}')\delta(\mathbf{r}' - \mathbf{r}) + \frac{\partial v}{\partial\nabla\rho}(\mathbf{r}')\nabla_{\mathbf{r}'}\delta(\mathbf{r}' - \mathbf{r}) + \frac{\partial v}{\partial\nabla^2\rho}(\mathbf{r}')\nabla_{\mathbf{r}'}^2\delta(\mathbf{r}' - \mathbf{r}). \quad (4.12)$$

Let us simplify these expressions before attempting to compare them. We introduce shorthand notation $P \equiv \partial v / \partial \rho$, $G \equiv \partial v / \partial \nabla \rho$, and $L \equiv \partial v / \partial \nabla^2 \rho$. We also change the arguments of delta functions in Eq. (4.11) from $(\mathbf{r} - \mathbf{r}')$ to $(\mathbf{r}' - \mathbf{r})$ using Eqs. (A.15) and (A.17) from Appendix A, and change the variables of differentiation in Eq. (4.12) from \mathbf{r}' to \mathbf{r} using Eq. (A.18) from the same Appendix. The result is

$$\frac{\delta v([\rho], \mathbf{r})}{\delta \rho(\mathbf{r}')} = P(\mathbf{r})\delta(\mathbf{r}' - \mathbf{r}) + G(\mathbf{r})\nabla\delta(\mathbf{r}' - \mathbf{r}) + L(\mathbf{r})\nabla^2\delta(\mathbf{r}' - \mathbf{r}), \quad (4.13)$$

$$\frac{\delta v([\rho]; \mathbf{r}')}{\delta \rho(\mathbf{r})} = P(\mathbf{r}')\delta(\mathbf{r}' - \mathbf{r}) - G(\mathbf{r}')\nabla\delta(\mathbf{r}' - \mathbf{r}) + L(\mathbf{r}')\nabla^2\delta(\mathbf{r}' - \mathbf{r}), \quad (4.14)$$

where the subscripts \mathbf{r} in ∇ are suppressed for brevity. Taking the difference of the two functional derivatives, we obtain

$$\frac{\delta v([\rho]; \mathbf{r})}{\delta \rho(\mathbf{r}')} - \frac{\delta v([\rho]; \mathbf{r}')}{\delta \rho(\mathbf{r})} = [G(\mathbf{r}) + G(\mathbf{r}')] \nabla\delta(\mathbf{r}' - \mathbf{r}) + [L(\mathbf{r}) - L(\mathbf{r}')] \nabla^2\delta(\mathbf{r}' - \mathbf{r}). \quad (4.15)$$

To evaluate this expression, we multiply it by an arbitrary function $f(\mathbf{r}')$ and integrate over \mathbf{r}' . The right-hand side of the identity above becomes

$$\int [G(\mathbf{r}) + G(\mathbf{r}')] \nabla\delta(\mathbf{r}' - \mathbf{r}) f(\mathbf{r}') d\mathbf{r}' + \int [L(\mathbf{r}) - L(\mathbf{r}')] \nabla^2\delta(\mathbf{r}' - \mathbf{r}) f(\mathbf{r}') d\mathbf{r}'. \quad (4.16)$$

Observe that functions $G(\mathbf{r})$ and $L(\mathbf{r})$, as well as the operators ∇ may be moved outside the integrals. With this, the last equation can be easily evaluated using the definition of the delta function. Switching back to the explicit expressions instead of P , G and L , we obtain

$$\frac{\partial v}{\partial \nabla \rho} \nabla f + \nabla \left(\frac{\partial v}{\partial \nabla \rho} f \right) + \frac{\partial v}{\partial \nabla^2 \rho} \nabla^2 f - \nabla^2 \left(\frac{\partial v}{\partial \nabla^2 \rho} f \right). \quad (4.17)$$

Expanding this equation and canceling out identical terms yields

$$2 \left[\frac{\partial v}{\partial \nabla \rho} - \nabla \left(\frac{\partial v}{\partial \nabla^2 \rho} \right) \right] \nabla f + \left[\nabla \left(\frac{\partial v}{\partial \nabla \rho} \right) - \nabla^2 \left(\frac{\partial v}{\partial \nabla^2 \rho} \right) \right] f. \quad (4.18)$$

For the kernel of Eq. (4.1) to be symmetric with respect to \mathbf{r} and \mathbf{r}' , the expression above needs to vanish. This is possible for an arbitrary $f(\mathbf{r})$ only when

$$\frac{\partial v}{\partial \nabla \rho} = \nabla \frac{\partial v}{\partial \nabla^2 \rho}. \quad (4.19)$$

We have a strong result: a trial potential of the type (4.8) is a functional derivative if and only if it satisfies Eq. (4.19). In particular, this implies that any model potential that depends on ρ and $\nabla\rho$, but not on $\nabla^2\rho$, is stray. We obtained this result in a different way in Chapter 3. The derivation here is more general and robust, because it is valid for *any* potential involving ρ , $\nabla\rho$ and $\nabla^2\rho$.

4.2.2 Integrability from the symmetry of second differential

Let us evaluate the second differential with the potential v . Using Eq. (4.5), the left-hand side of Eq. (4.7) for v is

$$\int \left(\frac{\partial v}{\partial \rho} k + \frac{\partial v}{\partial \nabla \rho} \cdot \nabla k + \frac{\partial v}{\partial \nabla^2 \rho} \nabla^2 k \right) h \, d\mathbf{r}. \quad (4.20)$$

We integrate the last term of this expression by parts. Since ρ , h , k are normed (vanish at infinity), we get

$$\int \left[\frac{\partial v}{\partial \rho} h k + \left(\frac{\partial v}{\partial \nabla \rho} - \nabla \frac{\partial v}{\partial \nabla^2 \rho} \right) \cdot h \nabla k - \frac{\partial v}{\partial \nabla^2 \rho} \nabla h \cdot \nabla k \right] d\mathbf{r}. \quad (4.21)$$

We now interchange the functions h and k in Eq. (4.21) and subtract the result from the original integral. According to Eq. (4.7), v is a functional derivative only if the difference is zero for every acceptable h , k , and ρ ,

$$\int \left(\frac{\partial v}{\partial \nabla \rho} - \nabla \frac{\partial v}{\partial \nabla^2 \rho} \right) \cdot (h \nabla k - k \nabla h) \, d\mathbf{r} = 0. \quad (4.22)$$

By the fundamental lemma of the calculus of variations, the latter is possible only if Eq. (4.19) is true.

The present derivation yields the same result as the direct evaluation of Eq. (4.1) discussed in the previous section, but is much simpler. We will now use the approach described here to derive integrability conditions for a broader class of model potentials.

4.3 Analytic integrability conditions

Consider a formal expression of the type

$$v = v(\rho, \{\rho_i\}, \{\rho_{ij}\}), \quad (4.23)$$

where $\rho_i \equiv \partial_i \rho$ and $\rho_{ij} \equiv \partial_i \partial_j \rho$, in which the operator ∂_i stands for differentiation with respect to the i th Cartesian real-space coordinate ($i = x, y, z$). To simplify our derivation, we will treat ρ_{ij} and ρ_{ji} as distinct variables. The left-hand side of Eq. (4.7) in this case is

$$\int \left(\frac{\partial v}{\partial \rho} k + \sum_i \frac{\partial v}{\partial \rho_i} k_i + \sum_i \sum_j \frac{\partial v}{\partial \rho_{ij}} k_{ij} \right) h \, d\mathbf{r}, \quad (4.24)$$

where $k_i \equiv \partial_i k$ and $k_{ij} \equiv \partial_i \partial_j k$. Integrating by parts each term containing k_{ij} with respect to j we obtain

$$\int \left\{ \frac{\partial v}{\partial \rho} h k + \sum_i \frac{\partial v}{\partial \rho_i} h k_i - \sum_i \sum_j \left[\partial_j \left(\frac{\partial v}{\partial \rho_{ij}} \right) h k_i + \frac{\partial v}{\partial \rho_{ij}} h_j k_i \right] \right\} d\mathbf{r}. \quad (4.25)$$

This integral is symmetric in h and k only if

$$\frac{\partial v}{\partial \rho_i} - \sum_j \partial_j \left(\frac{\partial v}{\partial \rho_{ij}} \right) = 0. \quad (4.26)$$

The system of equations (4.26) is the general integrability condition for expressions of the type (4.23).

Of course, physical density-functional approximations and Kohn–Sham potentials depend on ρ_i and ρ_{ij} only through their rotation-invariant combinations. Consider, for example, potentials associated with generalized-gradient approximations. The functional derivative of a GGA was computed in Sec. 3.2.1 and is given by Eq. (3.8). It involves four rotation-invariant variables: ρ , g , l , and w . Therefore, we can express the partial derivatives of v in Eq. (4.26) in terms of these variables to obtain the following integrability condition

$$\frac{\partial v}{\partial g} \frac{\nabla \rho}{g} - \frac{\partial v}{\partial w} (l \nabla \rho - g \nabla g) = \nabla \frac{\partial v}{\partial l} + \left(\nabla \frac{\partial v}{\partial w} \cdot \nabla \rho \right) \nabla \rho. \quad (4.27)$$

This condition may be applied to *any* analytic expression involving no variables other than ρ , g , l , w , and is always satisfied by the functional derivative of a GGA.

Let us look closer at GGA potentials. According to Eq. (3.8), derivatives $\partial v / \partial l$

and $\partial v/\partial w$ in Eq. (4.27) do not depend on either l or w , so we may write

$$\nabla \frac{\partial v}{\partial l} = \frac{\partial^2 v}{\partial \rho \partial l} \nabla \rho + \frac{\partial^2 v}{\partial g \partial l} \nabla g, \quad (4.28)$$

$$\nabla \frac{\partial v}{\partial w} = \frac{\partial^2 v}{\partial \rho \partial w} \nabla \rho + \frac{\partial^2 v}{\partial g \partial w} \nabla g. \quad (4.29)$$

If we substitute these expressions into Eq. (4.27), we can cast the result in the form $P\nabla\rho = G\nabla g$, where P and G are scalar functions. This condition must hold pointwise for every ρ . However, since the vectors ∇g and $\nabla\rho$ are related through a tensor ($g_i = g^{-1} \sum_j \rho_{ij} \rho_j$), they cannot in general be scalar multiples of each other at every \mathbf{r} . Therefore, in order for the condition $P\nabla\rho = G\nabla g$ to be satisfied at every \mathbf{r} , both P and G must vanish, that is,

$$\begin{cases} \frac{1}{g} \frac{\partial v}{\partial g} - l \frac{\partial v}{\partial w} - \frac{\partial^2 v}{\partial \rho \partial l} - g^2 \frac{\partial^2 v}{\partial \rho \partial w} - \frac{w}{g} \frac{\partial^2 v}{\partial g \partial w} = 0, \\ g \frac{\partial v}{\partial w} - \frac{\partial^2 v}{\partial g \partial l} = 0. \end{cases} \quad (4.30)$$

Integrability conditions such as Eq. (4.30) are entirely in the (ρ, g, l, w) -space and so are very convenient for constructing functional derivatives in the following manner.

4.4 Direct construction of integrable potentials

Suppose we have an expression of the type $v_0(\rho, g)$. Expressions that depend on g , but not on l or w , do not satisfy Eq. (4.30) and hence are stray. Let us assume that v_0 can be *made* a functional derivative of some GGA by introducing linear dependence on l and w . We write

$$v(\rho, g, l, w) = v_0(\rho, g) + X(\rho, g)l + Y(\rho, g)w, \quad (4.31)$$

where X and Y are unknown functions to be determined from the requirement that v be integrable. Substitution of Eq. (4.31) into Eq. (4.30) yields a system of two equations

$$\begin{cases} \frac{1}{g} \frac{\partial v_0}{\partial g} - \frac{\partial}{\partial \rho} (X + g^2 Y) = 0, \\ gY - \frac{\partial X}{\partial g} = 0. \end{cases} \quad (4.32)$$

We integrate the first of these equations with respect to ρ and use the second equation to write the result as

$$g \frac{\partial X}{\partial g} + X = \frac{1}{g} \int^\rho \frac{\partial v_0}{\partial g} d\rho + C_1(g), \quad (4.33)$$

where $C_1(g)$ is an arbitrary function of proper dimensionality. The general solution of Eq. (4.33), obtained by the method of section 9.2 in Ref. 5, is

$$X = \frac{1}{g} \int^g \left(\frac{1}{g} \int^\rho \frac{\partial v_0}{\partial g} d\rho \right) dg + \frac{1}{g} \left[\int^g C_1(g) dg + C_2(\rho) \right], \quad (4.34)$$

where $C_2(\rho)$ is another arbitrary function of appropriate dimensionality. Once X is obtained from v_0 by Eq. (4.34), Y may be found by the second equation of the system (4.32). Let us illustrate this with specific examples.

As a warm-up, consider the expression $v_0 = g^2/8\rho^2$ which is clearly not a functional derivative. If we assume that v_0 is an incomplete functional derivative of a GGA, Eq. (4.34) yields $X = -1/4\rho + g^{-1} [\int^g C_1(g) dg + C_2(\rho)]$. Setting $C_1 = C_2 = 0$ in this solution, so that $Y = 0$, we obtain the expression

$$v = \frac{1}{8} \frac{g^2}{\rho^2} - \frac{1}{4} \frac{l}{\rho}. \quad (4.35)$$

One may instantly recognize in this result the functional derivative of $\int (g^2/8\rho) d\mathbf{r}$, the Weizsäcker gradient correction to the Thomas–Fermi kinetic-energy functional.

Our second example involves the expression $v_0 = g/\rho$ briefly discussed in Sec. 1.4.3. In this case Eq. (4.34) gives $X = g^{-1} [(\ln \rho) \ln g + \int^g C_1(g) dg + C_2(\rho)]$. Choosing $C_1 = C_2 = 0$, we obtain $Y = -g^{-3} [(\ln \rho) \ln g - \ln \rho]$. Thus, a functional derivative “grown” from $v_0 = g/\rho$ is

$$v = \frac{g}{\rho} + \frac{l}{g} \ln \rho \ln g - \frac{w}{g^3} (\ln \rho \ln g - \ln \rho). \quad (4.36)$$

Model Kohn–Sham potentials for exchange and correlation are usually developed in terms of ρ and dimensionless counterparts of the variables g, l, w given by Eq. (3.9). It is straightforward to show that with the dimensionless variables s, q and u , and

under the assumption that v is linear in q and u , Eq. (4.30) becomes

$$\begin{cases} \frac{1}{s} \frac{\partial v}{\partial s} + \frac{5}{3} \frac{\partial v}{\partial q} + \frac{\partial v}{\partial u} \left(\frac{17}{3} s^2 - q \right) - \rho \frac{\partial^2 v}{\partial \rho \partial q} - s^2 \rho \frac{\partial^2 v}{\partial \rho \partial u} + \frac{\partial^2 v}{\partial s \partial u} \left(\frac{4}{3} s^3 - \frac{u}{s} \right) = 0, \\ s \frac{\partial v}{\partial u} - \frac{\partial^2 v}{\partial s \partial q} = 0. \end{cases} \quad (4.37)$$

Let us now show how one can design integrable exchange potentials using the variables ρ , s , q , and u . Exchange potentials are homogeneous of degree one [Eq. (1.61)] under the uniform density scaling of Eq. (1.60), which implies that $v \sim \rho^{1/3}$. From Eq. (3.8) we also know that if v descends from a GGA, it must be linear in q and u . The general form of v that satisfies these requirements is

$$v(\rho, s, q, u) = \rho^{1/3} [R(s) + Q(s)q + U(s)u], \quad (4.38)$$

where the functions R , Q , U are at our disposal. Note that this formula is equivalent to Eq. (3.21) that we derived in Chapter 3. Suppose the function R is known. To find Q and U we insert Eq. (4.38) into Eq. (4.37) and get

$$\begin{cases} \frac{1}{s} \frac{dR}{ds} + \frac{4}{3} Q + \frac{16}{3} s^2 U + \frac{4}{3} s^3 \frac{dU}{ds} = 0, \\ U - \frac{1}{s} \frac{dQ}{ds} = 0. \end{cases} \quad (4.39)$$

Substitution of the second equation into the first yields

$$s^2 \frac{d^2 Q}{ds^2} + 3s \frac{dQ}{ds} + Q = -\frac{3}{4s} \frac{dR}{ds}. \quad (4.40)$$

Integrating Eq. (4.40) as explained in sections 9.5 and 9.6 of Ref. 5 we write the general solution as

$$Q(s) = -\frac{1}{s} [c_1 + c_2 \ln s - I_1(s) + (\ln s + 1)I_0(s)], \quad (4.41)$$

where c_1 and c_2 are integration constants and

$$I_n(s) = \frac{3}{4} \int^s \frac{R(s)}{s^2} \ln^n s ds, \quad n = 0, 1. \quad (4.42)$$

The function U is then found from Eq. (4.39) to be

$$U(s) = \frac{1}{s^3} \left[c_1 - c_2 + c_2 \ln s - I_1(s) + I_0(s) \ln s - \frac{3}{4} \frac{R(s)}{s} \right]. \quad (4.43)$$

The constants c_1 and c_2 may be employed to satisfy known exact constraints. For instance, to recover the correct second-order gradient expansion of the exact exchange potential [6], one should choose $c_1 = c_2 = 0$.

4.5 Conclusion

The general strategy for developing integrable model Kohn–Sham potentials that emerges from this work is as follows: (i) choose a set of explicitly density-dependent ingredients of the approximation $(\rho, \nabla\rho, \nabla^2\rho, \dots)$ and use Eq. (4.7) to derive the corresponding integrability conditions; (ii) assume some general analytic form of v and construct one term; (iii) use the integrability conditions to derive the other terms. In particular, for exchange potentials of the GGA type, one can start with the function $R(s)$ and then use Eqs. (4.41)–(4.43) to obtain $Q(s)$ and $U(s)$.

In Chapter 3 we proposed a method for developing integrable Kohn–Sham potentials by analyzing the structure of functional derivatives. Integrability conditions provide an equivalent solution to this problem. For example, we could apply Eqs. (4.41) and (4.43) to the model potential of van Leeuwen and Baerends [7] and construct the fd-LB94 and fd-revLB94 approximations discussed in that Chapter. Unlike the approach proposed before, the integrability conditions involve *only* the derivatives of the potential and, formally, at no point use the functional explicitly.

Clearly, when designing integrable model potentials one implicitly designs density functionals. This raises the question of whether approximating potentials makes possible anything that is not afforded by approximating functionals. Our answer is yes because working in terms of integrable potentials is equivalent to working in terms of energy expressions containing integrals such as Eq. (4.42) which may not be expressible in elementary functions but clearly go beyond conventional forms of density-functional approximations.

Bibliography

- [1] R. van Leeuwen and E. J. Baerends, “Energy expressions in density-functional theory using line integrals”, *Phys. Rev. A* **51**, 170 (1995).
- [2] H. Ou-Yang and M. Levy, “Theorem for functional derivatives in density-functional theory”, *Phys. Rev. A* **44**, 54 (1991).
- [3] V. Volterra, *Theory of Functionals and of Integral and Integro-Differential Equations*, Dover Publications, Inc., New York (1959).
- [4] M. M. Vainberg, *Variational Methods for the Study of Nonlinear Operators*, Holden–Day, San Francisco (1964).
- [5] G. B. Arfken and H. J. Weber, *Mathematical Methods for Physicists*, Academic Press, San Diego, 6th ed. (2005).
- [6] Y. Wang, J. P. Perdew, J. A. Chevary, L. D. Macdonald, and S. H. Vosko, “Exchange potentials in density-functional theory”, *Phys. Rev. A* **41**, 78 (1990).
- [7] R. van Leeuwen and E. J. Baerends, “Exchange-correlation potential with correct asymptotic behavior”, *Phys. Rev. A* **49**, 2421 (1994).

Chapter 5

Energy functionals based on model Kohn–Sham potentials

5.1 Introduction

When the Kohn–Sham potential is approximated directly, there arises the question of finding the energy corresponding to that potential. The usual way to assign an energy to model exchange potentials is via the Levy–Perdew virial relation given by Eq. (1.62) [1, 2]. The problem with this approach, clearly recognized before us [3–5], is that the functional $E_X[\rho]$ constructed from $v_X([\rho]; \mathbf{r})$ is not assured to be translationally and rotationally invariant. (For an explanation refer to Sec. 1.4.4.) The energies assigned to stray potentials by the Levy–Perdew relation are position-dependent. No such problems exist for integrable potentials that originate from some density functional. This means that the Levy–Perdew virial relation is an acceptable way to assign energies only to integrable exchange potentials. Almost all model potentials existing today are stray (Chapter 2). This calls for a method that yields properly invariant energy expressions from arbitrary potentials. The aim of this Chapter is to propose such a method. As an example, we construct a competitively accurate density functional from the model potential of van Leeuwen and Baerends [3].

Reprinted in part with permission from **A. P. Gaiduk** and V. N. Staroverov, “A generalized gradient approximation for exchange derived from the model potential of van Leeuwen and Baerends”, *J. Chem. Phys.* **136**, 064116 (2012). Copyright 2012, American Institute of Physics.

5.2 Methodology

Our starting point is to realize that the Levy–Perdew relation is not the only way to go from potentials to the functionals. In fact, it is a special case of a more general method based on the line integrals [6, 7] which was discussed in Chapter 1. According to this method, a density functional can be obtained from the potential $v_{\text{XC}}([\rho]; \mathbf{r})$ by taking an integral given by Eq. (1.58) along a line (path) of a parametrized density $\rho_t(\mathbf{r})$. If $v_{\text{XC}}([\rho]; \mathbf{r})$ is a true functional derivative of some $E_{\text{XC}}[\rho]$, then Eq. (1.58) recovers the parent functional in one of its equivalent forms [8], and functional differentiation of that functional returns $v_{\text{XC}}([\rho]; \mathbf{r})$. But if $v_{\text{XC}}([\rho]; \mathbf{r})$ is stray, its parent functional does not exist and Eq. (1.58) predicts different energy values for different paths. Nevertheless, one can lend a meaning to this unphysical result by saying that the line integral of a stray potential taken along a particular path $\rho_t(\mathbf{r})$ *defines* a new energy functional. Of course, functional differentiation of any functional constructed in this manner will not recover the original stray potential.

Any “reasonable” parametrization of the density can be used with Eq. (1.58), such as scaling [7, 8], spatial redistribution of $\rho(\mathbf{r})$ [7] or even filling the density electron-by-electron in accordance with the *Aufbau* principle [9]. From a practical point of view, a convenient choice of parametrization is density scaling. A number of scaling transformations has been discussed in the literature [10–17]. The most well-known of them is, perhaps, the uniform density scaling [10, 11] of Eq. (1.60), termed the Λ -path in Sec. 1.4.2. Here, we write it with the scaling parameter t instead of λ ,

$$\rho_t(\mathbf{r}) = t^3 \rho(t\mathbf{r}), \quad 0 \leq t \leq 1. \quad (5.1)$$

Application of this path to Eq. (1.58) yields

$$E_{\text{XC}}[\rho] = \int d\mathbf{r} [3\rho(\mathbf{r}) + \mathbf{r} \cdot \nabla \rho(\mathbf{r})] \int_0^1 \frac{dt}{t} v_{\text{XC}} \left([\rho_t]; \frac{\mathbf{r}}{t} \right). \quad (5.2)$$

In the particular case of exchange potentials, this line integral becomes the Levy–Perdew relation of Eq. (1.62). Note that it is the coordinate scaling that is responsible for the presence of \mathbf{r} in Eq. (1.62), and ultimately, for the lack of translational and rotational invariance of Levy–Perdew relation when applied to stray model potentials.

Consider now the density scaling [13, 14] of Eq. (1.59) called the Q-path in Sec. 1.4.2. We rewrite it here as

$$\rho_t(\mathbf{r}) = t\rho(\mathbf{r}), \quad 0 \leq t \leq 1. \quad (5.3)$$

The energy expression corresponding to this path is

$$E_{\text{XC}}[\rho] = \int d\mathbf{r} \rho(\mathbf{r}) \int_0^1 dt v_{\text{XC}}([\rho_t]; \mathbf{r}). \quad (5.4)$$

This functional does not depend on the position vector \mathbf{r} explicitly, so it is translationally and rotationally invariant as long as $v_{\text{XC}}([\rho]; \mathbf{r})$ is itself invariant. Our idea is to assign energies to model potentials using Eq. (5.4) rather than Eq. (5.2). Note that if $v_{\text{XC}}([\rho]; \mathbf{r})$ is a functional derivative, then the functional of Eq. (5.4) is equivalent to the functional of Eq. (5.2) up to a gauge transformation of the energy density. For a stray potential, the functionals of Eq. (5.2) and (5.4) are different.

5.3 Application

5.3.1 Λ -LB94 and Q-LB94 functionals

To put our idea to practice, we chose a model potential of van Leeuwen and Baerends [3], a gradient-dependent approximation designed to mimic the Coulombic $(-1/r)$ asymptotic behavior of the exact potential. The exchange-like part of the LB94 potential is given by Eq. (1.45). Let us rewrite it as

$$v_{\text{X}}^{\text{LB94}} = v_{\text{X}}^{\text{LDA}} - \rho^{1/3} G(s), \quad (5.5)$$

where $v_{\text{X}}^{\text{LDA}}$ is the local density approximation for exchange given by Eq. (1.29) and

$$G(s) = \frac{\beta \xi s^2}{1 + 3\beta \xi s \sinh^{-1}(\xi s)}. \quad (5.6)$$

Recall that $\beta = 0.05$ is an empirical parameter, $\xi = 2^{1/3}$ is a factor arising in transition to the spin-unpolarized form, and s is the dimensionless reduced density gradient of Eq. (3.9).

Consider now two exchange functionals constructed from the LB94 as line integrals. The first functional, which we call Λ -LB94, is obtained by integrating the LB94 along the Λ -path, that is, by Eq. (5.2). It is defined as

$$E_{\text{X}}^{\Lambda\text{-LB94}}[\rho] = \int v_{\text{X}}^{\text{LB94}}([\rho]; \mathbf{r})(3\rho + \mathbf{r} \cdot \nabla\rho) d\mathbf{r}, \quad (5.7)$$

or, equivalently,

$$E_X^{\Lambda\text{-LB94}}[\rho] = E_X^{\text{LDA}}[\rho] - \int \rho^{1/3} G(s) (3\rho + \mathbf{r} \cdot \nabla \rho) d\mathbf{r}. \quad (5.8)$$

The second functional, called Q-LB94, is obtained by integrating the LB94 potential along the Q-path, that is, by Eq. (5.4). We write that functional as

$$E_X^{\text{Q-LB94}}[\rho] = E_X^{\text{LDA}}[\rho] - \int \rho^{4/3} Q(s) d\mathbf{r}, \quad \text{where} \quad (5.9)$$

$$Q(s) = \beta \xi s^2 \int_0^1 \frac{dt}{t^{1/3} + 3\beta \xi s \sinh^{-1}(t^{-1/3} \xi s)}. \quad (5.10)$$

The LB94 potential is not a functional derivative, so the functionals of Eqs. (5.8) and (5.9) yield different energy values (Chapter 2).

To obtain the functional derivative of the Λ -LB94 functional, we use Eq. (B.20) derived in the Appendix B. The result is

$$\begin{aligned} v_X^{\Lambda\text{-LB94}} &= v_X^{\text{LB94}} - \rho^{1/3} \left[\frac{4}{3} \frac{d^2 G}{ds^2} \frac{s^2}{\rho} - \frac{5}{3} \frac{dG}{ds} \frac{s}{\rho} - \frac{dG}{ds} \frac{q}{\rho s} + \left(\frac{dG}{ds} - \frac{d^2 G}{ds^2} s \right) \frac{u}{\rho s^3} \right] \\ &\times (3\rho + \mathbf{r} \cdot \nabla \rho) + 2\rho^{1/3} \frac{dG}{ds} \mathbf{r} \cdot \nabla s, \end{aligned} \quad (5.11)$$

where $G(s)$ is given by Eq. (5.6), and q and u are density-dependent variables defined in Eq. (3.9). Note that $v_X^{\Lambda\text{-LB94}}$ turns out to be the original LB94 plus a correction. This correction completes stray LB94 to a functional derivative, so that LB94 and Λ -LB94 yield the same energy via the Levy–Perdew relation:

$$\int v_X^{\text{LB94}} (3\rho + \mathbf{r} \cdot \nabla \rho) d\mathbf{r} = \int v_X^{\Lambda\text{-LB94}} (3\rho + \mathbf{r} \cdot \nabla \rho) d\mathbf{r},$$

the result which we verified numerically.

The functional derivative of the Q-LB94 functional can be obtained using Eqs. (3.20)–(3.25). Explicitly,

$$v_X^{\text{Q-LB94}} = v_X^{\text{LDA}} - \rho^{1/3} \left[\frac{4}{3} \left(\frac{d^2 Q}{ds^2} s^2 - \frac{dQ}{ds} s + Q \right) - \frac{dQ}{ds} \frac{q}{s} + \left(\frac{dQ}{ds} - s \frac{d^2 Q}{ds^2} \right) \frac{u}{s^3} \right], \quad (5.12)$$

where $Q(s)$ is given by Eq. (5.10).

We implemented the functionals of Eqs. (5.8) and (5.9) in the development version of the GAUSSIAN program [18]. To evaluate the function $Q(s)$ and its derivatives we

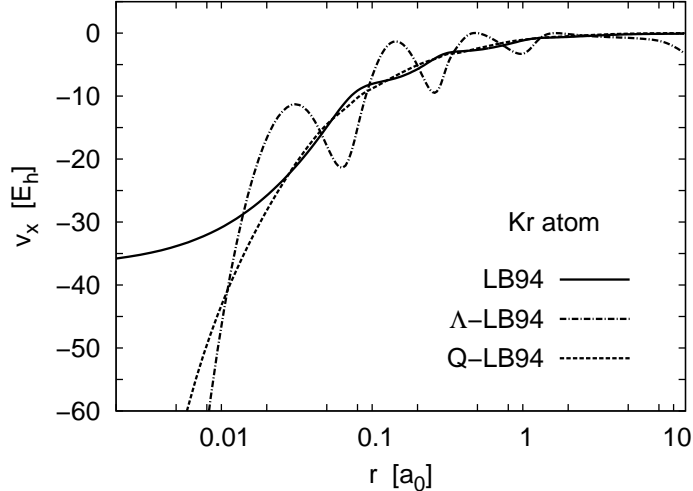


Figure 5.1: Exchange part of the LB94 potential and functional derivatives of the Λ -LB94 and Q-LB94 exchange functionals. The potentials are evaluated using HF/UGBS density of the Kr atom.

used the 256-point Gauss-Legendre quadrature formula [19]. The large number of points was chosen to ensure an accuracy of at least $10^{-5} E_h$ in the total energy.

Figure 5.1 compares the functional derivatives of Λ -LB94 and Q-LB94 functionals to the original LB94 potential. All three curves here are clearly different, which reflects the fact that LB94 is not a functional derivative. The Λ -LB94 has a pronounced oscillatory behavior, which might explain why the self-consistent-field (SCF) procedure with this potential was difficult to converge. Both Λ -LB94 and Q-LB94 are singular at the nucleus, a feature that is common to functional derivatives of generalized gradient approximations (*cf.* Fig. 3.2).

To test translational properties of the Λ -LB94 and Q-LB94 functionals, we calculated the total energy of an H_2O molecule in two different positions relative to the coordinate axes. The results are reported in Table 5.1. This test shows that the Λ -LB94 functional is not translationally invariant, but the Q-LB94 functional is. The difference between the Λ -LB94 energies for the initial and the displaced positions in Table 5.1 is precisely equal to

$$\Delta E = \mathbf{R} \cdot \int v_{\mathbf{x}}^{\text{LB94}}(\mathbf{r}) \nabla \rho(\mathbf{r}) d\mathbf{r}, \quad (5.13)$$

in agreement with Eq. (1.97).

To get an idea of the accuracy of the Λ -LB94 and Q-LB94 functionals we compared the above values to the HF/cc-pVQZ energy, which is a good approximation to the

Table 5.1: Tests of translational invariance of the Λ -LB94 and Q-LB94 functionals. All energies are evaluated using the cc-pVQZ basis set at the HF/cc-pVQZ density of the H₂O molecule. Symmetry was disabled with the NoSymm keyword.

Position	Total energy (E_h)		
	Λ -LB94	Q-LB94	HF
Initial ^a	-76.45904	-79.48049	-76.06374
Displaced ^b	-75.92645	-79.48049	-76.06374

^aInitial position: the oxygen is at (0, 0, 0); the hydrogens are at (0, ± 0.763208 , -0.596582) Å.

^bDisplaced position: the molecule is translated by $-\mathbf{R}$, where $\mathbf{R} = (0, 0, 5)$ Å.

exact exchange-only value. As seen from Table 5.1, the Λ -LB94 energy evaluated at the *initial* position is quite reasonable, but varies at a rate of about $0.1 E_h/\text{Å}$ as the molecule is moved. The Q-LB94 energy of H₂O is already too low by $3.4 E_h$.

This leads us to a choice: Q-LB94 functional is invariant with respect to molecular orientation but yields the energies that are too low. The Λ -LB94 functional is reasonably accurate but has problems with molecular translations and an unphysical behavior of functional derivative. An attempt to solve the problem of position-dependence was made by Kurzweil and Head-Gordon [5], who imposed the zero-force [Eq. (1.99)] and zero-torque [Eq. (1.100)] conditions on model potentials (which, in turn, make Levy–Perdew energies invariant with respect to translation and rotation). We will show that instead of trying to salvage the Λ -LB94 energy expression it is easier to repair the Q-LB94 functional.

5.3.2 Refinement of the Q-LB94 functional

To understand why the Q-LB94 functional gives unphysically low energies, let us consider its behavior in the uniform-gas limit, $s \rightarrow 0$. The Q-LB94 functional belongs to a class of GGAs for exchange. It is well known [20] that in the $s \rightarrow 0$ limit, GGAs reduce to density-gradient expansion (DGE),

$$E_X[\rho] = E_X^{\text{LDA}}[\rho] - \gamma \int \rho^{4/3} s^2 d\mathbf{r} + \dots, \quad (5.14)$$

where γ is a parameter. The non-empirical value of γ that makes Eq. (5.14) exact for a slowly varying electron gas is $\gamma_{\text{DGE}} = (10/81)[3/16\pi(3\pi^2)^{1/3}] \approx 0.0023817$ [21]. In order for a GGA to be accurate for atoms and molecules, Perdew and coworkers [16] demonstrated that the parameter γ must be approximately twice as large, $\gamma \approx 2\gamma_{\text{DGE}}$.

For example, the Perdew–Burke–Ernzerhof GGA [22] has $\gamma = 0.0042348$, while the Becke exchange GGA [23] has $\gamma = 0.0052917$.

We will now show that the Q-LB94 functional recovers the DGE up to the second order but its coefficient γ is very different from the exact result. In the limit of small s , the function $Q(s)$ of Eq. (5.10) becomes

$$Q(s) = \frac{3}{2^{2/3}}\beta s^2 + \dots \quad (s \rightarrow 0). \quad (5.15)$$

It has the desired quadratic behavior in s , but the second-order gradient expansion coefficient of the Q-LB94 is $\gamma = 3\beta/2^{2/3} \approx 0.094494$, a value 40 times greater than γ_{DGE} ! Since γ is too high, the function $Q(s)$ is too large, and the energies are too low.

Physically, there is no reason why the value of β in the Q-LB94 functional should be the same as in the original LB94 potential. First, the LB94 potential is not the functional derivative of the Q-LB94 functional. Second, the value of β in the LB94 potential is an empirical parameter that was fitted to reproduce the correct shape of the exchange-correlation potential, not accurate energies. The argument of Perdew and coworkers [16] applied to Eq. (5.15) suggests that, in order to make the Q-LB94 functional accurate for chemically relevant systems, we should revise the value of β from 0.05 to

$$\beta_{\text{rev}} = \frac{2^{2/3}}{3}(2\gamma_{\text{DGE}}) \approx 0.0025. \quad (5.16)$$

We call the functional utilizing the updated value of β Q-revLB94. To be clear, the Q-revLB94 functional is given by the same Eq. (5.9) as the Q-LB94, but uses $\beta_{\text{rev}} = 0.0025$ instead of $\beta = 0.05$.

5.3.3 Performance of the Q-revLB94 functional

Table 5.2 compares the total energies computed using Λ -LB94, Q-LB94, Q-revLB94 functionals with the energies from standard exchange-only density-functional approximations, B88 and PBE. All calculations were performed in a post-SCF fashion using HF/UGBS densities. This was done for fair comparison with Λ -LB94 and Q-LB94, which are difficult to converge for certain atoms. There were no convergence problems with the Q-revLB94 functional. One can see that the energies from the Λ -LB94 functional are not very accurate, with a mean absolute percentage error (MAPE) of 1.07%. The Q-LB94 energies are even worse, with MAPE = 6.35%. But the Q-revLB94 (MAPE = 0.070%) is a dramatic improvement over the Λ -LB94 and Q-LB94 approximations. In fact, it is comparable in accuracy to the B88 and PBE function-

Table 5.2: Total ground-state energies (in units of E_h) of a set of spherical atoms computed using various exchange-only approximations. All calculations are a single SCF cycle over the HF/UGBS density.

Atom	Λ -LB94	Q-LB94	Q-revLB94	B88	PBE	Exact ^a
H	-0.4664	-0.6310	-0.5009	-0.4973	-0.4934	-0.5000
He	-2.8206	-3.3139	-2.8727	-2.8614	-2.8495	-2.8617
Li	-7.3559	-8.1970	-7.4439	-7.4268	-7.4088	-7.4325
Be	-14.5424	-15.7067	-14.5846	-14.5640	-14.5419	-14.5724
N	-54.5963	-56.9662	-54.4165	-54.3940	-54.3500	-54.4034
Ne	-129.4297	-133.0534	-128.5854	-128.5766	-128.5054	-128.5455
Na	-162.8592	-166.9852	-161.8774	-161.8718	-161.7920	-161.8567
Mg	-200.8990	-205.4029	-199.6198	-199.6208	-199.5351	-199.6116
P	-342.4060	-348.5952	-340.6852	-340.6989	-340.5796	-340.7151
Ar	-529.1727	-537.0223	-526.7534	-526.7859	-526.6285	-526.8123
Ca	-679.7703	-688.5452	-676.6900	-676.7393	-676.5625	-676.7520
Zn	-1785.4706	-1799.2681	-1777.9199	-1778.0704	-1777.7348	-1777.8345
Kr	-2761.9209	-2779.4431	-2751.8578	-2752.0704	-2751.6239	-2752.0431
MAPE ^b (%)	1.07	6.35	0.070	0.059	0.200	

^aExact exchange-only total energies from Ref. 24.

^bMean absolute percentage error: $\text{MAPE} = \frac{1}{n} \sum_{i=1}^n \left| \frac{E_i - E_{\text{exact},i}}{E_{\text{exact},i}} \right|$.

als. Compared to the Λ -LB94 energy expression, the Q-revLB94 functional is not only more accurate but also gives energies that are position-independent. This makes the Q-revLB94 approximation suitable for calculating forces acting on the nuclei and for performing geometry optimizations.

5.3.4 The Q-revLB94 exchange potential

The functional derivative of Q-revLB94 has a shape similar to that of other popular approximations for exchange, as Fig. 5.2 shows. The exchange-only GGA potentials B88, PBE, and Q-revLB94 are almost indistinguishable on the scale shown. This is due to the like behavior of accurate exchange functionals for slowly varying densities, which makes their functional derivatives similar near the nucleus, where s is small. Compared to the GGA potentials, LB94 is more negative almost everywhere and does not have a singularity at the origin. The differences in the large- r behavior of the four potentials examined here are emphasized by plots of $rv_X(r)$, which are shown in Fig. 5.3. It is seen from this figure that the LB94 potential decays roughly as $-1/r$, whereas the other three potentials decay much faster.

To deduce the asymptotic behavior of Q-revLB94 potential we need to analyze its $s \rightarrow \infty$ limit (because s becomes infinitely large as $r \rightarrow \infty$). From Eq. (5.10) we have $Q(s) \sim 8s(\xi s)^3 E_1(3 \ln 2\xi s)$, where $E_1(z)$ is the exponential integral [25]. Using the asymptotic expansion formula for $E_1(z)$ (identity 5.1.20 in Ref. 25), we obtain

$$Q(s) \sim \frac{1}{3} \frac{s}{\ln 2\xi s} \quad (s \rightarrow \infty), \quad (5.17)$$

which is similar to the asymptotic behavior of the B88 gradient correction, except that the B88 analog of $Q(s)$ has a prefactor $1/6$ instead of $1/3$. (This occurs because the Q-revLB94 functional is based on the LB94 potential which in turn uses a B88-style gradient correction.) Finally, substituting an exponentially decaying density $\rho = e^{-ar}$ into Eqs. (5.12) and (5.17), we find that

$$v_X^{\text{Q-revLB94}} \sim -\frac{5}{ar^2} \quad (r \rightarrow \infty), \quad (5.18)$$

where a is a constant. For comparison, the B88 exchange potential decays as $-5/2ar^2$ (see Ref. 26), and PBE as $-ce^{-ar/3}$, where c is another constant.

Because the LB94 potential is more negative almost everywhere and decays more slowly than the Q-revLB94, B88, and PBE potentials, the quality of the highest occupied molecular orbital (HOMO) energies obtained with the LB94 potential is

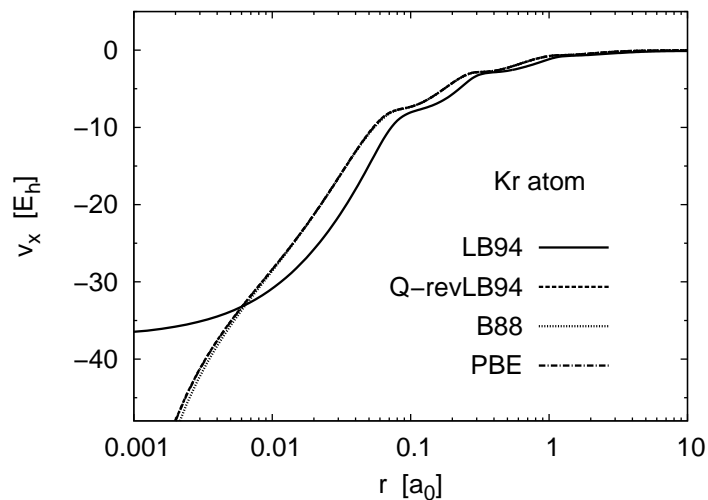


Figure 5.2: Exchange part of the LB94 model potential compared with functional derivatives of the Q-revLB94, B88, and PBE exchange functionals. All potentials are constructed for the Kr atom using the HF/UGBS density. The Q-revLB94, B88, and PBE curves are barely distinguishable at a given scale.

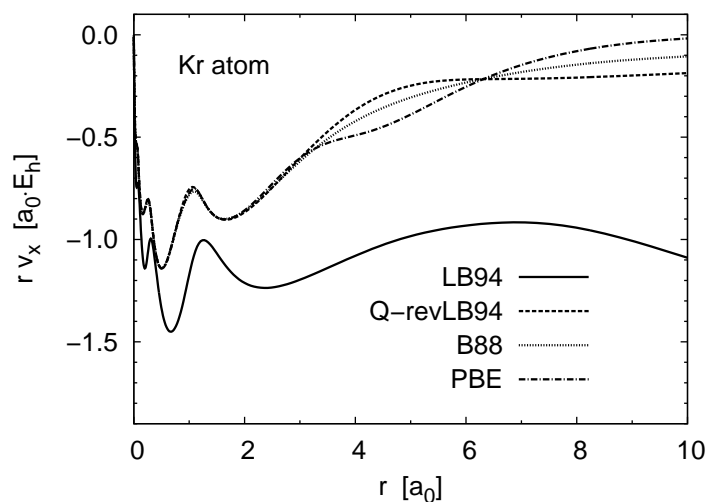


Figure 5.3: Same as Fig. 5.2 but with the potentials multiplied by r to emphasize the asymptotic region of the atom. The correct asymptote is a horizontal line at -1 .

Table 5.3: Negative of the HOMO energy (in units of eV) obtained from various exchange-only approximations. All calculations are self-consistent and use the UGBS.

Atom	Λ -LB94	Q-revLB94	B88	PBE	Exact ^a
H	11.32	7.39	7.41	7.37	13.61
He	21.62	15.02	15.08	15.05	24.98
Li	4.77	2.96	2.97	2.97	5.34
Be	7.67	4.90	4.94	4.94	8.41
N	12.94	7.64	7.74	7.74	15.54
Ne	19.69	12.21	12.37	12.39	23.15
Na	5.04	2.74	2.79	2.79	4.96
Mg	6.86	3.99	4.05	4.06	6.88
P	9.21	5.66	5.71	5.72	10.66
Ar	14.36	9.20	9.30	9.32	16.08
Ca	5.61	3.09	3.15	3.15	5.32
Zn	9.22	5.03	5.15	5.16	7.97
Kr	13.05	8.21	8.30	8.32	14.24
MAE ^b	1.46	5.32	5.24	5.24	

^aExact exchange-only HOMO eigenvalues from Ref. 24.

^bMean absolute error.

better than from the other three approximations (Table 5.3). This means that the Q-revLB94 potential will not perform better than the B88 and PBE approximations in calculations of response properties such as polarizabilities and excitation energies in time-dependent density functional theory.

5.4 Relation to other methods

Application of our method to the LB94 potential produces a competitively accurate exchange GGA. In Chapter 3 we described the construction of another GGA from the same model potential, using a different approach. In that case, we started with the LB94 potential, completed it to a functional derivative, and then recovered the parent functional. Here, we first assign a functional to the LB94 potential and then use that functional to obtain the functional derivative. Since neither completion to a functional derivative nor line integration is unique for stray potentials, the Q-revLB94 functional and the functional of Chapter 3 are different. The approach based on line integrals is more flexible.

Our method is also related to the procedure for constructing the “unambiguous energy density” proposed by Burke *et al.* [27, 28]. For exchange potentials, Burke’s

method amounts to defining the functional,

$$E_X[\rho] = -\frac{3}{4\pi} \int d\mathbf{r}' \int d\mathbf{r} \frac{\nabla \cdot [\rho(\mathbf{r}) \nabla v_X([\rho]; \mathbf{r})]}{|\mathbf{r} - \mathbf{r}'|}. \quad (5.19)$$

This expression is essentially a gauge transformation of the Levy–Perdew virial energy density carried out using the Helmholtz decomposition. Burke and co-workers intended Eq. (5.19) to be used with functional derivatives of standard density-functional approximations (such as LDA, PBE, and BLYP) as a way of eliminating the ambiguity of conventional energy densities. But, of course, their method may be also used to construct energy functionals from stray model potentials. Unfortunately, Eq. (5.19) is not very practical because it requires real-space integration over \mathbf{r} for each grid point \mathbf{r}' . Our method involves only a one-dimensional quadrature at every real-space grid point, so it is easier to implement and has a lower computational cost.

5.5 Conclusion

Assigning energy to stray model potentials always involves some degree of arbitrariness. Exchange energies computed via the Levy–Perdew virial relation (i.e., by line integration along a path of uniformly scaled density) are quite reasonable, provided that a model potential has a realistic shape. However, Levy–Perdew energies are not invariant with respect to molecular translations and rotations. By choosing an integration path that does not involve coordinate scaling, one can ensure proper invariance of the energies obtained from a stray model potential, but often at the expense of the accuracy of the resulting energy expression.

In this work, we adopt a different view of line integration as an instrument for designing new density-functional approximations using stray model potentials as starting points. The resulting functionals are not expected to automatically yield good energies and may require fine-tuning. The modification may be as simple as adjusting a parameter to satisfy an exact constraint. This strategy proved quite effective in deriving the Q-revLB94 functional starting with the LB94 model potential. This new functional is properly invariant and yields better energies than the Levy–Perdew relation.

Bibliography

- [1] M. Levy and J. P. Perdew, “Hellmann–Feynman, virial, and scaling requisites for the exact universal density functionals. Shape of the correlation potential and diamagnetic susceptibility for atoms”, *Phys. Rev. A* **32**, 2010 (1985).
- [2] O. Gritsenko, R. van Leeuwen, E. van Lenthe, and E. J. Baerends, “Self-consistent approximation to the Kohn–Sham exchange potential”, *Phys. Rev. A* **51**, 1944 (1995).
- [3] R. van Leeuwen and E. J. Baerends, “Exchange–correlation potential with correct asymptotic behavior”, *Phys. Rev. A* **49**, 2421 (1994).
- [4] D. J. Tozer, “The asymptotic exchange potential in Kohn–Sham theory”, *J. Chem. Phys.* **112**, 3507 (2000).
- [5] Y. Kurzweil and M. Head-Gordon, “Improving approximate-optimized effective potentials by imposing exact conditions: Theory and applications to electronic statics and dynamics”, *Phys. Rev. A* **80**, 012509 (2009).
- [6] V. Volterra, *Theory of Functionals and of Integral and Integro-Differential Equations*, Dover Publications, Inc., New York (1959).
- [7] R. van Leeuwen and E. J. Baerends, “Energy expressions in density-functional theory using line integrals”, *Phys. Rev. A* **51**, 170 (1995).
- [8] A. P. Gaiduk, S. K. Chulkov, and V. N. Staroverov, “Reconstruction of density functionals from Kohn–Sham potentials by integration along density scaling paths”, *J. Chem. Theory Comput.* **5**, 699 (2009).
- [9] P. D. Elkind and V. N. Staroverov, “Energy expressions for Kohn–Sham potentials and their relation to the Slater–Janak theorem”, *J. Chem. Phys.* **136**, 124115 (2012).

- [10] M. Levy, “Coordinate scaling requirements for approximating exchange and correlation”, in *Density Functional Theory*, edited by E. K. U. Gross and R. M. Dreizler, Plenum Press, New York, pp. 11–31 (1995).
- [11] M. Levy and J. P. Perdew, “Density functionals for exchange and correlation energies: Exact conditions and comparison of approximations”, *Int. J. Quantum Chem.* **49**, 539 (1994).
- [12] S. Liu and R. G. Parr, “Expansion of the correlation-energy density functional $E_c[\rho]$ and its kinetic-energy component $T_c[\rho]$ in terms of homogeneous functionals”, *Phys. Rev. A* **53**, 2211 (1996).
- [13] G. K.-L. Chan and N. C. Handy, “Kinetic-energy systems, density scaling, and homogeneity relations in density-functional theory”, *Phys. Rev. A* **59**, 2670 (1999).
- [14] Á. Nagy, “Density scaling and exchange-correlation energy”, *J. Chem. Phys.* **123**, 044105 (2005).
- [15] R. C. Morrison, P. W. Ayers, and Á. Nagy, “Density scaling and relaxation of the Pauli principle”, *J. Chem. Phys.* **126**, 124111 (2007).
- [16] J. P. Perdew, L. A. Constantin, and E. Sagvolden, “Relevance of the slowly varying electron gas to atoms, molecules, and solids”, *Phys. Rev. Lett.* **97**, 223002 (2006).
- [17] H. Ou-Yang and M. Levy, “Nonuniform coordinate scaling requirements in density-functional theory”, *Phys. Rev. A* **42**, 155 (1990).
- [18] M. J. Frisch, G. W. Trucks, H. B. Schlegel, G. E. Scuseria, M. A. Robb, J. R. Cheeseman, J. J. A. Montgomery, T. Vreven, G. Scalmani, B. Mennucci, V. Barone, G. A. Petersson, M. Caricato, H. Nakatsuji, M. Hada, M. Ehara, K. Toyota, R. Fukuda, J. Hasegawa, M. Ishida, T. Nakajima, Y. Honda, O. Kitao, H. Nakai, X. Li, H. P. Hratchian, J. E. Peralta, A. F. Izmaylov, K. N. Kudin, J. J. Heyd, E. Brothers, V. Staroverov, G. Zheng, R. Kobayashi, J. Normand, J. L. Sonnenberg, S. S. Iyengar, J. Tomasi, M. Cossi, N. Rega, J. C. Burant, J. M. Millam, M. Klene, J. E. Knox, J. B. Cross, V. Bakken, C. Adamo, J. Jaramillo, R. Gomperts, R. E. Stratmann, O. Yazyev, A. J. Austin, R. Cammi, C. Pomelli, J. W. Ochterski, P. Y. Ayala, K. Morokuma, G. A. Voth, P. Salvador, J. J. Dannenberg, V. G. Zakrzewski, S. Dapprich, A. D. Daniels, M. C. Strain,

- Ö. Farkas, D. K. Malick, A. D. Rabuck, K. Raghavachari, J. B. Foresman, J. V. Ortiz, Q. Cui, A. G. Baboul, S. Clifford, J. Cioslowski, B. B. Stefanov, G. Liu, A. Liashenko, P. Piskorz, I. Komaromi, R. L. Martin, D. J. Fox, T. Keith, M. A. Al-Laham, C. Y. Peng, A. Nanayakkara, M. Challacombe, W. Chen, M. W. Wong, and J. A. Pople, “Gaussian Development Version, Revision F.02”, Gaussian Inc., Wallingford, CT (2006).
- [19] W. H. Press, S. A. Teukolsky, W. T. Vetterling, and B. P. Flannery, *Numerical Recipes. The Art of Scientific Computing*, Cambridge University Press, Cambridge, 3rd ed. (2007).
- [20] J. P. Perdew and S. Kurth, “Density functionals for non-relativistic Coulomb systems in the new century”, in *A Primer in Density Functional Theory*, edited by C. Fiolhais, F. Nogueira, and M. Marques, Springer, Berlin (2003).
- [21] P. R. Antoniewicz and L. Kleinman, “Kohn–Sham exchange potential exact to first order in $\rho(\mathbf{K})/\rho_0$ ”, *Phys. Rev. B* **31**, 6779 (1985).
- [22] J. P. Perdew, K. Burke, and M. Ernzerhof, “Generalized gradient approximation made simple”, *Phys. Rev. Lett.* **77**, 3865 (1996).
- [23] A. D. Becke, “Density-functional exchange-energy approximation with correct asymptotic behavior”, *Phys. Rev. A* **38**, 3098 (1988).
- [24] E. Engel and S. H. Vosko, “Accurate optimized-potential-model solutions for spherical spin-polarized atoms: Evidence for limitations of the exchange-only local spin-density and generalized-gradient approximations”, *Phys. Rev. A* **47**, 2800 (1993).
- [25] M. Abramowitz and I. A. Stegun, *Handbook of Mathematical Functions with Formulas, Graphs, and Mathematical Tables*, Dover, New York (1964).
- [26] E. Engel, J. A. Chevary, L. D. Macdonald, and S. H. Vosko, “Asymptotic properties of the exchange energy density and the exchange potential of finite systems: Relevance for generalized gradient approximations”, *Z. Phys. D: At., Mol. Clusters* **23**, 7 (1992).
- [27] K. Burke, F. G. Cruz, and K.-C. Lam, “Unambiguous exchange-correlation energy density”, *J. Chem. Phys.* **109**, 8161 (1998).

- [28] K. Burke, F. G. Cruz, and K.-C. Lam, “Unambiguous exchange-correlation energy density for Hooke’s atom”, *Int. J. Quantum Chem.* **70**, 583 (1998).

Chapter 6

Self-interaction correction scheme for Kohn–Sham potentials

6.1 Introduction

In the Kohn–Sham density functional theory, electrons move in an electric field described by a multiplicative Kohn–Sham potential $v_s(\mathbf{r})$. The electronic part of v_s is the Hartree-exchange-correlation (HXC) potential v_{HXC} given by Eq. (1.14). The v_{HXC} describes interaction of each electron with the field created by the remaining $N - 1$ electrons in the system, and behaves asymptotically as $(N - 1)/r$. The v_{HXC} is further partitioned into a sum of the Hartree v_{H} [Eq. (1.15)] and the exchange-correlation v_{XC} potentials [Eq. (1.16)]. Of these two, the Hartree term includes the spurious self-interaction of each electron with itself and has the N/r asymptotic decay. This implies that the exact exchange-correlation potential should fall off as $-1/r$. Unfortunately, most approximations to v_{XC} decay faster than $-1/r$ and hence do not cancel out the self-interaction part of v_{H} completely. The resulting error in v_{HXC} , termed *self-interaction error*, causes the effective Kohn–Sham potential to be more repulsive than it should be at intermediate and large r [1, 2]. One immediate consequence of this aberration is a collapse of the virtual Kohn–Sham orbital eigenvalue spectrum, which translates into poor description of response properties [3–6].

In this Chapter, we propose a self-interaction correction (SIC) motivated by a

Reprinted in part with permission from **A. P. Gaiduk**, D. Mizzi, and V. N. Staroverov, “Self-interaction correction scheme for approximate Kohn–Sham potentials”, *Phys. Rev. A* **86**, 052518 (2012). Copyright 2012, American Physical Society.

Reprinted in part with permission from **A. P. Gaiduk**, D. S. Firaha, and V. N. Staroverov, “Improved electronic excitation energies from shape-corrected semilocal Kohn–Sham potentials”, *Phys. Rev. Lett.* **108**, 253005 (2012). Copyright 2012, American Physical Society.

fractional charge perspective on density functional theory [7]. We demonstrate application of our method to the calculation of vertical ionization and excitation energies. We also emphasize a unifying point of view according to which our method, the Slater transition-state technique [8–11], and the $X\alpha$ approximations [9] are all different forms of self-interaction correction for approximate exchange–correlation potentials.

6.2 Self-interaction error in Kohn–Sham potentials

Consider the ground-state hydrogen atom. For this system, $v_{\text{HXC}}(\mathbf{r})$ must vanish identically because a single electron does not interact with itself. Most approximate exchange–correlation potentials, however, violate the condition $v_{\text{HXC}}(\mathbf{r}) = 0$. This is illustrated in Fig. 6.1 for the local density approximation with the Perdew–Wang parametrization of the correlation energy [12].

In many-electron atoms and molecules, the exact v_{HXC} is of course no longer zero, but the symptoms of the self-interaction error are similar: a typical approximate v_{HXC} is not sufficiently negative at medium and large r , and decays too fast. This is illustrated in Fig. 6.2 by the example of an LDA calculation on the Ne atom. Note that here v_{HXC} is dominated by the Hartree potential, while the contribution of v_{XC} is relatively small. Generalized gradient approximations such as the Perdew–Burke–Ernzerhof exchange–correlation functional [13] yield similar curves (not shown), except that v_{XC} and v_{HXC} tend to $-\infty$ at the nucleus.

A useful measure of how strongly an approximate Hartree–exchange–correlation potential deviates from $v_{\text{HXC}}^{\text{exact}}$ is the corresponding HOMO eigenvalue, ϵ_{HOMO} . From Eqs. (1.12) and (1.13) we have

$$\epsilon_{\text{HOMO}} = \langle \phi_{\text{HOMO}} | -\frac{1}{2} \nabla^2 + v + v_{\text{HXC}} | \phi_{\text{HOMO}} \rangle. \tag{6.1}$$

For the H atom, the exact $v_{\text{HXC}} = 0$ with the exact $1s$ hydrogenic orbital $\phi(\mathbf{r}) = e^{-r}/\sqrt{\pi}$ yields the exact eigenvalue $\epsilon_{\text{HOMO}} = -0.5 E_{\text{h}}$, whereas the self-consistent LDA and PBE potentials give $\epsilon_{\text{HOMO}} = -0.269$ and $\epsilon_{\text{HOMO}} = -0.279 E_{\text{h}}$, respectively. Differences between exact and approximate ϵ_{HOMO} values for many-electron atoms are of similar magnitude.

The self-interaction error in Kohn–Sham potentials can be also analyzed by considering the behavior of ϵ_{HOMO} as a function of the HOMO occupation number. When

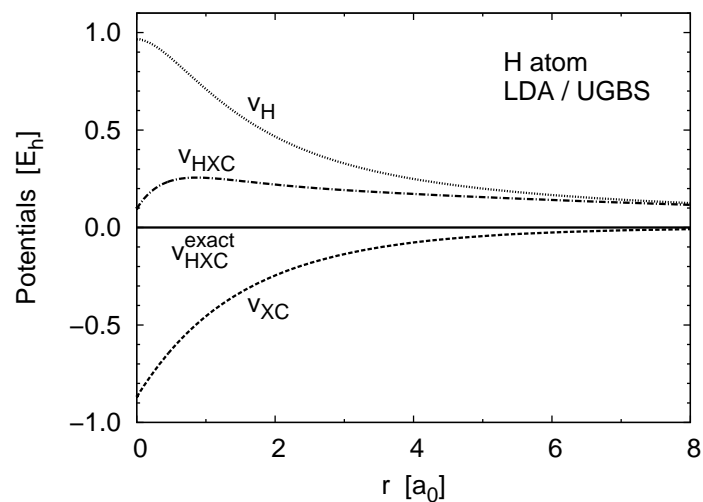


Figure 6.1: Self-consistent Hartree and LDA exchange-correlation potentials for the hydrogen atom. Here the entire difference between v_{HXC} and v_{HXC}^{exact} is the self-interaction error. The potentials depicted in this figure were calculated using the universal Gaussian basis set of Ref. 14.

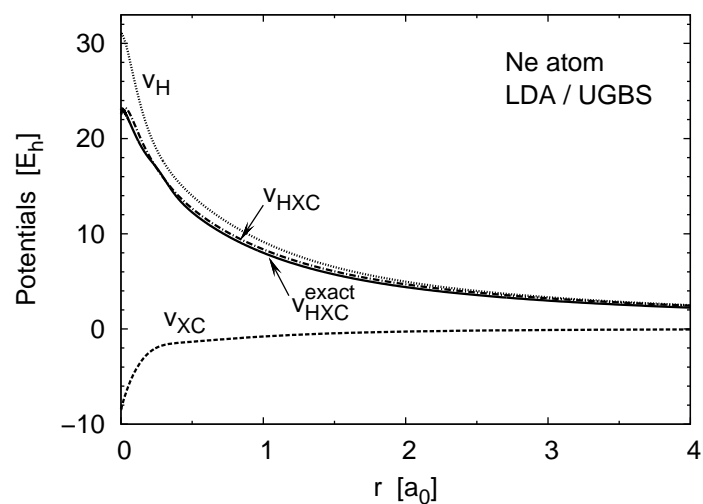


Figure 6.2: Self-consistent Hartree and LDA exchange-correlation potentials for the neon atom. The exact exchange-correlation potential is from Ref. 15.

a fraction δ of an electron is removed from the HOMO, the density becomes

$$\tilde{\rho}(\mathbf{r}) = \rho(\mathbf{r}) - \delta|\phi_{\text{HOMO}}(\mathbf{r})|^2. \quad (6.2)$$

Here and below, we call the parameter δ the HOMO depopulation. To study ϵ_{HOMO} as a function of δ , we construct the potential $v_{\text{HXC}}([\tilde{\rho}]; \mathbf{r})$ using the electron-deficient density $\tilde{\rho}(\mathbf{r})$ and then solve the Kohn–Sham equations self-consistently. Recall that in the fractional occupation formalism, ϵ_{HOMO} and the total electronic energy E are related by the Slater–Janak theorem [16],

$$\epsilon_{\text{HOMO}}(n) = \frac{\partial E(n)}{\partial n}, \quad (6.3)$$

where $n = 1 - \delta$. In the exact Kohn–Sham DFT, E is a linkage of straight-line segments between consecutive integer electron numbers [7, 17–19]; the slope of each segment between $J - 1$ and J is the vertical ionization energy (VIE) of the J -electron system. By Eq. (6.3) this implies that a plot of the exact ϵ_{HOMO} as a function of δ ($0 < \delta < 1$) should be a horizontal straight line drawn at $\epsilon_{\text{HOMO}} = -\text{VIE}$. It is known that nearly all approximate density functionals violate this constraint [20–23], as illustrated in Figs. (6.3) and (6.4) by the examples of the LDA, PBE, Tao–Perdew–Staroverov–Scuseria (TPSS) [24], and hybrid PBE (PBE0) [25] functionals. The deviation of $\epsilon_{\text{HOMO}}(n)$ from the exact horizontal line or, equivalently, the deviation of $E(n)$ from linearity have been termed the many-electron self-interaction error. Now let us show how this error can be reduced.

6.3 Self-interaction correction for Kohn–Sham potentials

Observe that each curve in Figs. 6.3 and 6.4 crosses the exact straight line near $\delta = 1/2$. This suggests that the shape of the LDA, PBE, TPSS, and PBE0 exchange–correlation potentials as functions of δ improves the most when about half an electron is removed from the HOMO. To verify this assumption for the H atom, we plotted the sum of Hartree and PBE exchange–correlation potentials for 10 values of δ varying between 0 and 0.9 (see Fig. 6.5). This figure shows that the smallest *average* deviation of $v_{\text{HXC}}([\tilde{\rho}]; \mathbf{r})$ from the exact $v_{\text{HXC}}(\mathbf{r})$ occurs at $\delta \approx 1/2$. Similar results were obtained for the H atom using the LDA exchange–correlation potential (not shown).

It is not difficult to see how the HOMO depopulation works. For a hydrogen

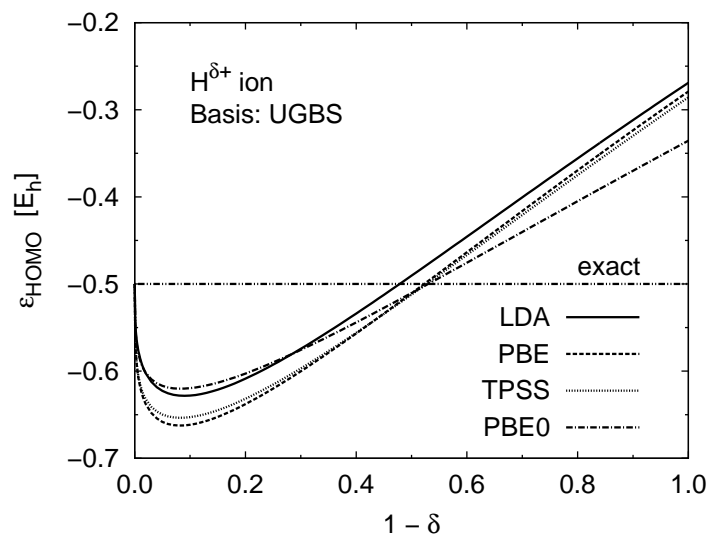


Figure 6.3: HOMO ($1s$) eigenvalue for a hydrogen atom as a function of the HOMO depopulation δ . All eigenvalues are from self-consistent potentials including exchange and correlation.

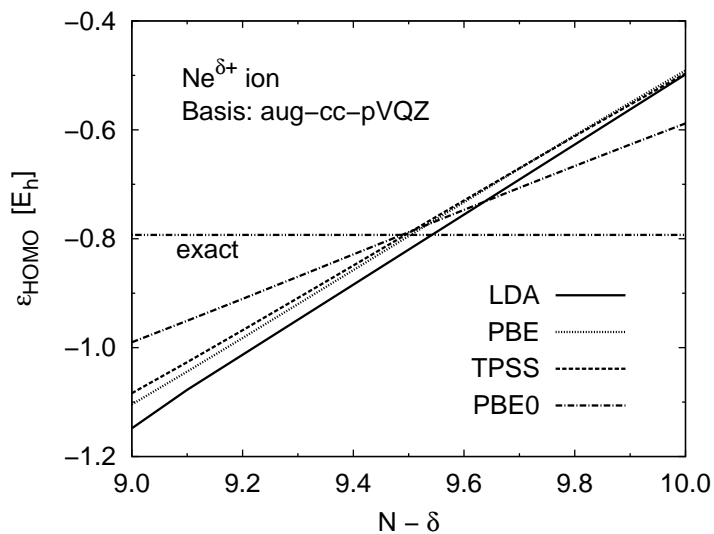


Figure 6.4: HOMO ($2p_z$) eigenvalue for a neon atom as a function of the HOMO depopulation δ . All eigenvalues are from self-consistent potentials including exchange and correlation.

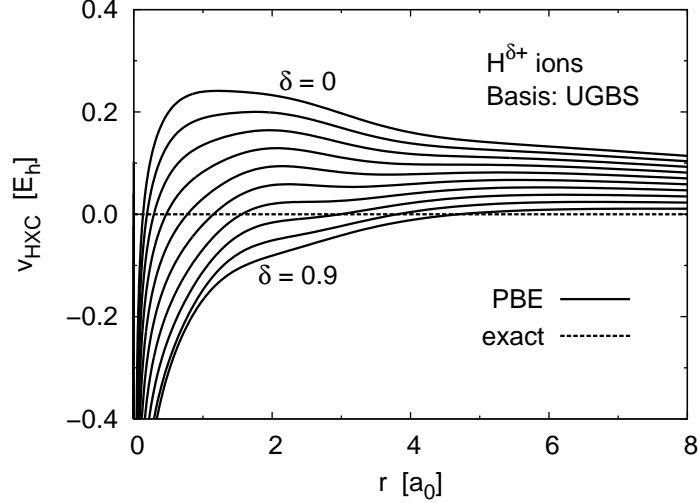


Figure 6.5: The sum of self-consistent Hartree and PBE exchange-correlation potentials of a hydrogen atom for 10 values of the HOMO depopulation from $\delta = 0$ to $\delta = 0.9$ with a step of 0.1.

atom, $v_H([\tilde{\rho}]; \mathbf{r})$ is linear in δ , whereas $v_{XC}([\tilde{\rho}]; \mathbf{r})$ scales roughly as $\delta^{1/3}$. As δ increases, $v_H([\tilde{\rho}]; \mathbf{r})$ decreases faster than $v_{XC}([\tilde{\rho}]; \mathbf{r})$ increases, so their sum $v_{HXC}([\tilde{\rho}]; \mathbf{r})$ becomes more negative. At $\delta \approx 1/2$, the potential $v_{HXC}([\tilde{\rho}]; \mathbf{r})$ is on average closest to the exact v_{HXC} in such a way that ϵ_{HOMO} becomes exact. The precise value of δ at which ϵ_{HOMO} becomes exact can be determined for any one-electron system by solving the equation

$$\langle \phi_{\text{HOMO}} | -\frac{1}{2} \nabla^2 + v + v_H[\tilde{\rho}] + v_{XC}[\tilde{\rho}] | \phi_{\text{HOMO}} \rangle = -\frac{1}{2}. \quad (6.4)$$

In particular, within the exchange-only LDA, analytic solution of Eq. (6.4) for the exact hydrogenic $1s$ orbital yields $\delta = 1 - 243\sqrt{5}/400\pi \approx 0.568$. For the self-consistent LDA, PBE, TPSS, and PBE0 potentials whose eigenvalues are plotted in Fig. 6.4, the solutions are $\delta = 0.522, 0.477, 0.473,$ and 0.470 , respectively.

In many-electron systems, the asymptotic region of the electron density is dominated by the HOMO, so the large- r behavior of v_{HXC} should be improved by depopulating the HOMO alone. Moreover, Fig. 6.4 suggests that the greatest improvement of the HOMO energy should again occur at $\delta \approx 1/2$. To verify this conjecture we could compare $v_{HXC}([\tilde{\rho}]; \mathbf{r})$ and $v_{HXC}([\rho]; \mathbf{r})$ to the exact Hartree-exchange-correlation potential. However, since the effect of HOMO depopulation in many-electron systems is very small on the scale of v_{HXC} , it is better to compare the uncorrected $v_{XC}([\rho]; \mathbf{r})$

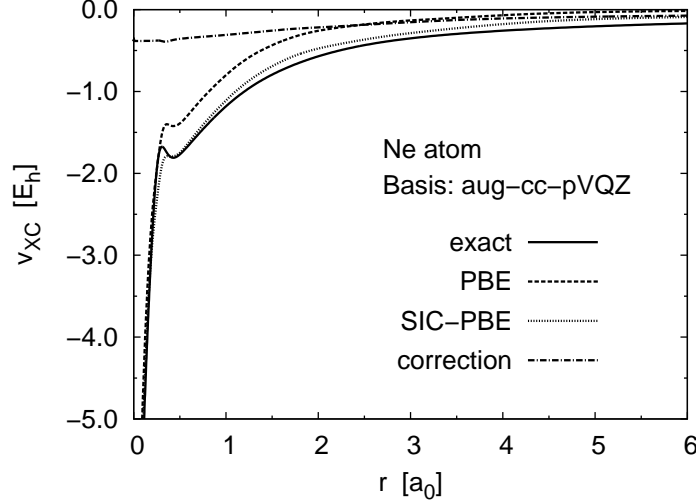


Figure 6.6: Self-consistent PBE exchange-correlation potential for the Ne atom with and without fractional depopulation of the spin-up $2p_z$ orbital ($\delta = 1/2$). The curve labeled SIC-PBE is the spin-up potential plotted along the z axis. The exact v_{XC} is from Ref. 15. The ‘correction’ is the difference between the SIC-PBE and PBE curves.

and the self-interaction-corrected potential defined by

$$v_{XC}^{\text{SIC}}(\mathbf{r}) = v_{\text{HXC}}([\tilde{\rho}]; \mathbf{r}) - v_{\text{H}}([\rho]; \mathbf{r}). \quad (6.5)$$

The SIC potential may be alternatively written as

$$v_{XC}^{\text{SIC}}(\mathbf{r}) = v_{XC}([\rho]; \mathbf{r}) + \Delta v_{XC}(\mathbf{r}), \quad (6.6)$$

where $\Delta v_{XC}(\mathbf{r})$ is the correction defined as

$$\Delta v_{XC}(\mathbf{r}) = v_{\text{HXC}}([\tilde{\rho}]; \mathbf{r}) - v_{\text{HXC}}([\rho]; \mathbf{r}). \quad (6.7)$$

Figure 6.6 shows that the SIC-PBE ($\delta = 1/2$) exchange-correlation potential of a Ne atom is indeed much closer to the exact v_{XC} than the uncorrected ($\delta = 0$) potential, especially in the middle- r range. Similar results are found for other systems and density functionals.

The effect of HOMO depopulation on $v_{XC}(\mathbf{r})$ in Fig. 6.6 resembles the effect of renormalizing the exchange-correlation charge [2, 26–29], which suggests that the physics underlying both approaches is similar. To a first approximation, HOMO depopulation creates a spherical layer (shell) of positive charge $+\delta$ distributed over

the valence region of the atom. The potential of this charged shell is constant inside the shell and decays as $-\delta/r$ outside the shell. According to this model, the asymptotic behavior of SIC-PBE exchange-correlation potential is $-1/2r$. This is not the exact $-1/r$ decay, but it is more realistic than the exponential decay of the uncorrected PBE potential. In any case, the shape of $v_{\text{XC}}(\mathbf{r})$ at $r \rightarrow \infty$ matters less than at $0.5 \lesssim r \lesssim 3a_0$, where the SIC-PBE potential mimics the exact $v_{\text{XC}}(\mathbf{r})$ quite well.

Let us summarize. The shape of Hartree-exchange-correlation potentials is improved if they are constructed from the density $\tilde{\rho}$ with the depopulated HOMO. Our correction amounts to reducing the self-interaction error in $v_{\text{HXC}}(\mathbf{r})$ and leads to better Kohn–Sham orbitals and orbital eigenvalues. In the following two sections, we will demonstrate the practical capabilities of our approach by computing vertical ionization energies and electronic excitation energies.

6.4 Vertical ionization energies

Our results suggest that the quality of approximate HOMO eigenvalues is at its best when the HOMO depopulation is $\delta \approx 1/2$. At this δ , the HOMO eigenvalue becomes a much better estimate of the VIE than at $\delta = 0$. The procedure for computing the VIE as $\epsilon_{\text{HOMO}}(\delta = 1/2)$ is actually a very old technique known as the Slater transition-state [8, 9] or half-ion [10, 11] method. In the usual justification of this procedure, the VIE is written using Eq. (6.3) as

$$\text{VIE} = E(N - 1) - E(N) = - \int_0^1 \epsilon_{\text{HOMO}}(n) \, dn, \tag{6.8}$$

where $n = 1 - \delta$. The argument is then made that the function $\epsilon_{\text{HOMO}}(n)$ is roughly linear (at least, for many-electron systems), so the integral in Eq. (6.8) must be well approximated as

$$\text{VIE} \approx -\epsilon_{\text{HOMO}}(n = 1/2). \tag{6.9}$$

Figures 6.3 and 6.4 provide an even more direct explanation of why Eq. (6.9) works—because the plot of $\epsilon_{\text{HOMO}}(n)$ crosses the exact value of ϵ_{HOMO} near $n = 1 - \delta = 1/2$. From this point of view, Slater’s transition-state method is a self-interaction correction scheme for approximate Hartree-exchange-correlation potentials.

The dramatic effect of switching from $v_{\text{HXC}}([\rho]; \mathbf{r})$ to $v_{\text{HXC}}([\tilde{\rho}]; \mathbf{r})$ is illustrated in Table 6.1. The mean absolute error in VIEs is reduced by more than an order of magnitude by applying the correction. The outliers are the halogenated hydrocar-

Table 6.1: Vertical ionization energies (in eV) determined as $-\epsilon_{\text{HOMO}}$ from LDA and PBE exchange-correlation potentials with and without HOMO depopulation. All calculations use the cc-pVQZ basis set. Some LDA calculations with fractional occupations could not be converged (‘n/c’).

System	LDA	SIC-LDA	PBE	SIC-PBE	Expt. ^a
	$\delta = 0$	$\delta = 1/2$	$\delta = 0$	$\delta = 1/2$	
He	15.49	24.56	15.73	24.92	24.59
Li	3.16	5.58	3.22	5.66	5.39
Be	5.60	9.06	5.61	9.04	9.32
Ne	13.37	n/c	13.14	21.61	21.56
Na	3.08	5.44	3.04	5.36	5.14
Mg	4.78	7.74	4.70	7.61	7.65
Ar	10.38	n/c	10.26	15.70	15.76
H ₂ O	7.16	13.08	7.01	12.73	12.62
CO	9.08	14.11	9.00	13.92	14.01
CH ₂ O	6.30	10.90	6.21	10.72	10.1
HCOOH	6.83	11.38	6.64	11.07	11.5
CH ₄	9.47	14.05	9.45	13.96	13.6
CH ₂ F ₂	8.16	12.50	8.06	12.36	13.27
CFCl ₃	7.84	10.98	7.70	10.81	11.76
CCl ₄	7.79	n/c	7.65	10.53	11.69
Acrolein	6.10	10.04	5.95	9.80	10.15
Furan	5.84	9.19	5.63	8.88	8.88
Thiophene	6.05	9.19	5.86	8.91	8.85
MAE ^b	4.41	0.34	4.50	0.35	

^aExperimental vertical ionization energies are from Ref. 32.

^bMean absolute error.

bons CH₂F₂, CFCl₃ and CCl₄, for which the error is reduced only by a factor of 4 (from roughly 4 eV to about 1 eV). Ionization energies of halogenated compounds are known to be inadequately described with standard density functionals [30, 31], so this underperformance has more to do with the LDA and PBE functionals than with the correction.

In terms of the effect on HOMO eigenvalues, the HOMO depopulation and transition-state schemes are similar to another technique proposed by Slater—the X α method [9]. In the original (nonempirical) version of the X α method, the LDA exchange potential is scaled by a constant $\alpha = 3/2$, which makes v_{HXC} more attractive and lowers the eigenvalues, just as in the transition-state scheme. The similarity between the transition state and scaling v_{X} was pointed out by Slater himself (see p. 55

in Ref. 9). We add that the optimal value α can be derived by solving the analog of Eq. (6.4), namely,

$$\langle \phi_{\text{HOMO}} | -\frac{1}{2} \nabla^2 + v + v_{\text{H}}[\rho] + \alpha v_{\text{X}}^{\text{LDA}}[\rho] | \phi_{\text{HOMO}} \rangle = \epsilon_{\text{HOMO}}^{\text{exact}}. \quad (6.10)$$

For the exact hydrogenic density, this gives $\alpha = 20(6\pi)^{2/3}/81 \approx 1.7488$, which is not far from $3/2$.

6.5 Electronic excitation energies

One of the effects of self-interaction error is inaccurate prediction of electronic excitation energies in time-dependent DFT calculations, especially for Rydberg states. This problem is successfully resolved using model potentials with correct asymptotic behavior [33]. Similar to model potentials, our self-interaction correction scheme improves the shape of exchange-correlation potentials, and may yield accurate valence-to-Rydberg excitation energies. We will test this assumption in the following Section.

6.5.1 Methodology

Before we begin, let us address one technical issue. In the transition-state method, removal of a fraction of a spin-up or spin-down electron from a doubly occupied HOMO leaves the system spin-polarized. In addition, for systems with degenerate HOMO, fractional depopulation of only one HOMO breaks the spatial symmetry of the total electron density. This is highly undesirable in TDDFT calculations. To preserve the spin state and spatial symmetry of many-electron systems with $\delta > 0$, we depopulate the entire HOMO level rather than a single orbital. That is, if a system has $m \geq 1$ occupied *spin*-orbitals at the highest occupied level, we replace the definition of $\tilde{\rho}$ in Eq. (6.2) with

$$\tilde{\rho}(\mathbf{r}) = \rho(\mathbf{r}) - \frac{\delta}{m} \sum_{i=1}^m |\phi_{\text{HOMO},i}(\mathbf{r})|^2, \quad (6.11)$$

For example, in a Be atom we remove $\delta/2$ spin-up and $\delta/2$ spin-down electrons from the $2s$ orbital. In a Ne atom, we remove $\delta/6$ electrons from each spin-orbital of the $2p$ subshell. The procedure for SIC-TDDFT calculations is similar to TDDFT with model potentials and consists of two steps: (1) do a self-consistent calculation for the $(N - \delta)$ -electron system using some standard density functional; (2) set up and solve Casida's TDDFT equations for the *all-electron* system using the orbitals, orbital energies and the functional from the first step.

The optimal δ for the SIC-TDDFT scheme described above is not guaranteed to be the same as for the vertical ionization energies. Vertical ionization energies depend on the eigenvalue of a single orbital, ϵ_{HOMO} , while excitation energies depend on the eigenvalue differences [34, 35], reproducing which may require a different value of δ . To analyze how the eigenvalue differences depend on δ , we plotted energies of the self-consistent Kohn–Sham LDA HOMO ($2s$) and the four lowest-lying virtual orbitals ($2p$, $3s$, $3p$, and $3d$) of a Be atom as functions of the HOMO depopulation (Fig. 6.7). The exact Kohn–Sham eigenvalues for the Be atom are known from the work of Savin *et al.* [34]. We see that the $2s$ and $2p$ orbital eigenvalues become exact near $\delta = 1/2$, but the $3s$, $3p$, and $3d$ eigenvalues become exact at much higher depopulations, $\delta \approx 0.8$. Nevertheless, the gaps between these orbitals become exact almost simultaneously near $\delta = 1/4$. This suggests that the LDA should give excellent excitation energies if the HOMO level is depopulated by about a quarter of electron.

Table 6.2 confirms that the use of $\delta = 1/4$ to improve the Kohn–Sham orbital gaps leads to dramatically improved Rydberg excitation energies. The uncorrected LDA is reasonably accurate in predicting the valence excitation of the Be atom ($2s \rightarrow 2p$), but Rydberg excitations are underestimated by as much as 1–1.5 eV. The SIC-LDA ($\delta = 1/4$) reduces this error to 0.1–0.4 eV and further improves the valence excitations.

6.5.2 Computational details

To benchmark our method, we applied it to a number of local, semilocal and hybrid functionals on an extensive test set. Our test set consists of 31 valence and 73 Rydberg excitation energies of three atoms (Be, Mg, and Zn) and six molecules (CO, CH₂O, C₂H₂, C₂H₄, H₂O, and N₂) at the experimental geometries [37]. To accommodate transitions to high-lying states, we used the d-aug-cc-pVQZ and d-aug-cc-pVTZ basis sets for the atoms and molecules, respectively. These are the standard aug-cc-pVQZ and aug-cc-pVTZ Gaussian basis sets taken from the EMSL Basis Set Library [38, 39] and augmented with one additional set of diffuse functions of each type (s , p , d , and so on). The exponents of these additional functions were chosen to continue the geometric progression of the two most diffuse exponents in the original basis sets and were rounded to 3 significant figures [40].

All calculations were performed using the GAUSSIAN 09 program [41] appropriately modified to allow for fractional occupations. In GAUSSIAN 09, Casida’s equations for a fixed set of Kohn–Sham orbitals and orbital eigenvalues stored in a checkpoint file can be solved using the keywords TD, Guess=Read, and SCF(MaxCyc=-1,NoVarAcc). The latter is needed to skip diagonalization of the Kohn–Sham Hamiltonian matrix, which

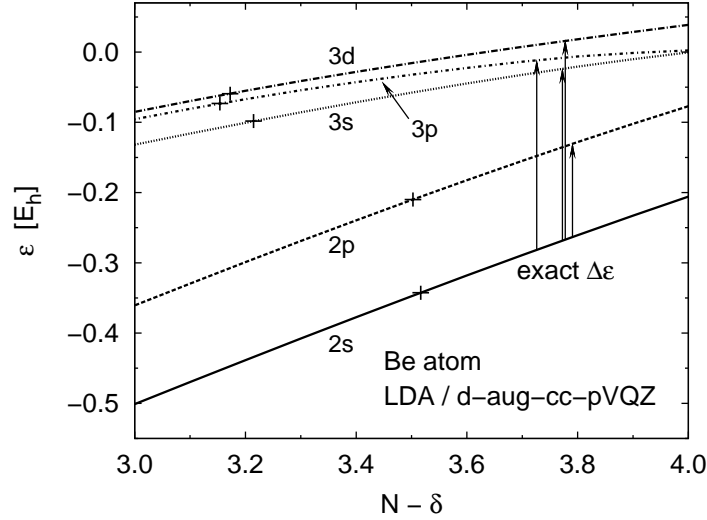


Figure 6.7: LDA orbital energies in a Be atom as functions of the HOMO depopulation. The crosses (+) mark the points where each ϵ becomes exact. The vertical arrows are drawn at those δ values for which the corresponding eigenvalue *differences* become exact. Note that the crosses are scattered whereas the arrows are clustered near $\delta = 1/4$. The exact eigenvalue of the $2s$ HOMO ($-0.3426 E_h$) was calculated as a negative of the non-relativistic fixed-nucleus ionization energy of a Be atom [36]; the exact eigenvalues of $2p$ ($-0.2099 E_h$), $3s$ ($-0.0982 E_h$), $3p$ ($-0.0732 E_h$), and $3d$ ($-0.0593 E_h$) virtual orbitals were computed from the orbital energy differences reported in Ref. 34.

Table 6.2: Kohn–Sham eigenvalue differences ($\Delta\epsilon$, eV) and TDDFT excitation energies (ω , eV) to valence (V) and Rydberg (R) states of a Be atom computed using LDA and SIC-LDA with $\delta = 1/4$. All calculations use d-aug-cc-pVQZ basis set. The computational details are the same as in Sec. 6.5.2.

State	Transition	LDA		SIC-LDA		Exact ^a	
		$\Delta\epsilon$	ω	$\Delta\epsilon$	ω	$\Delta\epsilon$	ω
3P	$2s \rightarrow 2p$ (V)	3.50	2.40	3.63	2.43	3.61	2.73
1P	$2s \rightarrow 2p$ (V)		4.85		5.19		5.28
3S	$2s \rightarrow 3s$ (R)	5.59	5.51	6.76	6.64	6.65	6.46
1S	$2s \rightarrow 3s$ (R)		5.62		6.85		6.78
3P	$2s \rightarrow 3p$ (R)	5.66	5.66	7.21	7.17	7.33	7.30
1P	$2s \rightarrow 3p$ (R)		5.66		7.23		7.46
3D	$2s \rightarrow 3d$ (R)	6.65	6.61	7.83	7.76	7.71	7.69
1D	$2s \rightarrow 3d$ (R)		6.52		7.69		7.99

^aFrom Ref. 34.

would otherwise alter the orbitals and orbital eigenvalues. All calculations employ the `UltraFine` integration grid.

The optimal δ for each density-functional approximation was determined by fitting calculated excitation energies to 14 experimental excitation energies of the CO molecule. This gave the following values: $\delta = 0.24$ for the LDA; 0.26 for the PBE approximation; 0.28 for the BLYP approximation; 0.23 for TPSS; 0.18 for the B3LYP hybrid functional [42–45]; 0.16 for the PBE0 hybrid; and 0.19 for the TPSS hybrid [31, 46]. Note the consistency with which functionals of the same type have similar δ values, and that hybrid functionals require smaller corrections. Also note that the fitted LDA value of $\delta = 0.24$ is almost exactly equal to the estimate $\delta = 1/4$ made in the previous Section for the optimal orbital gaps. Such an excellent agreement between two independent determinations of the optimal δ value justifies our assumption that the HOMO depopulation is an inherent characteristic of a given functional and is largely system-independent.

6.5.3 Results

Results of TDDFT calculations are summarized in Table 6.3 for four representative density functionals: LDA, BLYP, B3LYP, and TPSS. Without our correction, these functionals give good results for valence excitations (MAE = 0.26–0.35 eV), but severely underestimate the energies of Rydberg transitions (MAE = 0.97–1.63 eV). Our method reduces the MAEs for Rydberg excitations to 0.18–0.25 eV while preserving the already good performance for valence excitations. These trends appear statistically stable for all systems and functionals we tested (see Tables 6.4–6.12).

It is instructive to compare our method with long-range-corrected hybrids such as LC- ω PBE [47] and sophisticated empirical functionals such as M06-2X [48], which was specifically recommended for calculations of valence and Rydberg excitations. The LC- ω PBE functional has a low MAE for Rydberg excitations, but performs significantly worse than standard functionals for valence transitions. M06-2X is more accurate than any of the standard functionals for Rydberg excitations, but the same standard functionals corrected by our method outperform M06-2X by a wide margin.

6.6 Conclusion

Most existing schemes for reducing the self-interaction error in Kohn–Sham potentials correct energy functionals [57, 58] or orbital eigenvalues [59, 60], but approaches that

directly correct Kohn–Sham potentials [2, 29, 33, 61] are also becoming popular. In this Chapter, we described a simple and effective scheme of the latter type. Our method is based on the observation that an approximate Hartree-exchange-correlation potential $v_{\text{HXC}}(\mathbf{r})$ of a fractionally ionized system is a better representation of the exact $v_{\text{HXC}}(\mathbf{r})$ at intermediate and large r than the $v_{\text{HXC}}(\mathbf{r})$ constructed with the all-electron density. The HOMO depopulation method is applicable to any local, semilocal, or global hybrid density-functional approximation. If it were applied to the exact $v_{\text{HXC}}([\rho]; \mathbf{r})$, the resulting $v_{\text{HXC}}([\tilde{\rho}]; \mathbf{r})$ would still predict the exact HOMO energy because, in the exact Kohn–Sham DFT, ϵ_{HOMO} remains a constant for all $0 < \delta < 1$ [17, 20].

Our findings point to the physical reason behind the success of Slater’s transition state method for calculating vertical ionization energies. Namely, the HOMO eigenvalue of a Slater transition state is a good approximation to the exact HOMO energy because the quality of HOMO eigenvalues from approximate Kohn–Sham potentials peaks at $\delta \approx 1/2$. The HOMO depopulation method also works well in adiabatic TDDFT by improving Kohn–Sham orbital gaps. The optimal HOMO depopulation necessary to reproduce orbital gaps and excitation energies is about half of what is required to reproduce ionization energies. Our correction scheme lowers errors of Rydberg excitations from more than 1 eV to sub-eV values, and rivals the accuracy of the cutting-edge functionals such as LC- ω PBE and M06-2X.

To conclude, it appears that accurate response properties for a system of interest can be obtained by applying approximate density functionals to the same system with partially depopulated HOMO. The need for an auxiliary system reflects the limited accuracy of existing approximations, and their main problem, self-interaction error.

Table 6.3: Mean absolute errors (in eV) relative to experiment for 104 vertical excitation energies of three atoms (Be, Mg, Zn) and six molecules (CO, CH₂O, C₂H₂, C₂H₄, H₂O, N₂) calculated using TDDFT with various density functionals. The basis set is d-aug-cc-pVQZ for atoms and d-aug-cc-pVTZ for molecules.

Excitations	Uncorrected potentials				Corrected potentials					
	LDA	BLYP	B3LYP	TPSS	LDA	BLYP	B3LYP	TPSS		
	$\delta = 0$				$\delta = 0.23$					
					$\delta = 0.24$	$\delta = 0.28$	$\delta = 0.18$	$\delta = 0.23$	LC- ω PBE	M06-2X
Valence (6)	0.22	0.29	0.30	0.49	0.29	0.32	0.24	0.35	0.63	0.36
Rydberg (22)	1.01	1.29	0.96	1.12	0.23	0.18	0.29	0.22	0.29	1.10
All (28)	0.84	1.08	0.81	0.99	0.24	0.21	0.28	0.25	0.36	0.94
					Molecules					
Valence (25)	0.27	0.35	0.36	0.31	0.22	0.26	0.38	0.29	0.45	0.36
Rydberg (51)	1.37	1.78	0.98	1.45	0.25	0.18	0.15	0.19	0.19	0.40
All (76)	1.01	1.31	0.78	1.08	0.24	0.21	0.23	0.22	0.28	0.39
					Atoms and molecules					
Valence (31)	0.26	0.34	0.35	0.35	0.23	0.28	0.36	0.30	0.49	0.36
Rydberg (73)	1.26	1.63	0.97	1.35	0.25	0.18	0.19	0.19	0.22	0.61
All (104)	0.96	1.25	0.79	1.05	0.24	0.21	0.24	0.23	0.30	0.54

Table 6.4: Vertical excitation energies (in eV) for the ground-state Be atom ($1S$) calculated by TDDFT with various density-functional approximations. The basis set is d-aug-cc-pVQZ.

State	Transition	Uncorrected potentials				Corrected potentials				M06-2X	LC- ω PBE	Expt. ^a
		LDA	BLYP	B3LYP	TPSS	LDA	BLYP	B3LYP	TPSS			
		$\delta = 0$				$\delta = 0.23$						
						$\delta = 0.24$	$\delta = 0.28$	$\delta = 0.18$	$\delta = 0.23$			
3P	$2s \rightarrow 2p$	2.40	2.09	2.09	1.58	2.43	2.07	1.92	1.52	1.59	2.52	2.73
1P	$2s \rightarrow 2p$	4.85	4.85	4.89	5.05	5.17	5.24	4.98	5.36	4.97	4.76	5.28
3S	$2s \rightarrow 3s$	5.51	5.29	5.62	5.62	6.59	6.59	6.25	6.66	6.13	5.53	6.46
1S	$2s \rightarrow 3s$	5.62	5.40	5.80	5.75	6.80	6.82	6.49	6.88	6.57	5.89	6.78
3P	$2s \rightarrow 3p$	5.66	5.51	6.05	5.80	7.12	7.13	6.69	7.17	7.04	6.19	7.30
1P	$2s \rightarrow 3p$	5.66	5.52	6.13	5.80	7.17	7.22	6.77	7.25	7.22	6.40	7.46
3D	$2s \rightarrow 3d$	6.61	6.33	6.68	6.67	7.71	7.65	7.30	7.73	7.36	6.59	7.69
1D	$2s \rightarrow 3d$	6.52	6.28	6.62	6.66	7.64	7.62	7.25	7.73	7.43	6.68	7.99
Mean absolute errors with respect to experiment												
	Valence (2)	0.38	0.53	0.51	0.69	0.20	0.35	0.55	0.64	0.72	0.36	
	Rydberg (6)	1.35	1.56	1.13	1.23	0.17	0.17	0.49	0.16	0.32	1.07	
	All (8)	1.11	1.30	0.97	1.09	0.18	0.21	0.51	0.28	0.42	0.89	

^aRef. 49.

Table 6.5: Vertical excitation energies (in eV) for the ground-state Mg atom ($1S$) calculated by TDDFT with various density-functional approximations. The basis set is d-aug-cc-pVQZ.

Mg	State	Transition	Uncorrected potentials				Corrected potentials				M06-2X	Expt. ^a	
			LDA	BLYP	B3LYP	TPSS	LDA	BLYP	B3LYP	TPSS			
			$\delta = 0$	$\delta = 0.24$	$\delta = 0.28$	$\delta = 0.18$	$\delta = 0.23$	LC- ω PBE					
3P		$3s \rightarrow 3p$	2.76	2.66	2.61	2.16	2.96	2.87	2.63	2.29	1.91	3.05	2.71
1P		$3s \rightarrow 3p$	4.24	4.15	4.23	4.18	4.69	4.72	4.45	4.55	4.23	4.35	4.35
3S		$3s \rightarrow 4s$	4.67	4.40	4.66	4.63	5.53	5.46	5.18	5.43	4.98	4.62	5.11
1S		$3s \rightarrow 4s$	4.77	4.49	4.80	4.73	5.70	5.65	5.38	5.58	5.35	4.92	5.39
3D		$3s \rightarrow 3d$	5.10	4.78	5.23	5.05	6.21	6.04	5.92	6.06	5.99	5.61	5.95
1D		$3s \rightarrow 3d$	5.08	4.78	5.22	5.05	6.20	6.05	5.93	6.08	6.16	5.62	5.75
3P		$3s \rightarrow 4p$	4.88	4.62	5.06	4.84	6.05	5.97	5.77	5.89	5.79	5.19	5.93
1P		$3s \rightarrow 4p$	4.90	4.66	5.13	4.87	6.10	6.04	5.88	5.97	6.01	5.54	6.12
Mean absolute errors with respect to experiment													
		Valence (2)	0.08	0.12	0.11	0.36	0.29	0.26	0.09	0.31	0.46	0.17	
		Rydberg (6)	0.81	1.09	0.69	0.85	0.26	0.19	0.12	0.19	0.14	0.46	
		All (8)	0.63	0.85	0.55	0.72	0.27	0.21	0.11	0.22	0.22	0.39	

^aRef. 49.

Table 6.6: Vertical excitation energies (in eV) for the ground-state Zn atom ($1S$) calculated by TDDFT with various density-functional approximations. The basis set is d-aug-cc-pVQZ.

Zn		Uncorrected potentials				Corrected potentials				M06-2X	LC- ω PBE	Expt. ^a
		LDA	BLYP	B3LYP	TPSS	LDA	BLYP	B3LYP	TPSS			
State	Transition	$\delta = 0$				$\delta = 0.24$	$\delta = 0.28$	$\delta = 0.18$	$\delta = 0.23$			
3P	$4s \rightarrow 4p$	4.19	4.07	3.89	3.62	4.47	4.40	3.95	3.86	3.12	3.72	4.03
1P	$4s \rightarrow 4p$	5.58	5.42	5.42	5.35	6.14	6.12	5.70	5.84	5.31	5.02	5.80
3S	$4s \rightarrow 5s$	6.05	5.68	5.90	5.72	7.15	6.99	6.56	6.75	6.24	5.24	6.65
1S	$4s \rightarrow 5s$	6.12	5.76	6.02	5.83	7.27	7.14	6.74	6.90	6.57	5.51	6.92
3P	$4s \rightarrow 5p$	6.35	5.98	6.35	6.06	7.70	7.54	7.21	7.27	7.12	5.81	7.60
1P	$4s \rightarrow 5p$	6.42	6.09	6.45	6.15	7.75	7.63	7.31	7.36	7.32	6.22	7.80
3D	$4s \rightarrow 4d$	7.47	7.08	7.22	7.09	8.46	8.23	7.80	7.98	7.55	6.51	7.78
1D	$4s \rightarrow 4d$	7.36	7.02	7.15	7.07	8.37	8.19	7.75	7.97	7.62	6.48	7.74
3S	$4s \rightarrow 6s$	6.90	6.59	6.86	6.63	8.12	8.06	7.69	7.77	7.71	6.55	8.11
1S	$4s \rightarrow 6s$	7.04	6.75	7.01	6.78	8.22	8.17	7.81	7.86	7.85	6.67	8.19
3P	$4s \rightarrow 6p$	7.30	6.95	7.20	6.89	8.46	8.32	7.94	8.02	8.05	6.68	8.44
1P	$4s \rightarrow 6p$	7.56	7.29	7.48	7.25	8.63	8.52	8.13	8.24	8.20	7.11	8.51
Mean absolute errors with respect to experiment												
Valence (2)		0.19	0.21	0.26	0.43	0.39	0.34	0.09	0.11	0.70	0.54	
Rydberg (10)		0.92	1.25	1.01	1.23	0.25	0.19	0.29	0.27	0.35	1.50	
All (12)		0.80	1.08	0.88	1.09	0.27	0.21	0.25	0.24	0.41	1.34	

^aRef. 49.

Table 6.7: Vertical excitation energies (in eV) for the CO molecule ($X^1\Sigma^+$) calculated by TDDFT with various density-functional approximations. The basis set is d-aug-cc-pVTZ. Molecular geometry: $r(\text{CO}) = 1.128 \text{ \AA}$.

State	Transition	CO										
		Uncorrected potentials					Corrected potentials					
		LDA	BLYP	B3LYP	TPSS	TPSS	LDA	BLYP	B3LYP	TPSS	TPSS	
		$\delta = 0$	$\delta = 0.24$	$\delta = 0.28$	$\delta = 0.18$	$\delta = 0.23$	LC- ω PBE	M06-2X	Expt. ^a			
$^3\Pi$	$\sigma \rightarrow \pi^*$	5.97	5.82	5.86	5.79	6.24	6.11	5.83	6.01	5.81	6.24	6.32
$^3\Sigma^+$	$\pi \rightarrow \pi^*$	8.43	8.09	7.95	7.99	8.31	7.95	7.82	7.86	7.98	8.12	8.51
$^1\Pi$	$\sigma \rightarrow \pi^*$	8.17	8.23	8.39	8.45	8.51	8.61	8.41	8.74	8.54	8.20	8.51
$^3\Delta$	$\pi \rightarrow \pi^*$	9.19	8.68	8.64	8.64	9.11	8.57	8.54	8.55	8.70	9.24	9.36
$^3\Sigma^-$	$\pi \rightarrow \pi^*$	9.88	9.77	9.72	10.06	9.84	9.74	9.67	10.05	9.02	9.14	9.88
$^1\Sigma^-$	$\pi \rightarrow \pi^*$	9.88	9.77	9.73	10.06	9.84	9.74	9.67	10.05	10.67	9.14	9.88
$^1\Delta$	$\pi \rightarrow \pi^*$	10.33	10.01	10.04	10.16	10.33	10.00	10.00	10.16	10.27	10.20	10.23
$^3\Sigma^+$	$\sigma \rightarrow 3s\sigma$	9.04	8.74	9.56	9.12	10.66	10.62	10.53	10.68	10.31	9.99	10.4
$^1\Sigma^+$	$\sigma \rightarrow 3s\sigma$	9.22	8.94	9.86	9.34	10.95	10.94	10.92	10.99	10.84	10.39	10.78
$^3\Sigma^+$	$\sigma \rightarrow 3p\sigma$	9.50	9.21	10.18	9.60	11.37	11.37	11.32	11.38	11.17	10.74	11.3
$^1\Sigma^+$	$\sigma \rightarrow 3p\sigma$	9.50	9.22	10.20	9.65	11.41	11.44	11.39	11.45	11.33	10.87	11.40
$^3\Pi$	$\sigma \rightarrow 3p\pi$	9.52	9.24	10.25	9.63	11.46	11.50	11.41	11.53	11.29	10.79	11.55
$^1\Pi$	$\sigma \rightarrow 3p\pi$	9.54	9.28	10.29	9.68	11.46	11.52	11.49	11.51	11.42	10.92	11.53
$^1\Sigma^+$	$\sigma \rightarrow 3d\sigma$	10.26	9.99	11.04	10.40	12.20	12.28	12.29	12.25	12.41	11.86	12.4
Mean absolute errors with respect to experiment												
Valence (7)		0.15	0.33	0.34	0.32	0.10	0.31	0.39	0.34	0.49	0.34	
Rydberg (7)		1.83	2.11	1.14	1.70	0.13	0.10	0.08	0.12	0.10	0.54	
All (14)		0.99	1.22	0.74	1.01	0.11	0.20	0.24	0.23	0.30	0.44	

^aRef. 50.

Table 6.8: Vertical excitation energies (in eV) for the CH₂O molecule (\tilde{X}^1A_1) calculated by TDDFT with various density-functional approximations. The basis set is d-aug-cc-pVTZ. Molecular geometry: $r(\text{CO}) = 1.205 \text{ \AA}$, $r(\text{CH}) = 1.111 \text{ \AA}$, $\theta(\text{HCO}) = 121.9^\circ$.

State	Transition	Uncorrected potentials					Corrected potentials					M06-2X	LC- ω PBE	Expt. ^a	
		LDA	BLYP	B3LYP	TPSS	$\delta = 0$	LDA	BLYP	B3LYP	TPSS	$\delta = 0.23$				$\delta = 0.18$
3A_2	$n \rightarrow \pi^*$	3.09	3.15	3.22	3.26	3.35	3.46	3.21	3.50	3.15	3.19	3.50	3.19	3.15	3.50
1A_2	$n \rightarrow \pi^*$	3.70	3.84	3.94	4.06	3.97	4.16	3.93	4.31	3.93	3.71	3.94	3.71	3.93	3.94
3A_1	$\pi \rightarrow \pi^*$	6.24	5.80	5.46	5.59	6.38	5.98	5.59	5.75	5.31	5.71	5.53	5.71	5.31	5.53
3B_2	$n \rightarrow 3sa_1$	5.81	5.53	6.32	5.85	7.02	6.91	6.98	7.01	7.07	7.00	6.83	7.00	7.07	6.83
1B_2	$n \rightarrow 3sa_1$	5.87	5.62	6.44	5.96	7.16	7.12	7.17	7.22	7.28	7.12	7.09	7.12	7.28	7.09
3A_1	$n \rightarrow 3pb_2$	6.47	5.80	7.13	6.49	8.00	7.92	7.97	7.97	7.98	7.83	7.79	7.83	7.98	7.79
1A_1	$n \rightarrow 3pb_2$	6.48	6.22	7.18	6.52	8.08	8.03	8.08	8.08	8.13	7.96	7.97	7.96	8.13	7.97
3B_2	$n \rightarrow 3pa_1$	6.58	6.30	7.12	6.61	7.96	7.89	7.87	7.97	7.81	7.69	7.96	7.69	7.81	7.96
1B_2	$n \rightarrow 3pa_1$	6.59	6.34	7.19	6.65	8.04	8.01	8.01	8.08	8.02	7.82	8.12	7.82	8.02	8.12
1B_1	$\sigma \rightarrow \pi^*$	8.76	8.78	9.00	9.01	8.98	9.05	9.17	9.23	9.21	8.84	8.68	8.84	9.21	8.68
1A_2	$n \rightarrow 3pb_1$	6.69	6.41	7.38	6.73	8.35	8.32	8.36	8.33	8.28	8.12	8.38	8.12	8.28	8.38
1A_2	$n \rightarrow 3pb_1$	7.53	7.25	8.20	7.56	9.20	9.21	9.27	9.17	9.32	9.10	9.22	9.10	9.32	9.22
Mean absolute errors with respect to experiment															
Valence (4)		0.36	0.20	0.17	0.19	0.33	0.27	0.21	0.28	0.28	0.22	0.28	0.28	0.28	0.22
Rydberg (8)		1.42	1.74	0.80	1.37	0.09	0.07	0.10	0.10	0.15	0.15	0.15	0.15	0.15	0.15
All (12)		1.06	1.23	0.59	0.98	0.17	0.14	0.14	0.16	0.20	0.17	0.17	0.20	0.20	0.17

^aRef. 51.

Table 6.9: Vertical excitation energies (in eV) for the C₂H₂ molecule ($\tilde{X}^1\Sigma_g^+$) calculated by TDDFT with various density-functional approximations. The basis set is d-aug-cc-pVTZ. Molecular geometry: $r(\text{CC}) = 1.203 \text{ \AA}$, $r(\text{CH}) = 1.063 \text{ \AA}$.

State	Transition	Uncorrected potentials				Corrected potentials				M06-2X	Expt. ^a	
		LDA	BLYP	B3LYP	TPSS	LDA	BLYP	B3LYP	TPSS			
		$\delta = 0$				$\delta = 0.23$						
$^3\Sigma_u^+$	$\pi_u \rightarrow \pi_g$	5.52	5.22	5.02	4.95	5.69	5.39	5.03	5.08	4.63	5.35	5.2
$^3\Delta_u$	$\pi_u \rightarrow \pi_g$	6.21	5.77	5.70	5.76	6.43	6.00	5.75	5.94	5.50	6.54	6.0
$^1\Delta_u$	$\pi_u \rightarrow \pi_g$	7.02	6.76	6.79	6.96	7.35	7.15	6.93	7.27	6.95	7.11	7.2
$^3\Pi_u$	$\pi_u \rightarrow 3s\sigma_g$	7.16	6.68	7.22	6.98	8.41	8.11	8.01	8.18	8.11	7.60	8.07
$^1\Pi_u$	$\pi_u \rightarrow 3s\sigma_g$	7.17	6.71	7.26	7.02	8.44	8.16	8.08	8.24	8.25	7.64	8.16
$^3\Pi_g$	$\pi_u \rightarrow 3p\sigma_u$	7.37	6.87	7.43	7.19	8.53	8.16	8.14	8.30	8.55	7.88	8.90
$^3\Sigma_g^+$	$\pi_u \rightarrow 3p\pi_u$	7.71	7.23	7.87	7.49	9.15	8.89	8.81	8.87	8.84	8.27	8.98
$^1\Pi_g$	$\pi_u \rightarrow 3p\sigma_u$	7.42	6.94	7.55	7.26	8.70	8.37	8.35	8.51	8.75	7.99	9.00
$^3\Delta_g$	$\pi_u \rightarrow 3p\pi_u$	7.73	7.24	7.89	7.53	9.20	8.91	8.84	8.92	8.95	8.33	9.08
$^3\Pi_u$	$\pi_u \rightarrow 3d\sigma_g$	7.81	7.36	8.15	7.65	9.34	9.05	8.98	9.17	9.29	8.67	9.17
$^1\Sigma_g^+$	$\pi_u \rightarrow 3p\pi_u$	7.78	7.31	8.01	7.60	9.30	9.06	9.03	9.06	9.21	8.59	9.21
$^1\Pi_u$	$\pi_u \rightarrow 3d\sigma_g$	7.82	7.37	8.18	7.67	9.46	9.19	9.14	9.26	9.47	8.76	9.24 ^b
Mean absolute errors with respect to experiment												
Valence (3)		0.24	0.23	0.30	0.24	0.35	0.08	0.23	0.08	0.44	0.26	
Rydberg (9)		1.32	1.79	1.14	1.49	0.23	0.22	0.27	0.19	0.15	0.68	
All (12)		1.05	1.40	0.93	1.18	0.26	0.19	0.26	0.16	0.22	0.57	

^aAll experimental values except for the $^1\Pi_u$ state are from Ref. 52.

^bRef. 53.

Table 6.10: Vertical excitation energies (in eV) for the C_2H_4 molecule (\tilde{X}^1A_g) calculated by TDDFT with various density-functional approximations. The basis set is d-aug-cc-pVTZ. Molecular geometry: $r(CC) = 1.339 \text{ \AA}$, $r(CH) = 1.086 \text{ \AA}$, $\theta(HCC)=121.2^\circ$.

State	Transition	C_2H_4										Expt. ^a	
		Uncorrected potentials					Corrected potentials						
		LDA	BLYP	B3LYP	TPSS	$\delta = 0$	LDA	BLYP	B3LYP	TPSS	$\delta = 0.23$		LC- ω PBE
		$\delta = 0.24$	$\delta = 0.28$	$\delta = 0.18$									
$^3B_{1u}$	$\pi \rightarrow \pi^*(b_{2g})$	4.65	4.26	4.02	4.03	4.76	4.37	3.91	4.10	3.49	4.49	4.36	
$^3B_{3u}$	$\pi \rightarrow 3s(a_g)$	6.55	6.08	6.49	6.38	7.57	7.26	7.04	7.37	7.37	6.86	6.98	
$^1B_{3u}$	$\pi \rightarrow 3s(a_g)$	6.59	6.14	6.56	6.44	7.65	7.36	7.14	7.47	7.53	6.90	7.11	
$^3B_{1g}$	$\pi \rightarrow 3p\sigma(b_{2u})$	6.96	6.54	7.05	6.83	8.22	7.11	7.41	7.37	7.51	7.43	7.79	
$^1B_{1g}$	$\pi \rightarrow 3p\sigma(b_{2u})$	7.03	6.55	7.08	6.85	8.26	7.68	7.73	8.00	8.11	7.43	7.80	
$^1B_{2g}$	$\pi \rightarrow 3p\sigma(b_{1u})$	7.02	6.52	7.07	6.82	8.28	7.94	7.77	8.03	8.28	7.50	7.90	
$^1B_{1u}$	$\pi \rightarrow \pi^*(b_{2g})$	7.35	7.00	7.30	7.26	7.85	7.73	7.48	7.83	7.60	7.45	8.0	
3A_g	$\pi \rightarrow 3p\pi(b_{3u})$	7.26	6.76	7.30	7.00	8.60	8.30	8.07	8.26	8.28	7.69	8.15	
1A_g	$\pi \rightarrow 3p\pi(b_{3u})$	7.29	6.79	7.37	7.07	8.67	8.39	8.18	8.38	8.50	7.87	8.28	
$^3B_{3u}$	$\pi \rightarrow 3d\sigma(a_g)$	7.30	6.84	7.53	7.12	8.83	8.60	8.46	8.57	8.87	8.19	8.57	
$^1B_{3u}$	$\pi \rightarrow 3d\sigma(a_g)$	7.32	6.87	7.55	7.15	8.85	8.63	8.49	8.59	8.96	8.24	8.62	
$^1B_{3u}$	$\pi \rightarrow 3d\delta(a_g)$	7.62	7.13	7.77	7.42	9.10	8.84	8.68	8.82	9.18	8.48	8.90	
$^1B_{2u}$	$\pi \rightarrow 3d\delta(b_{1g})$	8.20	7.70	8.22	8.00	9.50	9.20	8.98	9.23	9.28	8.62	9.05	
$^1B_{1u}$	$\pi \rightarrow 3d\pi(b_{2g})$	7.80	7.44	7.95	7.68	9.26	9.00	8.86	8.97	9.40	8.71	9.33	
Mean absolute errors with respect to experiment													
Valence (2)		0.47	0.55	0.52	0.53	0.27	0.14	0.48	0.21	0.64	0.34		
Rydberg (12)		0.96	1.43	0.88	1.15	0.37	0.18	0.15	0.20	0.28	0.38		
All (14)		0.89	1.30	0.83	1.06	0.36	0.18	0.20	0.20	0.33	0.37		

^aRef. 54.

Table 6.11: Vertical excitation energies (in eV) for the H₂O molecule (\tilde{X}^1A_1) calculated by TDDFT with various density-functional approximations. The basis set is d-aug-cc-pVTZ. Molecular geometry: $r(\text{OH}) = 0.958 \text{ \AA}$, $\theta(\text{HOH})=104.478^\circ$.

H ₂ O		Uncorrected potentials				Corrected potentials				M06-2X	Expt. ^a	
		LDA	BLYP	B3LYP	TPSS	LDA	BLYP	B3LYP	TPSS			
State	Transition	$\delta = 0$				$\delta = 0.24$	$\delta = 0.28$	$\delta = 0.18$	$\delta = 0.23$	LC- ω PBE		
³ B ₁	$b_1 \rightarrow 3sa_1$	6.30	5.95	6.56	6.28	7.74	7.57	7.30	7.64	7.04	7.13	7.0
¹ B ₁	$b_1 \rightarrow 3sa_1$	6.55	6.24	6.92	6.57	8.10	7.99	7.74	8.03	7.50	7.46	7.4
³ A ₂	$b_1 \rightarrow 3pb_2$	7.59	7.25	8.18	7.50	9.58	9.40	9.17	9.36	8.91	8.77	8.9
¹ A ₂	$b_1 \rightarrow 3pb_2$	7.60	7.27	8.28	7.53	9.69	9.58	9.36	9.51	9.10	8.92	9.1
³ A ₁	$a_1 \rightarrow 3sa_1$	8.27	7.97	8.60	8.34	9.45	9.32	9.47	9.51	9.11	9.24	9.3
¹ A ₁	$a_1 \rightarrow 3sa_1$	8.62	8.36	9.11	8.75	9.91	9.86	9.95	10.14	9.54	9.53	9.7
³ A ₁	$b_1 \rightarrow 3pb_1$	7.98	7.60	8.58	7.83	10.11	10.03	9.82	9.82	9.36	9.38	9.81
³ B ₁	$b_1 \rightarrow 3pa_1$	7.72	7.41	8.60	7.65	10.13	10.12	9.96	9.91	9.50	9.43	9.98
¹ B ₁	$b_1 \rightarrow 3pa_1$	7.75	7.44	8.62	7.69	10.14	10.15	9.99	9.94	9.57	9.52	10.01
¹ A ₁	$b_1 \rightarrow 3pb_1$	9.19	7.70	8.72	7.96	10.27	10.24	10.18	9.96	9.84	9.83	10.16
Mean absolute errors with respect to experiment												
Rydberg (10)		1.38	1.82	0.92	1.53	0.37	0.29	0.17	0.32	0.22	0.25	
All (10)		1.38	1.82	0.92	1.53	0.37	0.29	0.17	0.32	0.22	0.25	

^aRef. 55.

Table 6.12: Vertical excitation energies (in eV) for the N₂ molecule ($X^1\Sigma_g^+$) calculated by TDDFT with various density-functional approximations. The basis set is d-aug-cc-pVTZ. Molecular geometry: $r(\text{NN}) = 1.098 \text{ \AA}$.

N ₂	State	Transition	Uncorrected potentials				Corrected potentials				M06-2X	Expt. ^a	
			LDA	BLYP	B3LYP	TPSS	LDA	BLYP	B3LYP	TPSS			
			$\delta = 0$				$\delta = 0.24$	$\delta = 0.28$	$\delta = 0.18$	$\delta = 0.23$	LC- ω PBE		
$^3\Sigma_u^+$	π_u	$\rightarrow \pi_g$	7.91	7.48	7.10	7.27	7.91	7.46	7.06	7.25	6.99	7.50	7.75
$^3\Pi_g$	σ_g	$\rightarrow \pi_g$	7.58	7.45	7.58	7.46	7.74	7.61	7.45	7.57	7.72	7.75	8.04
$^3\Delta_u$	π_u	$\rightarrow \pi_g$	8.84	8.22	7.97	8.10	8.87	8.23	7.96	8.11	7.90	8.89	8.88
$^1\Pi_g$	σ_g	$\rightarrow \pi_g$	9.07	9.09	9.27	9.26	9.29	9.33	9.18	9.44	9.47	9.04	9.31
$^3\Sigma_u^-$	π_u	$\rightarrow \pi_g$	9.68	9.58	9.33	9.88	9.74	9.66	9.36	9.95	9.32	8.44	9.67
$^1\Sigma_u^-$	π_u	$\rightarrow \pi_g$	9.68	9.58	9.33	9.88	9.74	9.66	9.36	9.95	9.32	8.44	9.92
$^1\Delta_u$	π_u	$\rightarrow \pi_g$	10.23	9.86	9.72	10.01	10.32	9.97	9.77	10.10	9.88	9.98	10.27
$^3\Pi_u$	σ_u	$\rightarrow \pi_g$	10.38	10.32	10.64	10.64	10.51	10.47	10.67	10.77	10.86	11.36	11.19
$^3\Sigma_g^+$	σ_g	$\rightarrow 3s\sigma_g$	10.42	10.06	11.02	10.39	12.00	11.87	11.95	11.91	11.74	11.58	12.0
$^1\Sigma_g^+$	σ_g	$\rightarrow 3s\sigma_g$	10.61	10.26	11.29	10.60	12.26	12.16	12.28	12.19	12.21	11.97	12.2
$^1\Pi_u$	σ_g	$\rightarrow 3p\pi_u$	10.94	10.60	11.71	10.95	12.75	12.70	12.83	12.69	12.70	12.51	12.90
$^1\Sigma_u^+$	σ_g	$\rightarrow 3p\sigma_u$	10.83	10.50	11.69	10.84	12.74	12.69	12.83	12.67	12.72	12.57	12.98
$^1\Pi_u$	π_u	$\rightarrow 3s\sigma_g$	11.97	11.37	12.06	11.73	13.49	13.12	13.16	13.21	13.02	12.46	13.24
$^1\Pi_u$	σ_u	$\rightarrow \pi_g$	13.01	13.13	13.58	13.64	13.27	13.46	13.77	13.90	13.95	13.97	13.63
Mean absolute errors with respect to experiment													
	Valence (9)		0.29	0.44	0.46	0.33	0.20	0.32	0.48	0.34	0.47	0.48	
	Rydberg (5)		1.71	2.11	1.11	1.76	0.14	0.16	0.09	0.13	0.19	0.45	
	All (14)		0.80	1.03	0.69	0.84	0.18	0.26	0.34	0.26	0.37	0.47	

^aRef. 56.

Bibliography

- [1] R. Baer, E. Livshits, and U. Salzner, “Tuned range-separated hybrids in density functional theory”, *Annu. Rev. Phys. Chem.* **61**, 85 (2010).
- [2] N. I. Gidopoulos and N. N. Lathiotakis, “Constraining density functional approximations to yield self-interaction free potentials”, *J. Chem. Phys.* **136**, 224109 (2012).
- [3] S. J. A. van Gisbergen, V. P. Osinga, O. V. Gritsenko, R. van Leeuwen, J. G. Snijders, and E. J. Baerends, “Improved density functional theory results for frequency-dependent polarizabilities, by the use of an exchange-correlation potential with correct asymptotic behavior”, *J. Chem. Phys.* **105**, 3142 (1996).
- [4] M. E. Casida, C. Jamorski, K. C. Casida, and D. R. Salahub, “Molecular excitation energies to high-lying bound states from time-dependent density-functional response theory: Characterization and correction of the time-dependent local density approximation ionization threshold”, *J. Chem. Phys.* **108**, 4439 (1998).
- [5] D. J. Tozer and N. C. Handy, “Improving virtual Kohn–Sham orbitals and eigenvalues: Application to excitation energies and static polarizabilities”, *J. Chem. Phys.* **109**, 10180 (1998).
- [6] P. R. T. Schipper, O. V. Gritsenko, S. J. A. van Gisbergen, and E. J. Baerends, “Molecular calculations of excitation energies and (hyper)polarizabilities with a statistical average of orbital model exchange-correlation potentials”, *J. Chem. Phys.* **112**, 1344 (2000).
- [7] J. P. Perdew, M. Levy, and J. L. Balduz, “Density-functional theory for fractional particle number: Derivative discontinuities of the energy”, *Phys. Rev. Lett.* **49**, 1691 (1982).
- [8] J. Slater and K. Johnson, “Self-consistent-field $X\alpha$ cluster method for polyatomic molecules and solids”, *Phys. Rev. B* **5**, 844 (1972).

- [9] J. C. Slater, *Quantum Theory of Molecules and Solids, Vol. 4: The Self-Consistent Field for Molecules and Solids*, McGraw-Hill, Inc., New York (1974).
- [10] L. Ferreira, M. Marques, and L. Teles, “Approximation to density functional theory for the calculation of band gaps of semiconductors”, *Phys. Rev. B* **78**, 125116 (2008).
- [11] L. G. Ferreira, M. Marques, and L. K. Teles, “Slater half-occupation technique revisited: the LDA-1/2 and GGA-1/2 approaches for atomic ionization energies and band gaps in semiconductors”, *AIP Adv.* **1**, 032119 (2011).
- [12] J. P. Perdew and Y. Wang, “Accurate and simple analytic representation of the electron-gas correlation energy”, *Phys. Rev. B* **45**, 13244 (1992).
- [13] J. P. Perdew, K. Burke, and M. Ernzerhof, “Generalized gradient approximation made simple”, *Phys. Rev. Lett.* **77**, 3865 (1996).
- [14] E. V. R. de Castro and F. E. Jorge, “Accurate universal Gaussian basis set for all atoms of the periodic table”, *J. Chem. Phys.* **108**, 5225 (1998).
- [15] C. Filippi, X. Gonze, and C. J. Umrigar, “Generalized gradient approximations to density functional theory: Comparison with exact results”, in *Recent Developments and Applications of Modern Density Functional Theory, Theoretical and Computational Chemistry*, Vol. 4, edited by J. M. Seminario, Elsevier, pp. 295–326 (1996).
- [16] J. F. Janak, “Proof that $\partial E/\partial n_i = \epsilon_i$ in density-functional theory”, *Phys. Rev. B* **18**, 7165 (1978).
- [17] J. P. Perdew, “What do the Kohn–Sham orbital energies mean? How do atoms dissociate?”, in *Density Functional Methods in Physics*, edited by R. M. Dreizler and J. da Providência, Plenum, New York, pp. 265–308 (1985).
- [18] W. Yang, Y. Zhang, and P. Ayers, “Degenerate ground states and a fractional number of electrons in density and reduced density matrix functional theory”, *Phys. Rev. Lett.* **84**, 5172 (2000).
- [19] E. R. Johnson, W. Yang, and E. R. Davidson, “Spin-state splittings, highest-occupied-molecular-orbital and lowest-unoccupied-molecular-orbital energies, and chemical hardness”, *J. Chem. Phys.* **133**, 164107 (2010).

- [20] O. A. Vydrov, G. E. Scuseria, and J. P. Perdew, “Tests of functionals for systems with fractional electron number”, *J. Chem. Phys.* **126**, 154109 (2007).
- [21] A. J. Cohen, P. Mori-Sánchez, and W. Yang, “Insights into current limitations of density functional theory”, *Science* **321**, 792 (2008).
- [22] P. Mori-Sánchez, A. J. Cohen, and W. Yang, “Discontinuous nature of the exchange-correlation functional in strongly correlated systems”, *Phys. Rev. Lett.* **102**, 066403 (2009).
- [23] A. J. Cohen, P. Mori-Sánchez, and W. Yang, “Challenges for density functional theory”, *Chem. Rev.* **112**, 289 (2012).
- [24] J. Tao, J. P. Perdew, V. N. Staroverov, and G. E. Scuseria, “Climbing the density functional ladder: Nonempirical meta-generalized gradient approximation designed for molecules and solids”, *Phys. Rev. Lett.* **91**, 146401 (2003).
- [25] A. Carlo and V. Barone, “Toward reliable density functional methods without adjustable parameters: The PBE0 model”, *J. Chem. Phys.* **110**, 6158 (1999).
- [26] A. Görling, “New KS method for molecules based on an exchange charge density generating the exact local KS exchange potential”, *Phys. Rev. Lett.* **83**, 5459 (1999).
- [27] S. Liu, P. W. Ayers, and R. G. Parr, “Alternative definition of exchange-correlation charge in density functional theory”, *J. Chem. Phys.* **111**, 6197 (1999).
- [28] P. W. Ayers and M. Levy, “Sum rules for exchange and correlation potentials”, *J. Chem. Phys.* **115**, 4438 (2001).
- [29] X. Andrade and A. Aspuru-Guzik, “Prediction of the derivative discontinuity in density functional theory from an electrostatic description of the exchange and correlation potential”, *Phys. Rev. Lett.* **107**, 183002 (2011).
- [30] D. P. Chong, O. V. Gritsenko, and E. J. Baerends, “Interpretation of the Kohn–Sham orbital energies as approximate vertical ionization potentials”, *J. Chem. Phys.* **116**, 1760 (2002).
- [31] V. N. Staroverov, G. E. Scuseria, J. Tao, and J. P. Perdew, “Comparative assessment of a new nonempirical density functional: Molecules and hydrogen-bonded complexes”, *J. Chem. Phys.* **119**, 12129 (2003).

- [32] P. J. Linstrom and W. G. Mallard, Eds., *NIST Chemistry WebBook, NIST Standard Reference Database Number 69*, National Institute of Standards and Technology, Gaithersburg MD, 20899, <http://webbook.nist.gov> (retrieved October 21, 2012).
- [33] M. E. Casida and D. R. Salahub, “Asymptotic correction approach to improving approximate exchange–correlation potentials: Time-dependent density-functional theory calculations of molecular excitation spectra”, *J. Chem. Phys.* **113**, 8918 (2000).
- [34] A. Savin, C. Umrigar, and X. Gonze, “Relationship of Kohn–Sham eigenvalues to excitation energies”, *Chem. Phys. Lett.* **288**, 391 (1998).
- [35] C. J. Umrigar, A. Savin, and X. Gonze, “Are unoccupied Kohn–Sham eigenvalues related to excitation energies?”, in *Electronic Density Functional Theory: Recent Progress and New Directions*, edited by J. F. Dobson, G. Vignale, and M. P. Das, Plenum, New York, p. 167 (1998).
- [36] S. J. Chakravorty, S. R. Gwaltney, E. R. Davidson, F. A. Parpia, and C. F. Fischer, “Ground-state correlation energies for atomic ions with 3 to 18 electrons”, *Phys. Rev. A* **47**, 3649 (1993).
- [37] R. D. Johnson III (Ed.), “NIST Computational Chemistry Comparison and Benchmark Database, NIST Standard Reference Database Number 101”, Release 15b, August 2011, <http://cccbdb.nist.gov/>.
- [38] D. Feller, “The role of databases in support of computational chemistry calculations”, *J. Comp. Chem.* **17**, 1571 (1996).
- [39] K. L. Schuchardt, B. T. Didier, T. Elsethagen, L. Sun, V. Gurumoorthi, J. Chase, J. Li, and T. L. Windus, “Basis set exchange: A community database for computational sciences”, *J. Chem. Inf. Model.* **47**, 1045 (2007).
- [40] D. E. Woon and T. H. Dunning, Jr., “Gaussian basis sets for use in correlated molecular calculations. IV. Calculation of static electrical response properties”, *J. Chem. Phys.* **100**, 2975 (1994).
- [41] M. J. Frisch, G. W. Trucks, H. B. Schlegel, G. E. Scuseria, M. A. Robb, J. R. Cheeseman, G. Scalmani, V. Barone, B. Mennucci, G. A. Petersson, H. Nakatsuji, M. Caricato, X. Li, H. P. Hratchian, A. F. Izmaylov, J. Bloino, G. Zheng, J. L.

- Sonnenberg, M. Hada, M. Ehara, K. Toyota, R. Fukuda, J. Hasegawa, M. Ishida, T. Nakajima, Y. Honda, O. Kitao, H. Nakai, T. Vreven, J. A. Montgomery, Jr., J. E. Peralta, F. Ogliaro, M. Bearpark, J. J. Heyd, E. Brothers, K. N. Kudin, V. N. Staroverov, R. Kobayashi, J. Normand, K. Raghavachari, A. Rendell, J. C. Burant, S. S. Iyengar, J. Tomasi, M. Cossi, N. Rega, J. M. Millam, M. Klene, J. E. Knox, J. B. Cross, V. Bakken, C. Adamo, J. Jaramillo, R. Gomperts, R. E. Stratmann, O. Yazyev, A. J. Austin, R. Cammi, C. Pomelli, J. W. Ochterski, R. L. Martin, K. Morokuma, V. G. Zakrzewski, G. A. Voth, P. Salvador, J. J. Dannenberg, S. Dapprich, A. D. Daniels, Ö. Farkas, J. B. Foresman, J. V. Ortiz, J. Cioslowski, and D. J. Fox, "Gaussian 09, Revision A.1", Gaussian Inc., Wallingford, CT (2009).
- [42] A. D. Becke, "Density-functional exchange-energy approximation with correct asymptotic behavior", *Phys. Rev. A* **38**, 3098 (1988).
- [43] C. Lee, W. Yang, and R. G. Parr, "Development of the Colle–Salvetti correlation-energy formula into a functional of the electron density", *Phys. Rev. B* **37**, 785 (1988).
- [44] A. D. Becke, "Density-functional thermochemistry. III. The role of exact exchange", *J. Chem. Phys.* **98**, 5648 (1993).
- [45] P. J. Stephens, F. J. Devlin, C. F. Chabalowski, and M. J. Frisch, "*Ab initio* calculation of vibrational absorption and circular dichroism spectra using density functional force fields", *J. Phys. Chem.* **98**, 11623 (1994).
- [46] V. N. Staroverov, G. E. Scuseria, J. Tao, and J. P. Perdew, "Erratum: "Comparative assessment of a new nonempirical density functional: Molecules and hydrogen-bonded complexes" [J. Chem. Phys. 119, 12129 (2003)]", *J. Chem. Phys.* **121**, 11507(E) (2004).
- [47] O. A. Vydrov and G. E. Scuseria, "Assessment of a long-range corrected hybrid functional", *J. Chem. Phys.* **125**, 234109 (2006).
- [48] Y. Zhao and D. G. Truhlar, "The M06 suite of density functionals for main group thermochemistry, thermochemical kinetics, noncovalent interactions, excited states, and transition elements: two new functionals and systematic testing of four M06-class functionals and 12 other functionals", *Theor. Chem. Acc.* **120**, 215 (2008).

- [49] Yu. Ralchenko, A. E. Kramida, J. Reader, and NIST ASD Team, NIST Atomic Spectra Database (ver. 4.1.0), <http://physics.nist.gov/asd>.
- [50] E. S. Nielsen, P. Jørgensen, and J. Oddershede, “Transition moments and dynamic polarizabilities in a second order polarization propagator approach”, *J. Chem. Phys.* **73**, 6238 (1980).
- [51] D. J. Clouthier and D. A. Ramsay, “The spectroscopy of formaldehyde and thioformaldehyde”, *Ann. Rev. Phys. Chem.* **34**, 31 (1983).
- [52] R. Dressler and M. Allan, “A dissociative electron attachment, electron transmission, and electron energy-loss study of the temporary negative ion of acetylene”, *J. Chem. Phys.* **87**, 4510 (1987).
- [53] A. S. Zyubin and A. M. Mebel, “Accurate prediction of excitation energies to high-lying Rydberg electronic states: Rydberg states of acetylene as a case study”, *J. Chem. Phys.* **119**, 6581 (2003).
- [54] L. Serrano-Andrés, M. Merchán, I. Nebot-Gil, R. Lindh, and B. O. Roos, “Towards an accurate molecular orbital theory for excited states: Ethene, butadiene, and hexatriene”, *J. Chem. Phys.* **98**, 3151 (1993).
- [55] A. Chutjian, R. I. Hall, and S. Trajmar, “Electron-impact excitation of H₂O and D₂O at various scattering angles and impact energies in the energy-loss range 4.2–12 eV”, *J. Chem. Phys.* **63**, 892 (1975).
- [56] S. B. Ben-Shlomo and U. Kaldor, “N₂ excitations below 15 eV by the multireference coupled-cluster method”, *J. Chem. Phys.* **92**, 3680 (1990).
- [57] J. P. Perdew and A. Zunger, “Self-interaction correction to density-functional approximations for many-electron systems”, *Phys. Rev. B* **23**, 5048 (1981).
- [58] A. J. Cohen, P. Mori-Sánchez, and W. Yang, “Development of exchange-correlation functionals with minimal many-electron self-interaction error”, *J. Chem. Phys.* **126**, 191109 (2007).
- [59] H. Chermette, I. Ciofini, F. Mariotti, and C. Daul, “A posteriori corrections to systematic failures of standard density functionals: The dissociation of two-center three-electron systems”, *J. Chem. Phys.* **115**, 11068 (2001).
- [60] I. Dabo, A. Ferretti, N. Poilvert, Y. Li, N. Marzari, and M. Cococcioni, “Koopmans’ condition for density-functional theory”, *Phys. Rev. B* **82**, 115121 (2010).

- [61] M. Grüning, O. V. Gritsenko, S. J. A. van Gisbergen, and E. J. Baerends, “On the required shape corrections to the local density and generalized gradient approximations to the Kohn–Sham potentials for molecular response calculations of (hyper)polarizabilities and excitation energies”, *J. Chem. Phys.* **116**, 9591 (2002).

Chapter 7

Summary and outlook

Most approximations in density functional theory predict accurate total electronic energies but fail for response properties such as electronic excitations, ionization energies, and molecular polarizabilities. These properties are highly sensitive to the quality of the Kohn–Sham potential; thus, their description can be improved by directly approximating the exchange–correlation potential [1–4] and imparting it with the essential analytical properties such as the exact Coulombic decay [5], shell structure, and derivative discontinuities [6, 7].

A model exchange–correlation potential is unlikely to be a functional derivative of any functional unless explicitly constrained to be one. Non-integrable potentials do not have a unique energy associated with them and lack the translational and rotational invariance, which leads to artifacts such as energies dependent on molecular orientations, and causes problems with geometry optimizations [2, 8]. As a result, applications of stray model potentials have long been limited to calculations of molecular response properties [7, 9]. To be useful for a wider range of applications, model potentials must be integrable.

Before our work, there existed only scattered results related to the integrability of model potentials [2, 10, 11]. We have proposed numerical and analytical tests to detect non-integrable potentials, as well as several methods to construct integrable potentials directly. Our work laid the foundation for the development of universal potential approximations in density functional theory that can perform equally well for computing both energies and response properties. We also proposed a self-interaction correction scheme that improves the shape of standard exchange–correlation potentials and, in this sense, amounts to generating model potentials *on the fly*. What remains to be done is to learn how to improve the accuracy of potential approximations. We will now discuss several strategies for designing better model Kohn–Sham potentials.

One of the big open questions is how to develop accurate approximation to the entire exchange-correlation potential. The vast majority of model potentials existing today are exchange-only [4, 12–14], and even the few exchange-correlation approximations such as the LB94 [3] and U06 [15] actually have the exchange-like behavior. The true correlation potential is more difficult to approximate because its properties are studied less than the properties of the exchange potential. Perhaps, one might get a better idea of what to approximate by analyzing exact correlation potentials extracted from highly-correlated densities of various systems [16–18].

One could get additional flexibility for the development of model potentials by constructing them from the Kohn–Sham orbitals. Numerous exchange potentials such as the Becke–Johnson [4], Räsänen–Pittalis–Proetto [13], and the recently proposed ϵ -consistent potential (Sec. 1.4.1) use Kohn–Sham orbitals as a basic ingredient. It would also be interesting to design the *entire* exchange-correlation potential from the orbitals. Note that the energy from orbital-dependent potentials can be computed by line-integration along the Λ -path [Eq. (1.60)] but not along the Q- [Eq. (1.59)] or Z-paths [Eq. (1.63)] because the scaling of Kohn–Sham orbitals is known only under the λ -transformation of the density. One could try to extend the line-integral method of Ref. 19 to orbital-dependent potentials. For example, it should be possible to take the derivative of the exchange-correlation functional with respect to the Kohn–Sham orbitals $\phi_i(\mathbf{r})$ [2, 20, 21]

$$\frac{\delta E_{\text{XC}}[\rho]}{\delta \phi_i^*(\mathbf{r})} = v_{\text{XC}}([\rho]; \mathbf{r}) \phi_i, \quad (7.1)$$

and rewrite the van Leeuwen–Baerends line integral in terms of the derivatives $\delta E_{\text{XC}}[\rho]/\delta \phi_i^*(\mathbf{r})$ rather than $\delta E_{\text{XC}}[\rho]/\delta \rho(\mathbf{r})$. It would also be interesting to study the scaling of the Kohn–Sham orbitals under the q - and ζ -density transformations.

Another important problem is to design models with exact Coulombic decay. So far this proved to be quite difficult because the electron density falls off exponentially, and any approximation that uses only the density and its derivatives will inherit the exponential decay [17, 22, 23]. We envision at least three different ways to capture the exact asymptotic behavior of the potential. One possibility is to extract r from quantities like $\ln \rho$ or $\ln s$. In fact, the LB94 model [3] does just that because it contains the term $\sinh^{-1}(s) = \ln(s + \sqrt{1 + s^2})$. Unfortunately, the logarithmic function increases too slowly, so the LB94 potential reaches the correct asymptotic decay too late [15]. Another possibility is to get the term $-1/r$ from the Laplacian of the density

[Eq. (3.16)]. This idea was implemented in the functional of Engel and Vosko [24],

$$E_X[\rho] = -\frac{1}{2} \int \rho^{4/3}(\mathbf{r}) s(\mathbf{r}) d\mathbf{r}. \quad (7.2)$$

The corresponding potential has the correct asymptotic decay but is too negative in the region near the nucleus. Furthermore, this approximation does not recover the density-gradient expansion of the slowly varying electron gas and is therefore not very accurate. Still, one might employ this idea to design simple gradient-dependent functionals with the correct long-range behavior of the potential.

Probably, the most promising approach is to develop potentials in the form of the electrostatic integral, as pointed out by Li, Ayers, and Parr [25, 26], and by Görling [27],

$$v_{XC}(\mathbf{r}) = \int \frac{q_{XC}(\mathbf{r}')}{|\mathbf{r}' - \mathbf{r}|} d\mathbf{r}'. \quad (7.3)$$

The potential v_{XC} becomes asymptotically correct if the exchange-correlation charge q_{XC} integrates to -1 [28, 29]. The development of model potentials then reduces to finding a suitable representation of q_{XC} . One of the possible choices is $q_{XC} = -\rho/N$, which gives rise to the Fermi–Amaldi model of Eq. (1.40). The success of the approach focusing on exchange-correlation charge has been recently demonstrated by Andrade [30] and Gidopoulos [31], who designed new potentials with correct long-range decay by normalizing approximate q_{XC} . Even our self-interaction correction scheme discussed in Chapter 6 partially recovers the correct normalization of the underlying exchange-correlation charge, and thereby improves the shape of the potential.

There are many other interesting problems one could address. I finish this thesis in the hope that the potential-driven approach will soon play a prominent role in the development of density functional theory.

Bibliography

- [1] R. van Leeuwen, O. V. Gritsenko, and E. J. Baerends, “Analysis and modelling of atomic and molecular Kohn–Sham potentials”, *Top. Curr. Chem.* **180**, 107 (1996).
- [2] R. Neumann, R. H. Nobes, and N. C. Handy, “Exchange functionals and potentials”, *Mol. Phys.* **87**, 1 (1996).
- [3] R. van Leeuwen and E. J. Baerends, “Exchange-correlation potential with correct asymptotic behavior”, *Phys. Rev. A* **49**, 2421 (1994).
- [4] A. D. Becke and E. R. Johnson, “A simple effective potential for exchange”, *J. Chem. Phys.* **124**, 221101 (2006).
- [5] J. P. Perdew and A. Zunger, “Self-interaction correction to density-functional approximations for many-electron systems”, *Phys. Rev. B* **23**, 5048 (1981).
- [6] J. P. Perdew, M. Levy, and J. L. Balduz, “Density-functional theory for fractional particle number: Derivative discontinuities of the energy”, *Phys. Rev. Lett.* **49**, 1691 (1982).
- [7] M. E. Casida and D. R. Salahub, “Asymptotic correction approach to improving approximate exchange-correlation potentials: Time-dependent density-functional theory calculations of molecular excitation spectra”, *J. Chem. Phys.* **113**, 8918 (2000).
- [8] D. J. Tozer, “The asymptotic exchange potential in Kohn–Sham theory”, *J. Chem. Phys.* **112**, 3507 (2000).
- [9] M. Grüning, O. V. Gritsenko, S. J. A. van Gisbergen, and E. J. Baerends, “On the required shape corrections to the local density and generalized gradient approximations to the Kohn–Sham potentials for molecular response calculations

- of (hyper)polarizabilities and excitation energies”, *J. Chem. Phys.* **116**, 9591 (2002).
- [10] H. Ou-Yang and M. Levy, “Theorem for exact local exchange potential”, *Phys. Rev. Lett.* **65**, 1036 (1990).
- [11] A. Karolewski, R. Armiento, and S. Kümmel, “Polarizabilities of polyacetylene from a field-counteracting semilocal functional”, *J. Chem. Theory Comput.* **5**, 712 (2009).
- [12] V. N. Staroverov, “A family of model Kohn–Sham potentials for exact exchange”, *J. Chem. Phys.* **129**, 134103 (2008).
- [13] E. Räsänen, S. Pittalis, and C. R. Proetto, “Universal correction for the Becke–Johnson exchange potential”, *J. Chem. Phys.* **132**, 044112 (2010).
- [14] F. Della Sala and A. Görling, “Efficient localized Hartree–Fock methods as effective exact-exchange Kohn–Sham methods for molecules”, *J. Chem. Phys.* **115**, 5718 (2001).
- [15] N. Umezawa, “Explicit density-functional exchange potential with correct asymptotic behavior”, *Phys. Rev. A* **74**, 032505 (2006).
- [16] Q. Zhao, R. C. Morrison, and R. G. Parr, “From electron densities to Kohn–Sham kinetic energies, orbital energies, exchange-correlation potentials, and exchange-correlation energies”, *Phys. Rev. A* **50**, 2138 (1994).
- [17] C. R. Jacob, “Unambiguous optimization of effective potentials in finite basis sets”, *J. Chem. Phys.* **135**, 244102 (2011).
- [18] I. G. Ryabinkin and V. N. Staroverov, “Determination of Kohn–Sham effective potentials from electron densities using the differential virial theorem”, *J. Chem. Phys.* **137**, 164113 (2012).
- [19] R. van Leeuwen and E. J. Baerends, “Energy expressions in density-functional theory using line integrals”, *Phys. Rev. A* **51**, 170 (1995).
- [20] A. V. Arbuznikov, M. Kaupp, V. G. Malkin, R. Reviakine, and O. L. Malkina, “Validation study of meta-GGA functionals and of a model exchange-correlation potential in density functional calculations of EPR parameters”, *Phys. Chem. Chem. Phys.* **4**, 5467 (2002).

- [21] A. V. Arbuznikov and M. Kaupp, “The self-consistent implementation of exchange-correlation functionals depending on the local kinetic energy density”, *Chem. Phys. Lett.* **381**, 495 (2003).
- [22] P. R. T. Schipper, O. V. Gritsenko, and E. J. Baerends, “Kohn–Sham potentials corresponding to Slater and Gaussian basis set densities”, *Theor. Chem. Acc.* **98**, 16 (1997).
- [23] M. E. Mura, P. J. Knowles, and C. A. Reynolds, “Accurate numerical determination of Kohn–Sham potentials from electronic densities: I. Two-electron systems”, *J. Chem. Phys.* **106**, 9659 (1997).
- [24] E. Engel, J. A. Chevary, L. D. Macdonald, and S. H. Vosko, “Asymptotic properties of the exchange energy density and the exchange potential of finite systems: Relevance for generalized gradient approximations”, *Z. Phys. D: At., Mol. Clusters* **23**, 7 (1992).
- [25] S. Liu, P. W. Ayers, and R. G. Parr, “Alternative definition of exchange-correlation charge in density functional theory”, *J. Chem. Phys.* **111**, 6197 (1999).
- [26] P. W. Ayers and M. Levy, “Sum rules for exchange and correlation potentials”, *J. Chem. Phys.* **115**, 4438 (2001).
- [27] A. Görling, “New KS method for molecules based on an exchange charge density generating the exact local KS exchange potential”, *Phys. Rev. Lett.* **83**, 5459 (1999).
- [28] G. B. Arfken and H. J. Weber, *Mathematical Methods for Physicists*, Academic Press, San Diego, 6th ed. (2005).
- [29] P. W. Ayers, R. C. Morrison, and R. G. Parr, “Fermi–Amaldi model for exchange-correlation: atomic excitation energies from orbital energy differences”, *Mol. Phys.* **103**, 2061 (2005).
- [30] X. Andrade and A. Aspuru-Guzik, “Prediction of the derivative discontinuity in density functional theory from an electrostatic description of the exchange and correlation potential”, *Phys. Rev. Lett.* **107**, 183002 (2011).
- [31] N. I. Gidopoulos and N. N. Lathiotakis, “Constraining density functional approximations to yield self-interaction free potentials”, *J. Chem. Phys.* **136**, 224109 (2012).

Appendix A

Properties of the delta function

The Dirac delta function $\delta(x)$ is defined by its two properties:

$$\delta(x) = \begin{cases} 0 & \text{for } x \neq 0 \\ \infty & \text{for } x = 0 \end{cases} \quad \text{and} \quad \int_{-\infty}^{\infty} f(x)\delta(x) dx = f(0), \quad (\text{A.1})$$

where $f(x)$ is some probe function. As a special case, $\int_{-\infty}^{\infty} \delta(x) dx = 1$. The delta function may be interpreted as an infinitely sharp spike at the origin with a total area of one under the spike. Dirac delta is not a function in the usual sense: It belongs to a class of generalized functions, or distributions, and is meaningful only as part of an integral. In this spirit, the linear operator $\int dx \delta(x)$ acts on $f(x)$ to yield $f(0)$.

Here we review the properties of $\delta(x)$ relevant to the present work. Let $\delta(x - x')$ be delta function shifted by x' along the coordinate axis. To evaluate the integral with $\delta(x - x')$, we change the variable to $y \equiv x - x'$ and use the definition [Eq. (A.1)] to write

$$\int_{-\infty}^{\infty} f(x)\delta(x - x') dx = \int_{-\infty}^{\infty} f(y + x')\delta(y) dy = f(x'), \quad (\text{A.2})$$

Thus, the function $\delta(x)$ is a special case of $\delta(x - x')$ with $x' = 0$.

Dirac delta is an even function, i.e., $\delta(x - x') = \delta(x' - x)$. To see this, consider the integral with $\delta(x' - x)$ multiplied by a test function $f(x)$. We change the integration variable from x to $y \equiv x' - x$ so that $dy = -dx$, and get

$$\int_{-\infty}^{\infty} f(x)\delta(x' - x) dx = - \int_{\infty}^{-\infty} f(x' - y)\delta(y) dy = \int_{-\infty}^{\infty} f(x' - y)\delta(y) dy = f(x'), \quad (\text{A.3})$$

the same result as Eq. (A.2).

To evaluate derivatives of the delta function, we insert $\frac{d}{dx} \delta(x - x')$ into the integral

with $f(x)$ and perform integration by parts,

$$\int_{-\infty}^{\infty} f(x) \frac{d}{dx} \delta(x - x') dx = - \int_{-\infty}^{\infty} \frac{d}{dx} f(x) \delta(x - x') dx = - \left\{ \frac{df(t)}{dt} \right\}_{t=x'} \quad (\text{A.4})$$

In a similar way,

$$\int_{-\infty}^{\infty} f(x) \frac{d^n}{dx^n} \delta(x - x') dx = (-1)^n \left\{ \frac{d^n f(t)}{dt^n} \right\}_{t=x'} \quad (\text{A.5})$$

There are two important properties of the derivative of the Dirac delta. First, the operator d/dx can be replaced by d/dx' , but this operation changes the sign of the derivative,

$$\frac{d}{dx} \delta(x - x') = - \frac{d}{dx'} \delta(x - x'). \quad (\text{A.6})$$

Second, the first derivative of $\delta(x - x')$ is an odd function,

$$\left\{ \frac{d\delta(t)}{dt} \right\}_{t=x-x'} = - \left\{ \frac{d\delta(t)}{dt} \right\}_{t=x'-x} \quad (\text{A.7})$$

The first statement is proved by moving the differential outside the integral sign:

$$\int_{-\infty}^{\infty} f(x) \frac{d}{dx'} \delta(x - x') dx = \frac{d}{dx'} \int_{-\infty}^{\infty} f(x) \delta(x - x') dx = \left\{ \frac{df(t)}{dt} \right\}_{t=x'} \quad (\text{A.8})$$

The second statement requires a clarification. Since the operations of taking the derivative and changing the sign of the argument of a function do not commute, the result will depend on their order. In Eq. (A.7), differentiation precedes changing the argument of the derivative function. On the other hand, if differentiation is performed *after* replacing $(x - x')$ by $(x' - x)$, the sign of the derivative does not change. To distinguish between the two (potentially confusing) cases, we indicate the order of the operations using square brackets:

$$\left[\frac{d\delta}{dx} \right] (x - x') = - \left[\frac{d\delta}{dx} \right] (x' - x), \quad \text{but} \quad (\text{A.9})$$

$$\frac{d}{dx} [\delta(x - x')] = \frac{d}{dx} [\delta(x' - x)]. \quad (\text{A.10})$$

The Dirac delta function is easily generalized to the case of three dimensions:

$$\delta(\mathbf{r} - \mathbf{r}') \equiv \delta(x - x') \delta(y - y') \delta(z - z'). \quad (\text{A.11})$$

All properties derived for the one-dimensional delta function also apply to the three-dimensional function. Let us write out the results:

$$\int f(\mathbf{r})\delta(\mathbf{r} - \mathbf{r}') d\mathbf{r} = f(\mathbf{r}') \quad (\text{A.12})$$

$$\int f(\mathbf{r})\nabla_{\mathbf{r}}\delta(\mathbf{r} - \mathbf{r}') d\mathbf{r} = -\nabla_{\mathbf{r}'}f(\mathbf{r}') \quad (\text{A.13})$$

$$\int f(\mathbf{r})\nabla_{\mathbf{r}}^2\delta(\mathbf{r} - \mathbf{r}') d\mathbf{r} = \nabla_{\mathbf{r}'}^2f(\mathbf{r}') \quad (\text{A.14})$$

$$\delta(\mathbf{r} - \mathbf{r}') = \delta(\mathbf{r}' - \mathbf{r}) \quad (\text{A.15})$$

$$[\nabla_{\mathbf{r}}\delta](\mathbf{r} - \mathbf{r}') = -[\nabla_{\mathbf{r}}\delta](\mathbf{r}' - \mathbf{r}) \quad (\text{A.16})$$

$$\nabla_{\mathbf{r}}[\delta(\mathbf{r} - \mathbf{r}')] = \nabla_{\mathbf{r}}[\delta(\mathbf{r}' - \mathbf{r})] \quad (\text{A.17})$$

$$\nabla_{\mathbf{r}}\delta(\mathbf{r} - \mathbf{r}') = -\nabla_{\mathbf{r}'}\delta(\mathbf{r} - \mathbf{r}'). \quad (\text{A.18})$$

Appendix B

Functional derivative of the Levy–Perdew energy expression

Here we derive a convenient formula [Eq. (B.20)] for evaluating functional derivatives of functionals of the form

$$F[\rho] = \int v(\rho, g)(3\rho + \mathbf{r} \cdot \nabla\rho) d\mathbf{r}, \quad (\text{B.1})$$

where $g \equiv |\nabla\rho|$ and $v(\rho, g)$ is some gradient-corrected Kohn–Sham model potential. Equation (B.1) belongs to a class of functionals of the type

$$F[\rho] = \int f(\mathbf{r}, \rho, \nabla\rho) d\mathbf{r}. \quad (\text{B.2})$$

Functional derivatives of such quantities are given by the general formula of the calculus of variations,

$$\frac{\delta F}{\delta\rho} = \frac{\partial f}{\partial\rho} - \nabla \cdot \left(\frac{\partial f}{\partial\nabla\rho} \right), \quad (\text{B.3})$$

in which $\partial f/\partial\nabla\rho$ means a vector with the components $(\partial f/\partial\rho_x, \partial f/\partial\rho_y, \partial f/\partial\rho_z)$ with $\rho_i \equiv \partial\rho/\partial i$ ($i = x, y, z$). Applying formula (B.3) to Eq. (B.1) one has

$$\frac{\delta F}{\delta\rho} = \frac{\partial v}{\partial\rho}(3\rho + \mathbf{r} \cdot \nabla\rho) + 3v - \nabla \cdot \left[\frac{\partial v}{\partial\nabla\rho}(3\rho + \mathbf{r} \cdot \nabla\rho) + \mathbf{r}v \right]. \quad (\text{B.4})$$

We observe that

$$\nabla \cdot (\mathbf{r}v) = 3v + \mathbf{r} \cdot \nabla v \quad (\text{B.5})$$

and use this identity to rearrange Eq. (B.4) as follows

$$\frac{\delta F}{\delta \rho} = \left[\frac{\partial v}{\partial \rho} - \nabla \cdot \left(\frac{\partial v}{\partial \nabla \rho} \right) \right] (3\rho + \mathbf{r} \cdot \nabla \rho) - \frac{\partial v}{\partial \nabla \rho} \cdot \nabla (3\rho + \mathbf{r} \cdot \nabla \rho) - \mathbf{r} \cdot \nabla v. \quad (\text{B.6})$$

Let us elaborate each of the three terms on the right-hand side of Eq. (B.6), starting with the last. Using the chain rule of differentiation for $v(\rho, g)$ we have

$$\mathbf{r} \cdot \nabla v = \frac{\partial v}{\partial \rho} \mathbf{r} \cdot \nabla \rho + \frac{\partial v}{\partial g} \mathbf{r} \cdot \nabla g. \quad (\text{B.7})$$

The dot product $\mathbf{r} \cdot \nabla \rho$ can be evaluated trivially. To evaluate $\mathbf{r} \cdot \nabla g$, we observe that each of the three components of the Cartesian vector $\nabla g \equiv (g_x, g_y, g_z)$ can be written as $g_i = g^{-1} \sum_j \rho_{ij} \rho_j$, where $i, j = x, y, z$ and ρ_{ij} are the components of the Hessian tensor of the density. This gives the following ready-to-program formula

$$\mathbf{r} \cdot \nabla g = \frac{1}{g} \sum_{ij} i \rho_{ij} \rho_j \quad (i, j = x, y, z). \quad (\text{B.8})$$

Now for the second term of Eq. (B.6). Using the chain rule of differentiation for $v(\rho, g)$ we have

$$\frac{\partial v}{\partial \nabla \rho} = \frac{\partial v}{\partial g} \frac{\partial g}{\partial \nabla \rho} = \frac{\partial v}{\partial g} \frac{\nabla \rho}{g}. \quad (\text{B.9})$$

This allows us to write the second term of Eq. (B.6) as

$$\frac{\partial v}{\partial \nabla \rho} \cdot \nabla (3\rho + \mathbf{r} \cdot \nabla \rho) = \frac{\partial v}{\partial g} \left[3g + \frac{\nabla \rho \cdot \nabla (\mathbf{r} \cdot \nabla \rho)}{g} \right]. \quad (\text{B.10})$$

Here

$$\frac{\nabla \rho \cdot \nabla (\mathbf{r} \cdot \nabla \rho)}{g} = \frac{g^2 + \sum_{ij} i \rho_{ij} \rho_j}{g} = g + \mathbf{r} \cdot \nabla g, \quad (\text{B.11})$$

where we have used the definition of $\mathbf{r} \cdot \nabla g$ by Eq. (B.8). Substitution of Eq. (B.11) into Eq. (B.10) yields

$$\frac{\partial v}{\partial \nabla \rho} \cdot \nabla (3\rho + \mathbf{r} \cdot \nabla \rho) = \frac{\partial v}{\partial g} (4g + \mathbf{r} \cdot \nabla g). \quad (\text{B.12})$$

Next consider the quantity inside square brackets in the first term of Eq. (B.6). Expressions of this type were worked out in Sec. 3.2.1. Referring to Eqs. (3.3) and (3.8),

we can immediately write

$$\frac{\partial v}{\partial \rho} - \nabla \cdot \left(\frac{\partial v}{\partial \nabla \rho} \right) = \frac{\partial v}{\partial \rho} - \frac{\partial^2 v}{\partial \rho \partial g} g - \frac{\partial v}{\partial g} \frac{\nabla^2 \rho}{g} + \left(\frac{\partial v}{\partial g} - g \frac{\partial^2 v}{\partial g^2} \right) \frac{w}{g^3}, \quad (\text{B.13})$$

where $w = \sum_{ij} \rho_i \rho_{ij} \rho_j$ [cf. Eq. (3.7)].

Finally, we substitute Eqs. (B.7), (B.12), and (B.13) into Eq. (B.6) and write the result as

$$\frac{\delta F}{\delta \rho} = 3\rho \frac{\partial v}{\partial \rho} - 2(2g + \mathbf{r} \cdot \nabla g) \frac{\partial v}{\partial g} - \left[\frac{\partial^2 v}{\partial \rho \partial g} g + \frac{\partial v}{\partial g} \frac{\nabla^2 \rho}{g} - \left(\frac{\partial v}{\partial g} - g \frac{\partial^2 v}{\partial g^2} \right) \frac{w}{g^3} \right] (3\rho + \mathbf{r} \cdot \nabla \rho). \quad (\text{B.14})$$

Equation (B.14) is not easy to use unless the potential v is specified in terms of the *reduced* (dimensionless) density gradient s rather than g . To adapt our formula to functionals of the type

$$F[\rho] = \int v(\rho, s) (3\rho + \mathbf{r} \cdot \nabla \rho) d\mathbf{r}, \quad (\text{B.15})$$

we change variables in Eq. (B.14) from (ρ, g) to (ρ, s) using the following transformation rules from Sec. 3.2.1

$$\frac{\partial v}{\partial \rho} \rightarrow \frac{\partial v}{\partial \rho} - \frac{4}{3} \frac{\partial v}{\partial s} \frac{s}{\rho}, \quad (\text{B.16})$$

$$\frac{\partial v}{\partial g} \rightarrow \frac{\partial v}{\partial s} \frac{s}{g}, \quad (\text{B.17})$$

$$\frac{\partial^2 v}{\partial \rho \partial g} \rightarrow \frac{\partial^2 v}{\partial \rho \partial s} \frac{s}{g} - \frac{4}{3} \frac{\partial^2 v}{\partial s^2} \frac{s^2}{\rho g} - \frac{4}{3} \frac{\partial v}{\partial s} \frac{s}{\rho g}, \quad (\text{B.18})$$

$$\frac{\partial^2 v}{\partial g^2} \rightarrow \frac{\partial^2 v}{\partial s^2} \frac{s^2}{g^2} \quad (\text{B.19})$$

The result may be written as

$$\begin{aligned} \frac{\delta F}{\delta \rho} = & 3 \frac{\partial v}{\partial \rho} \rho + \left[\frac{4}{3} \frac{\partial^2 v}{\partial s^2} \frac{s^2}{\rho} - \frac{\partial^2 v}{\partial \rho \partial s} s - \frac{4}{3} \frac{\partial v}{\partial s} \frac{s}{\rho} - \frac{\partial v}{\partial s} \frac{q}{\rho s} + \left(\frac{\partial v}{\partial s} - \frac{\partial^2 v}{\partial s^2} s \right) \frac{u}{\rho s^3} \right] (3\rho + \mathbf{r} \cdot \nabla \rho) \\ & - 2 \frac{\partial v}{\partial s} \mathbf{r} \cdot \nabla s, \end{aligned} \quad (\text{B.20})$$

where q and u are given by Eq. (3.9) and

$$\mathbf{r} \cdot \nabla s = \left(\frac{\mathbf{r} \cdot \nabla g}{g} - \frac{4}{3} \frac{\mathbf{r} \cdot \nabla \rho}{\rho} \right) s. \quad (\text{B.21})$$

The dot product $\mathbf{r} \cdot \nabla g$ is computed using Eq. (B.8). In Eq. (B.20), as in Eq. (3.13)

of Sec. 3.2.1, the derivatives of $v(\rho, s)$ with respect to ρ refer *only* to the explicit dependence of v on ρ ; the implicit dependence on ρ through s is taken into account by the variable transformation.

Appendix C

Copyright permissions

C.1 ACS Permission



Title: Reconstruction of Density Functionals from Kohn–Sham Potentials by Integration along Density Scaling Paths

Author: Alex P. Gaiduk, Sergey K. Chulkov, and Viktor N. Staroverov

Publication: Journal of Chemical Theory and Computation

Publisher: American Chemical Society

Date: Apr 1, 2009

Copyright © 2009, American Chemical Society

Logged in as:
Alex Gaiduk

[LOGOUT](#)

PERMISSION/LICENSE IS GRANTED FOR YOUR ORDER AT NO CHARGE

This type of permission/license, instead of the standard Terms & Conditions, is sent to you because no fee is being charged for your order. Please note the following:

- Permission is granted for your request in both print and electronic formats, and translations.
- If figures and/or tables were requested, they may be adapted or used in part.
- Please print this page for your records and send a copy of it to your publisher/graduate school.
- Appropriate credit for the requested material should be given as follows: "Reprinted (adapted) with permission from (COMPLETE REFERENCE CITATION). Copyright (YEAR) American Chemical Society." Insert appropriate information in place of the capitalized words.
- One-time permission is granted only for the use specified in your request. No additional uses are granted (such as derivative works or other editions). For any other uses, please submit a new request.

C.2 ACS Terms and Conditions

Journal of Chemical Theory and Computation

Permission type: Republish or display content

Type of use: Reuse in a Thesis/Dissertation

American Chemical Society's Policy on Theses and Dissertations

If your university requires you to obtain permission, you must use the RightsLink permission system. See RightsLink instructions at <http://pubs.acs.org/page/copyright/permissions.html>.

This is regarding request for permission to include your paper(s) or portions of text from your paper(s) in your thesis. Permission is now automatically granted; please pay special attention to the implications paragraph below. The Copyright Subcommittee of the Joint Board/Council Committees on Publications approved the following:

Copyright permission for published and submitted material from theses and dissertations: ACS extends blanket permission to students to include in their theses and dissertations their own articles, or portions thereof, that have been published in ACS journals or submitted to ACS journals for publication, provided that the ACS copyright credit line is noted on the appropriate page(s).

Publishing implications of electronic publication of theses and dissertation material: Students and their mentors should be aware that posting of theses and dissertation material on the Web prior to submission of material from that thesis or dissertation to an ACS journal may affect publication in that journal. Whether Web posting is considered prior publication may be evaluated on a case-by-case basis by the journal's editor. If an ACS journal editor considers Web posting to be "prior publication", the paper will not be accepted for publication in that journal. If you intend to submit your unpublished paper to ACS for publication, check with the appropriate editor prior to posting your manuscript electronically.

Reuse/Republication of the Entire Work in Theses or Collections: Authors may reuse all or part of the Submitted, Accepted or Published Work in a thesis or dissertation that the author writes and is required to submit to satisfy the criteria of degree-granting institutions. Such reuse is permitted subject to the ACS' "Ethical Guidelines to Publication of Chemical Research" (<http://pubs.acs.org/page/policy/ethics/index.html>); the author should secure written confirmation (via letter or email) from the respective ACS journal editor(s) to avoid potential conflicts with journal prior publication¹/embargo policies. Appropriate citation of the Published Work must be made. If the thesis or dissertation to be published is in electronic format, a direct link to the Published Work must also be included using the ACS Articles on Request author-directed link—see <http://pubs.acs.org/page/policy/articlesonrequest/index.html>.

If your paper has not yet been published by ACS, please print the following credit


¹Prior publication policies of ACS journals are posted on the ACS website at <http://pubs.acs.org/page/policy/prior/index.html>.


line on the first page of your article: “Reproduced (or ‘Reproduced in part’) with permission from [JOURNAL NAME], in press (or ‘submitted for publication’). Unpublished work copyright [CURRENT YEAR] American Chemical Society.” Include appropriate information.



If your paper has already been published by ACS and you want to include the text or portions of the text in your thesis/dissertation, please print the ACS copyright credit line on the first page of your article: “Reproduced (or ‘Reproduced in part’) with permission from [FULL REFERENCE CITATION.] Copyright [YEAR] American Chemical Society.” Include appropriate information.

Submission to a Dissertation Distributor: If you plan to submit your thesis to UMI or to another dissertation distributor, you should not include the unpublished ACS paper in your thesis if the thesis will be disseminated electronically, until ACS has published your paper. After publication of the paper by ACS, you may release the entire thesis (not the individual ACS article by itself) for electronic dissemination through the distributor; ACS’s copyright credit line should be printed on the first page of the ACS paper.

C.3 AIP Permissions

Order detail ID:	63166358	Permission Status:	 Granted
Order License Id:	3023980256963	Permission type:	Republish or display content
Article Title:	Virial exchange energies from model exact-exchange potentials	Type of use:	reuse in a thesis/dissertation
Author(s):	Gaiduk, Alex P. ; Staroverov, Viktor N.	Requestor type	Author (original article)
DOI:	10.1063/1.2920197	Format	Print and electronic
Date:	Jan 01, 2008	Portion	Excerpt (> 800 words)
ISSN:	0021-9606	Will you be translating?	No
Publication Type:	Journal	Title of your thesis / dissertation	Theory of model Kohn-Sham potentials and its applications
Volume:	128	Expected completion date	Jan 2013
Issue:	20	Estimated size (number of pages)	150
Start page:			
Publisher:	AMERICAN INSTITUTE OF PHYSICS.		
Author/Editor:	AMERICAN INSTITUTE OF PHYSICS		

Order detail ID:	63166359	Permission Status:	 Granted
Order License Id:	3023980411561	Permission type:	Republish or display content
Article Title:	How to tell when a model Kohn-Sham potential is not a functional derivative	Type of use:	reuse in a thesis/dissertation
Author(s):	Gaiduk, Alex P. ; Staroverov, Viktor N.	Requestor type	Author (original article)
DOI:	10.1063/1.3176515	Format	Print and electronic
Date:	Jan 01, 2009	Portion	Excerpt (> 800 words)
ISSN:	0021-9606	Will you be translating?	No
Publication Type:	Journal	Title of your thesis / dissertation	Theory of model Kohn-Sham potentials and its applications
Volume:	131	Expected completion date	Jan 2013
Issue:	4	Estimated size (number of pages)	150
Start page:			
Publisher:	AMERICAN INSTITUTE OF PHYSICS.		
Author/Editor:	AMERICAN INSTITUTE OF PHYSICS		

Order detail ID:	63166399	Permission Status:	 Granted
Order License Id:	3023990572396	Permission type:	Republish or display content
Article Title:	Communication: Explicit construction of functional derivatives in potential-driven density-functional theory	Type of use:	reuse in a thesis/dissertation
Author(s):	Gaiduk, Alex P. ; Staroverov, Viktor N.	Requestor type	Author (original article)
DOI:	10.1063/1.3483464	Format	Print and electronic
Date:	Sep 14, 2010	Portion	Excerpt (> 800 words)
ISSN:	0021-9606	Will you be translating?	No
Publication Type:	Journal	Title of your thesis / dissertation	Theory of model Kohn-Sham potentials and its applications
Volume:	133	Expected completion date	Jan 2013
Issue:	10	Estimated size (number of pages)	150
Start page:			
Publisher:	AMERICAN INSTITUTE OF PHYSICS.		
Author/Editor:	AMERICAN INSTITUTE OF PHYSICS		
Order detail ID:	63166400	Permission Status:	 Granted
Order License Id:	3023990723854	Permission type:	Republish or display content
Article Title:	A generalized gradient approximation for exchange derived from the model potential of van Leeuwen and Baerends	Type of use:	reuse in a thesis/dissertation
Author(s):	Gaiduk, Alex P. ; Staroverov, Viktor N.	Requestor type	Author (original article)
DOI:	10.1063/1.3684261	Format	Print and electronic
Date:	Feb 14, 2012	Portion	Excerpt (> 800 words)
ISSN:	0021-9606	Will you be translating?	No
Publication Type:	Journal	Title of your thesis / dissertation	Theory of model Kohn-Sham potentials and its applications
Volume:	136	Expected completion date	Jan 2013
Issue:	6	Estimated size (number of pages)	150
Start page:			
Publisher:	AMERICAN INSTITUTE OF PHYSICS.		
Author/Editor:	AMERICAN INSTITUTE OF PHYSICS		

C.4 AIP Terms and conditions

The Journal of Chemical Physics

Permission type: Republish or display content

Type of use: Reuse in a thesis/dissertation

American Institute of Physics – Terms and Conditions: Permissions Uses

American Institute of Physics (“AIP”) hereby grants to you the non-exclusive right and license to use and/or distribute the Material according to the use specified in your order, on a one-time basis, for the specified term, with a maximum distribution equal to the number that you have ordered. Any links or other content accompanying the Material are not the subject of this license.

1. You agree to include the following copyright and permission notice with the reproduction of the Material: “Reprinted with permission from [FULL CITATION]. Copyright [PUBLICATION YEAR], American Institute of Physics.” For an article, the copyright and permission notice must be printed on the first page of the article or book chapter. For photographs, covers, or tables, the copyright and permission notice may appear with the Material, in a footnote, or in the reference list.
2. If you have licensed reuse of a figure, photograph, cover, or table, it is your responsibility to ensure that the material is original to AIP and does not contain the copyright of another entity, and that the copyright notice of the figure, photograph,

cover, or table does not indicate that it was reprinted by AIP, with permission, from another source. Under no circumstances does AIP, purport or intend to grant permission to reuse material to which it does not hold copyright.

3. You may not alter or modify the Material in any manner. You may translate the Material into another language only if you have licensed translation rights. You may not use the Material for promotional purposes. AIP reserves all rights not specifically granted herein.
4. The foregoing license shall not take effect unless and until AIP or its agent, Copyright Clearance Center, receives the Payment in accordance with Copyright Clearance Center Billing and Payment Terms and Conditions, which are incorporated herein by reference.
5. AIP or the Copyright Clearance Center may, within two business days of granting this license, revoke the license for any reason whatsoever, with a full refund payable to you. Should you violate the terms of this license at any time, AIP, American Institute of Physics, or Copyright Clearance Center may revoke the license with no refund to you. Notice of such revocation will be made using the contact information provided by you. Failure to receive such notice will not nullify the revocation.
6. AIP makes no representations or warranties with respect to the Material. You agree to indemnify and hold harmless AIP, American Institute of Physics, and their officers, directors, employees or agents from and against any and all claims arising out of your use of the Material other than as specifically authorized herein.
7. The permission granted herein is personal to you and is not transferable or assignable without the prior written permission of AIP. This license may not be amended except in a writing signed by the party to be charged.
8. If purchase orders, acknowledgments or check endorsements are issued on any forms containing terms and conditions which are inconsistent with these provisions, such inconsistent terms and conditions shall be of no force and effect. This document, including the CCC Billing and Payment Terms and Conditions, shall be the entire agreement between the parties relating to the subject matter hereof.

This Agreement shall be governed by and construed in accordance with the laws of the State of New York. Both parties hereby submit to the jurisdiction of the courts of New York County for purposes of resolving any disputes that may arise hereunder.

C.5 APS Permission

From: Associate Publisher <...>
 Date: Thu, Nov 1, 2012 at 12:08 PM
 Subject: Re: Copyright Permission Request
 To: Alex Gaiduk <...>

Dear Alex Gaiduk

Thank you for your email. As the author, you have the right to use the article or a portion of the article in a thesis or dissertation without requesting permission from APS, provided the bibliographic citation and the APS copyright credit line are given on the appropriate pages.

Best wishes,

Jasmine Martin

American Physical Society

----- Original Message -----

From: Alex Gaiduk <...>
 To: Associate Publisher <...>
 Sent: Tuesday, October 30, 2012 3:50:54 PM
 Subject: Copyright Permission Request

Dear Sir or Madam:

I am the author of several papers in the APS journals, and I would like to include them into my Ph.D. thesis titled “Theory of model Kohn-Sham potentials and its applications”, to be published by the University of Western Ontario (Canada). The papers are:

- 1) A. P. Gaiduk, D. Mizzi, and V. N. Staroverov, “A self-interaction correction scheme for approximate Kohn-Sham potentials”, submitted to Phys. Rev. A.
- 2) A. P. Gaiduk, D. S. Firaha, and V. N. Staroverov, “Improved electronic excitation energies from shape-corrected semilocal Kohn-Sham potentials” Phys. Rev. Lett. 108, 253005 (2012).
- 3) A. P. Gaiduk and V. N. Staroverov, “Construction of integrable model Kohn-Sham potentials by analysis of the structure of functional derivatives”, Phys. Rev. A 83, 012509 (2011).

My thesis will be available in full-text on the Internet for reference, study and/or copy. Except in situations where a thesis is under embargo or restriction, the electronic version will be accessible through the University of Western Ontario Libraries web pages, the Library's web catalogue, and also through web search engines.

I am asking for your permission to include the papers listed above into my thesis.

Sincerely yours,

Alex Gaiduk

Curriculum Vitæ

Name:	Alex P. Gaiduk
Post-Secondary Education and Degrees:	Ph.D. in Chemistry (2013) University of Western Ontario, London, Canada Advisor: Professor Viktor N. Staroverov B.Sc. in Chemistry (2008) Belarus State University, Minsk, Belarus Advisor: Dr. Vitaly E. Matulis
Honours and Awards:	Graduate Thesis Research Award (2011) Ontario Graduate Scholarship (2009–2011) Lumsden Graduate Fellowship (2011) Best poster award, 17th Canadian Symposium on Theoretical Chemistry (2010) Best poster award, 9th Annual Centre for Research in Molecular Modeling Symposium (2009) Christian Sivertz Scholarship (2008) Best undergraduate performance award (2008) Best undergraduate research award (2008) Belarus President’s Scholarship (2007) Best talk award, 16th International Conference “Radiation Physics of Solids” (2006) Francysk Skaryna Scholarship (2005)
Related Work Experience:	Teaching Assistant (2008–2012) University of Western Ontario Coach for the National Chemistry Olympiad (2008) Belarus State University

Publications:

11. A. A. Kananenka, S. V. Kohut, **A. P. Gaiduk**, I. G. Ryabinkin, and V. N. Staroverov, “Generation of model potentials using the Kohn–Sham inversion procedure”, manuscript in preparation.
10. **A. P. Gaiduk**, D. Mizzi, and V. N. Staroverov, “Self-interaction correction scheme for approximate Kohn–Sham potentials”, *Phys. Rev. A* **2012**, 86, 052518/1–7.
9. **A. P. Gaiduk**, D. S. Firaha, and V. N. Staroverov, “Improved electronic excitation energies from shape-corrected semilocal Kohn–Sham potentials”, *Phys. Rev. Lett.* **2012**, 108, 253005/1–5.
8. **A. P. Gaiduk** and V. N. Staroverov, “A generalized gradient approximation for exchange derived from the model potential of van Leeuwen and Baerends”, *J. Chem. Phys.* **2012**, 136, 064116/1–8.
7. **A. P. Gaiduk** and V. N. Staroverov, “Construction of integrable model Kohn–Sham potentials by analysis of the structure of functional derivatives”, *Phys. Rev. A* **2011**, 83, 012509/1–7.
6. **A. P. Gaiduk** and V. N. Staroverov, “Explicit construction of functional derivatives in potential-driven density-functional theory”, *J. Chem. Phys.* **2010**, 133, 101104/1–4.
5. **A. P. Gaiduk** and V. N. Staroverov, “How to tell when a model Kohn–Sham potential is not a functional derivative”, *J. Chem. Phys.* **2009**, 131, 044107/1–7.
4. **A. P. Gaiduk**, S. K. Chulkov, and V. N. Staroverov, “Reconstruction of density functionals from Kohn–Sham potentials by integration along density scaling paths”, *J. Chem. Theory Comput.* **2009**, 5, 699–707.
3. **A. P. Gaiduk** and V. N. Staroverov, “Virial exchange energies from model exact-exchange potentials”, *J. Chem. Phys.* **2008**, 128, 204101/1–6.
2. **A. P. Gaiduk**, P. I. Gaiduk, and A. Nylandsted Larsen, “Chemical bath deposition of PbS nanocrystals: Effect of substrate”, *Thin Solid Films* **2008**, 516, 3791–3795.
1. **A. P. Gaiduk**, A. Nylandsted Larsen, J. Chevalier, and P. I. Gaiduk, “Decomposition of SiO₂(Ge) supersaturated alloys due to high-temperature treatment”, *Perspekt. Mater.* **2007**, 2, 29–35 (in Russian).

Talks at national and international meetings:

5. “Energy expressions for model exchange potentials: Beyond the Levy–Perdew virial relation”, 2012 March Meeting of the American Physical Society, Boston, Massachusetts, February 27–March 2, 2012.
4. “Accurate total energies from the model potential of van Leeuwen and Baerends”, Applied Mathematics, Modeling and Computational Science Conference, Wilfrid Laurier University, Waterloo, Ontario, July 25–29, 2011.
3. “Toward density-functional theory based on model Kohn–Sham potentials”, 26th Symposium on Chemical Physics, University of Waterloo, Waterloo, Ontario, November 5–7, 2010.
2. “Analytic structure of functional derivatives of density-functional approximations”, 240th American Chemical Society Meeting, Boston, Massachusetts, August 22–26, 2010.
1. “Evolution of the composition and phase structure of $\text{SiO}_2(\text{Ge})$ supersaturated alloys during their thermal treatment”, 16th International Conference “Radiation Physics of Solids”, Sevastopol, Ukraine, July 3–8, 2006.

Poster presentations:

5. “A self-interaction correction scheme for approximate Kohn–Sham potentials”, 25th Canadian Symposium on Theoretical and Computational Chemistry, Guelph, Ontario, July 22–27, 2012.
4. “Analytic integrability conditions for model Kohn–Sham potentials”, 17th Canadian Symposium on Theoretical Chemistry, Edmonton, Alberta, July 25–30, 2010.
3. “Functional derivatives and stray potentials in Kohn–Sham density-functional theory”, 92nd Canadian Chemistry Conference and Exhibition, Hamilton, Ontario, May 30 – June 3, 2009.
2. “Tests for functional derivatives in density-functional theory”, 9th Centre for Research in Molecular Modeling Symposium, Concordia University, Montréal, Québec, May 8–10, 2009.
1. “How to tell when a model Kohn–Sham potential is not a functional derivative”, 24th Symposium on Chemical Physics, University of Waterloo, Waterloo, Ontario, November 7–9, 2008.